SOLIDIFICATION AND STABILIZATION OF SPENT CATALYST FROM CATALYTIC CRACKING IN FLUDIZED BED-FLY ASH WITH PORTLAND CEMENT

Miss Onchuda Dumsri

A Thesis Submitted in Partial Fulfillment of Requirements
for the Degree of Master of Science in Environmental Management (Inter-Department)
Graduate School
Chulalongkorn University
Academic Year 2004

ISBN 974-17-7010-3

การหล่อแข็งและปรับเสถียรสารเร่งปฏิกิริยาที่ใช้แล้วจากกระบวนการกลั่นน้ำมัน-เถ้าถ่านหินด้วยปูนซีเมนต์

นางสาว อรชุดา ดำศรี

วิทยานิพนธ์นี้เป็นส่วนหนึ่งของการศึกษาตามหลักสูตรปริญญาวิทยาศาสตรมหาบัณฑิต
สาขาวิชาการจัดการสิ่งแวดล้อม (สหสาขาวิชา)
บัณฑิตวิทยาลัย จุฬาลงกรณ์มหาวิทยาลัย
ปีการศึกษา 2547
ISBN 974-17-7010-3

Thesis Title	Solidification and Stabilization of Spent Catalyst from Catalytic Cracking in Fluidized Bed–Fly Ash with Portland Cement
By	Miss Onchuda Dumsri
Field of Study	Environmental Management
Thesis Advisor	Manaskorn Rachakornkij, Ph.D.
Thesis Co-advisor	Walairat Bumrongjaroen, Ph.D.

Accepted by the Graduate School, Chulalongkorn University in Partial Fulfillment of the Requirements for the Master ’s Degree

…….. Dean of the Graduate School

(Assistant Professor M.R. Kalaya Tingsabadh, Ph.D.)

THESIS COMMITTEE

…….. Chairman

(Chantra Tongcumpou, Ph.D.)

…….…… Thesis Advisor

(Manaskorn Rachakornkij, Ph.D.)

…….. Thesis Co-advisor

(Walairat Bumrongjaroen, Ph.D.)

…….. Member

(Associate Professor Chai Jaturapitakkul, Ph.D.)

…….. Member

(Punjaporn Weschayanwiwat, Ph.D.)

อรชุดา ดำศรี : การหล่อแข็งและปรับเสถียรสารเร่งปฏิกิริยาที่ใช้แล้วจากกระบวนการกลั่นน้ำมัน-เถ้าถ่านหินด้วยปูนซีเมนต์. (Solidification and Stabilization of Spent Catalyst from Catalytic Cracking in Fluidized Bed–Fly Ash with Portland Cement) อ. ที่ปรึกษา: อ.ดร. มนัสกร ราชากรกิจ, อ. ที่ปรึกษาร่วม: ดร. วลัยรัตน์ บำรุงเจริญ 155 หน้า. ISBN 974-17-7010-3.

สารเร่งปฏิกิริยาที่ใช้แล้วจากกระบวนการกลั่นน้ำมันของหน่วยแตกน้ำมันหนัก จัดเป็นของเสียจากโรงกลั่นน้ำมันชนิดหนึ่ง ในปัจจุบันจึงได้มีการนำสารปฏิกิริยาที่ใช้แล้วเหล่านี้มาใช้ในงานก่อสร้าง เนื่องจากว่ามีคุณสมบัติเป็นวัสดุปอซโซลาน อีกทั้งยังสามารถปรับเสถียรโลหะหนักได้อีกด้วย งานวิจัยนี้มีวัตถุประสงค์เพื่อศึกษากลไกในการยึดจับโลหะหนักในสารเร่งปฏิกิริยาที่ใช้แล้วเมื่อนำมาผสมกับปูนซีเมนต์ และศึกษาการเปลี่ยนแปลงโครงสร้างระดับจุลภาค ตรวจสอบปริมาณแคลเซียมไฮดรอกไซด์ที่เปลี่ยนแปลงเพื่อนำมาใช้วิเคราะห์ปฏิกิริยาปอซโซลานที่เกิดขึ้น ทดสอบการเปลี่ยนแปลงขนาดโพรงและการชะของโลหะหนักจากก้อนเพสต์ และได้นำเถ้าถ่านหินมาผสมกับปูนซีเมนต์เพื่อศึกษาคุณสมบัติด้านต่างๆ อีกด้วย โดยอัตราส่วนที่นำมาใช้ตลอดการทดสอบคือทรายต่อวัสดุประสาน 2.75:1 และน้ำต่อวัสดุประสาน 0.55:1

ผลจากการวิจัยไม่พบการก่อตัวของโลหะหนักในซีเมนต์เพสต์ (ยกเว้นเหล็ก) เป็นเพราะว่าโลหะหนักจะอยู่ในโครงสร้างของ C-S-H ทำให้ไม่สามารถตรวจพบได้ หรืออธิบายโดยความสัมพันธ์ระหว่างอัตราการชะละลายและความเป็นกรดด่าง พบว่าโลหะหนักในสารเร่งปฏิกิริยาที่ใช้แล้วและเถ้าถ่านหินจะถูกชะออกมาได้ดีในระบบที่มีความเป็นด่างสูง แสดงให้เห็นว่าโลหะหนักจะละลายออกมาตั้งแต่ช่วงแรกของการบ่มเพราะในขณะนั้นค่าพีเอชในซีเมนต์เพสต์อาจสูงถึง 12 ส่วนผลการวิเคราะห์การชะของโลหะหนักจากก้อนมอร์ต้าร์ พบว่าเมื่ออายุการบ่มนานขึ้นอัตราการชะก็ต่ำลงเนื่องจากเกิดปฏิกิริยาไฮเดรชั่นและปฏิกิริยาปอซโซลานในสารเร่งปฏิกิริยาที่ใช้แล้วและเถ้าถ่านหินนั่นเอง โดยในช่วงเริ่มต้นจะเกิดจากปฏิกิริยาไฮเดรชั่นแต่เมื่อนานขึ้นจะเกิดจากปฏิกิริยาไฮเดรชั่นและปฏิกิริยาปอซโซลาน ทำให้โลหะหนักถูกดักจับไว้ในก้อนมอร์ต้าร์ได้ดี ผลที่ได้ยังสอดคล้องกับขนาดของโพรงในซีเมนต์เพสต์ที่เล็กลงอีกด้วย ผลการทดลองยังแสดงว่าการปริมาณการชะของโลหะและขนาดของโพรงจะลดลงมากเมื่อแทนที่สารเร่งปฏิกิริยาที่ใช้แล้วในปูนซีเมนต์ร้อยละ 15 โดยน้ำหนัก เถ้าถ่านหินร้อยละ 20 โดยน้ำหนัก แต่สารเร่งปฏิกิริยาที่ใช้แล้วผสมกับเถ้าถ่านหินเพียงร้อยละ 5-10 โดยน้ำหนักเท่านั้น.

สาขาวิชา...การจัดการสิ่งแวดล้อม.....ลายมือชื่อนิสิต.....

ปีการศึกษา.....2547.....ลายมือชื่ออาจารย์.....

ลายมือชื่ออาจารย์ที่ปรึกษาร่วม.....

4689522720 : MAJOR ENVIRONMENTAL MANAGEMENT
KEY WORD : SPENT CATALYST FROM FLUIDIZED-BED CATALYTIC CRACKING UNIT (FCC) / FLY ASH / LEACHABILITY / SOLIDIFICATION AND STABILIZATION

ONCHUDA DUMSRI : SOLIDIFICATION AND STABILIZATION OF SPENT CATALYST FROM CATALYTIC CRACKING IN FLUDIZED BED-FLY ASH WITH PORTLAND CEMENT. THESIS ADVISOR : MANASKORN RACHAKORNKIJ, Ph.D., THESIS COADVISOR : WALAIRAT BUMRONGJAROEN, 155 pp. ISBN 974-17-7010-3.

The spent catalyst from fluidized-bed catalytic cracking unit (FCC) is waste material since it is a waste from oil refinery. The use of spent FCC catalyst in construction has been proposed recently as it possesses pozzolanic activity and its heavy metal can be stabilized in the structure. The research is aimed to investigate the mechanism that stabilizes the heavy metal from FCC paste (CSP), fly ash paste (CFA) and FCC and fly ash paste (CSFA). Their microstructure developments were examined by X-Ray diffraction and scanning electron microscope (SEM). The pozzolanic reaction was monitored through calcium hydroxide consumption using XRD. The porosity and the leaching of heavy metals from the samples were measured in parallel with other tests. The experiment used sand to binder ratio of 2.75:1 and water to binder ratio of 0.55:1

Phase analysis by XRD reveals that no heavy metal phase exists (except Fe), suggesting that heavy metals from CSP, CFA, and CSFA do not form a new phase. This is because the heavy metals exist inside C-S-H structure of cement paste which can not be detected by XRD or all of metals can be dissolved out since pH in cement paste can reach to 12 within a few hours of mixing. The leaching test shows that the leaching rate at later age is much lower than at early age. As shown by the consumption of calcium hydroxide, the presence of FCC and fly ash prolongs the hydration process. As a result, there is less hydration product at early age to stabilize heavy metals. The hydration rate increases significantly at later age due to pozzolanic action of FCC and fly ash. Consequently, the heavy metals can be encapsulated inside these products. The permeability result also confirms the dense structure as the total porosity reduces significantly. It is a greater decrease for CSP 15 paste and CFA 20 paste but only 5-10% of CSFA pastes.

Field of study……Environmental Management…..Student’s signature……....

Academic year…...2004……...Advisor’s signature……...

Co-advisor’s signature……..

ACKNOWLEDGMENTS

I would like to express my sincerest gratitude to my thesis advisor, Dr. Manaskorn Rachakornkij for his encouragement, invaluable support, and insightful comments, throughout my thesis. I am also grateful to Dr. Walairat Bumrongjaroen, my thesis co-advisor, for her comments and suggestions not merely provide valuable knowledge, but broaden perspective in practical application as well. I would also like to express my gratitude my thesis committee members, Dr. Chantra Tongcumpou, Assoc. Prof. Dr. Chai Jaturapitakkul, and Dr. Punjaporn Weschayanwiwat

I am very grateful to the National Research Center for Environmental and Hazardous Waste Management Program (NRC-EHWM) for initial funding of the thesis. Special thanks must be giving to Toras Pozzolan, Limited, Thailand, for providing the spent FCC catalyst and fly ash used in this thesis and Department of Geology, Faculty of Science, for XRD supporting. The also thank to Khun Tanapon Phenrat for his helpful suggestions, all staff and friends at NRC-EHWM for their friendship.

Most particular, I fell pound to dedicate this thesis with due respect to my beloved mother and grandmother for their wholehearted understanding, constant source of encouragement and support throughout my life.

NOMENCLATURES

ASTM	American Society for Testing and Materials
C_2S	$2CaO•SiO_2$, dicalcium silicate
C_3A	$3CaO•Al_2O_3$, tricalcium aluminate
C_3S	$3CaO•SiO_2$, tricalcium silicate
C-S-H	Calcium silicate hydrate
CH	$Ca(OH)_2$, calcium hydroxide
$d_{10\%}$, $d_{50\%}$, $d_{90\%}$	Percentile points (microns) show the given percent of the volume
$d_{50\%}$	Median particle size
Fly Ash	Fine-grained material resulting from combustion of pulverized coal in power station furnaces and is collected in electrostatic separators
ICP	Inductively Coupled Plasma Spectroscopy
LOI	Loss on ignition (%) is defined by ASTM C311 as the weight fraction of material that is lost by heating the oven dried sample at 750 °C
LP-No.6	Notification of Ministry of Industry No. 6, B.E. 2540 (1997)
MIP	Mercury Intrusion Porosimetry
SEM	Scanning Electron Microscopy
Spent FCC Catalyst	Spent catalyst from fluid catalytic cracking unit of oil refinery
TCLP	Toxicity Characteristic Leaching Procedure
w/b	Water-to-binder ratio
XRD	X-ray Diffraction Spectroscopy
XRF	X-ray Fluorescence Spectroscopy

CONTENTS

Pages

Pages

Pages

Pages

Pages

LIST OF FIGURES

Figure **Pages**

Figure **Pages**

Figure **Pages**

Figure **Pages**

LIST OF TABLES

Table **Pages**

CHAPTER I

INTRODUCTION

1.1 General

Energy shortages have been a major problem in every country. The main natural resource for electric generation is crude oil. It is composed of different types of hydrocarbon all mixed together. They have long chain lengths, which are unusable. The petroleum refinery process separates crude oil by hydrocarbon chain length and its boiling point in distillation column. A catalyst is used to speed up this reaction by breaking large hydrocarbon chain to smaller chain.

The refinery operation consists of four processes: reforming, hydrocracking, hydrotreating, catalytic cracking and alkylation. The catalysts can be separated into two groups: solid and liquid acid catalysts. The liquid catalysts used in the alkylation process are acid catalyst such as HF and H_2SO_4. The liquid catalysts are the most widely used catalyst. Solid catalysts include non-noble and noble catalyst. Non-noble metal catalyst include base metal and zeolites. Noble metal catalyst includes a variety of precious metals from the platinum groups (Furimsky, 1996). In the past, the catalyst consumption accounted for more than half of the total worldwide but this trend will decrease in the future because of the advances in development of more active and stable catalysts (Su, Fang, Chen, and Liu, 2000). The catalytic cracking unit can be divided into two units: fluidized bed catalytic cracking (FCC) and hydrocracking process. This study investigates the spent catalyst from a fluidized bed in Rayong province in Thailand.

The FCC catalyst is supplied to the refinery in its solid form as micro-spheroidal particles, having been made by spray drying a silica alumina gel. These spheroidal catalyst particles consist of coherent aggregates of dense smooth spherical

particles about 45°A in diameter with a relatively narrow distribution in particle size (Paul and Thomas, 1979).

The spent FCC catalyst is a non-noble metal catalyst because it is mainly composed of solid support such as alumina, silica, silica-alumina and/or zeolite type. The flammability is significantly lower because of a more refractory nature of the deposited of coke, i.e. much lower H/C ratio. Also, the amount of coke on the spent FCC catalysts is much lower. The major components of the spent catalyst are silica-alumina and some heavy metals (cadmium, chromium, copper, iron, mercury, nickel, vanadium etc.) (Hopkins, 1938). The hazardous constituents in the spent catalyst can be divided into two groups, such as those present in the fresh catalyst and/or the fresh catalyst (e.g. alkylation catalyst), and those added to the catalyst during the operation. Among spent solid refinery catalysts, those from the upgrading of heavy feeds, much are more contaminated than spent FCC catalyst. The hazardous materials in spent catalyst are these heavy metal and coke. Coke is the residue product that comes from crude oil and easily to absorbs metal on its surface. The level of contamination by heavy metals and coke in the FCC catalyst is significantly lower because it has a much shorter contact time and the feedstock processed in the spent FCC catalyst is either of conventional origin or already catalytically treated. Even though, based on the RCRA regulations, the FCC catalyst is classified as non-hazardous. However, this classification might be changed in near future.

After several cycles in the catalytic cracking unit, the catalyst is removed from the bed and replaced by a new one to maintain the catalytic activity. Nowadays, there are seven oil refinery facilities but only three of them have the catalytic cracking process. They are Thai Oil Refinery, Esso Oil Refinery and Star Petroleum Oil Refinery. The annual production of spent catalyst for each plant is about 3,500 tons (Rattanasak, Jaturapitakkul, and Sudaprasert, 2001). Currently there are two ways to dispose spent catalysts from an oil refinery, in a landfill and through incineration in a cement plant. Most spent catalysts are sent to landfills because it is an easy to disposal method. In Thailand, there are only two industrial waste disposal companies, the General Environmental Conservation Public Company Limited (GENCO) and

Professional World Technology. For each company, the capacity of waste disposal is 125,000 tons per year while the quantity of industrial waste exceeds their treatment capabilities (Genco, 1998).

Due to the problem of landfill leachate contaminating with groundwater, the use of landfills is restricted. Although, the concentration of heavy metal in the spent FCC catalyst is low, it can accumulate and pose adverse effect in the long term. Thus, the petroleum refinery industry is now seeking an alternative process for disposal of spent catalyst. One of the options is to use them as construction material, which can make use of them and at the same time solidify and/or stabilize the hazardous materials in them.

Solidification and Stabilization (S/S) technologies are defined as treatment processes designed not only to improve waste-handling and physical characteristics, but also to reduce the surface area across which pollutants can transfer to leach, which limits the solubility of contaminant compounds and detoxifies the hazardous constitutions (Bishop, 1988). Stabilization is a process that employs additive (reagents) to reduce the hazardous nature of waste. After stabilization, the waste and its hazardous constituents are in a stable form that have a low migration rate into environment. Solidification is described as a technique that encapsulates the waste in a monolithic solid of high structural integrity. Solidification does not necessarily involve a chemical interaction between the waste and the solidifying reagents, but may mechanically bind the waste into the monolith. The difference between these two terms is that the solidification process may not necessarily decrease leachability, and the stabilization refers to a chemical reaction that has occurred to make waste constituents less leachable (Lagrega, Buckingham, and Evans, 2001).

In the S/S process, the binder and the heavy metal must interact with a chemical to create chemical binding. As a result, it cannot leach out into groundwater. S/S technology is comparable to other treatments or to the recovery, recycling or reuse processes. If the spent catalyst contains precious metals, such as platinum and palladium, metal recovery processes are highly profitable. However, spent FCC catalyst contains a small amount of metals and hazardous waste that are considered

not valuable metal. In addition, it is not possible to recover all of heavy metal in waste. Thus, S/S technologies are more cost effective, health safety and better for the long-term immobilization.

Fly ash is a by-product of the combustion process of pulverized coal in power plants furnaces. Coal is a complex material and widely used for as an energy source around the world. When pulverized, coal is burned to generate electrical power. The process produces large amounts of fly ash and bottom ash. The material is collected from the combustion gases before they are discharged into the open air. The term fly ash does not include the residue extracted from the bottom of boilers. In Thailand, the annual production of fly ash is about 3.3 million tons (Rattanasak et al., 2001). This number will increase in near future. Many studies have used fly ash in S/S processes. This utilization of fly ash not only contributes to environmental protection but also indirectly reduces the energy consumption in cement production.

The benefits of using fly ash in concrete includes economic value, workability, the improvement of concrete durability, reduction in the temperature rise in fresh concert, and the long-term strength of hardened concrete. In addition, it has been reported that it can reduce the leaching of heavy metals from hazardous waste when added to concrete (Bach, 1991). This could be due to the pozzolanic activity of both fly ash and spent FCC catalyst that enables them to add more hydration products into the cement matrix. This study attempts to investigate the S/S mechanism of using spent catalyst and fly ash in Portland cement paste. The important properties of solidified/stabilized materials that will be tested are leachability and strength. However, this work studied only leachability by observing the microstructure, glassy phase, permeability and mineralogical composition of the matrix.

1.2 Objectives

The main objective:

1. To investigate the stabilization and solidification process of spent FCC catalyst and fly ash with Portland Cement.

The specific objective are:

1. To investigate the mechanisms that stabilize the heavy metal in cement paste.

2. To investigate the pozzolanic reaction of the spent FCC catalyst and fly ash in the cement paste.

1.3 Scopes of the Study

This research was conducted to determine the physical and chemical properties of spent FCC catalyst and also determined fly ash from Mae Moh power plant. In addition, to evaluated the potential of solidified/ stabilized utilization from solidification and stabilization of spent FCC catalyst the suitable application of fly ash was evaluated, the environmental impact. The following point of research were conducted

1. Before carrying any of the test, the spent FCC catalyst was ground to a very small particle size and pass through a standard sieve No.325 (45 micrometer opening) while the fly ash sample was sieved through standard sieve No.200 (75 micrometer opening).

2. To investigate the chemical compositions of spent FCC catalyst and fly ash, Inductively Coupled Plasma Spectroscopy (ICP) was used.

3. The solidifization/stabilization ratio in differing amounts and combinations of binder materials was investigated. The ratios of the Portland cement to the spent FCC catalyst were: 1:0, 0.95:0.05, 0.90:0.10, 0.85:0.15, 0.80:0.20. The similar ratios were used with Portland cement to fly ash. For ratios of Portland cement : spent FCC catalyst : fly ash were 0.95:0.025:0.025, 0.90:0.05:0.05, 0.85:0.075:0.075, 0.80:0.10:0.10. The ratio of the binder materials to sand was 1.00:2.75 in accordance with ASTM C109-95 and the water to binder ratio was 0.55.

4. The S/S mechanism of heavy metal in the spent FCC catalyst and fly ash cement paste was investigated. The development of the hydration reaction and the solidified/stabilized matrices were observed at the ages of 3, 7, 14, 28, 56 and 90 days.

5. A study was conducted on the influence of the heavy metal on cement hydration by investigation the microstructure, phase formation and porosity. The Scanning Electron Microscope (SEM), X-ray Diffraction (XRD) Spectroscopy and Mercury Intrusion Porosimetry (MIP) were used in this study.

6. The standard regulatory method for determining the leaching of metal involved an extraction test, the Notification of Ministry No. 6, B.E. 2540 (1997), and the Toxic Characteristic Leaching Procedure (TCLP) was chosen to predict the leachability of the solidified and stabilized matrices at 28 and 90 days.

CHAPTER II

LETERATURE REVIEW

2.1 Characterization of Materials

2.1.1 Spent Catalyst

2.1.1.1 Formation and Compositions

The catalyst is used in petroleum refining practice to speed up the cracking reactions for takes large chain hydrocarbon and break them into smaller once. The catalyst usually changes the rate of the reaction by promoting a different mechanism for the reaction (Stuff works, 1998). The catalyst used in a fluid catalytic cracking (FCC) plant is developed from natural clays to synthetic gels from ground lumps to spray-dried micro-spheroids; all catalyst were built around the silica molecule (Sadeghbheigi, 2000). FCC catalytic as supplied to the refinery in the form of micro-spheroidal particles, has been made by spray drying a silica alumina gel. Each tetrahedron of FCC catalyst particle consists of a silicon or aluminum atom at the center of the tetrahedron, with oxygen atoms at the four corners (Figure 2.1). The microstructure observation shows that these spheroidal catalyst particles consist of coherent aggregates of dense smooth spherical particles about 45°A in diameters (Figure 2.2) with a relatively narrow distribution in particle size (Paul et al., 1979).

Spent FCC catalyst, the waste material from the FCC unit of oil refineries, is composed mainly of silica-alumina and/or zeolite type. The flammability of the spent FCC catalysts is significantly lower than spent hydroprocessing catalysts because of the more refractory nature of the deposited of coke, i.e. a much lower H/C ratio. As a result, the amount of coke on the spent FCC catalysts is much lower.

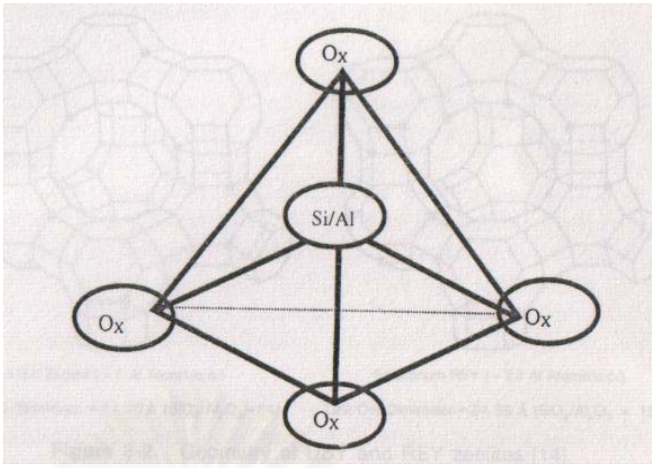

Figure 2.1 Spent FCC Catalyst Components in the Form of a Tetrahedron (Sadeghbheigi, 2000)

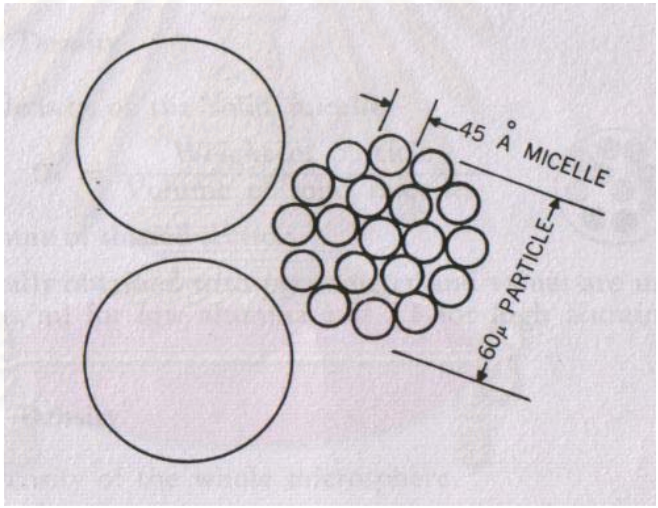

Figure 2.2 Average Particle Size of the Spent FCC Catalyst (Hopkin, 1938).

This catalyst was initially used in a FCC unit to cause hydrocarbon molecules to break into two or more smaller molecules. The FCC catalyst usually includes three vessels, i.e., a converter, a stripper and a regenerator. During the catalytic operation in the converter, some cracked products or coke will deposit on the catalyst particle. However, they are removed or burned off either in the stripper or in the regenerator. Some of the catalyst must be removed downstream of the regenerator and replaced with a fresh catalyst to maintain steady activity. This solid waste is removed at the

point following the generation; therefore, the amount of remaining coke is very small. In addition, fine particles are removed from the regenerator off-gas using electrostatic precipitator. These fines particle usually cannot be reuse in the refinery.

The hazardous constituents in spent catalyst can be divided into two groups: those present in the fresh catalysts and/or are the fresh catalysts (e.g. alkylation catalysts), and those added to the catalyst during the operation. Among spent solid refinery catalysts, those from the upgrading of heavy feeds are much more contaminated than spent FCC catalyst because the feedstock processed in the spent FCC catalyst are either of conventional origin or already catalytically treated (Marafi and Stanislaus, 2003). Vanadium and nickel were found as major contaminants on spent FCC catalyst at levels of 3518 ppm and 3225 ppm, respectively (Furimsky, 1996).

Therefore, spent catalyst from a FCC unit contains minute inorganic oxides and almost no organic compounds (Su, Chen, and Fang, 2001). Currently, spent catalyst from FCC unit are classified as non-hazardous materials.

2.1.1.2 Reclamation Technologies and Handling Options of Spent Catalyst

The refining industry uses large quantities of catalyst for the purification and upgrading of the various petroleum streams and residues. The catalysts deactivate with time and the spent catalysts are usually discarded as solid wastes. The quantity of spent catalysts discharged from different processing units depends largely on the amount of fresh catalysts used, their life, and the deposited formed on them during their use in the reactor. Normally, after two or three cycle times the catalyst can no longer be used due to irreversible loss of catalyst and/or mechanical properties. The volume of spent catalyst from various catalytic operations in the petroleum refinery process discarded as solid wastes has increased significantly due to a steady increase in the processing. In Thailand, the amount of spent catalyst from catalytic cracking in fluidized (FCC) beds alone produces more than 3,500 tons/year (Rattanasak et al., 2001).

The most important hazardous characteristic of spent catalyst from different catalytic processing units such as reforming, hydrocracking, hydrotreating, and alkylation are their toxic nature. Chemicals such as V, Ni, Mo, Co, Fe, etc. are present in the catalyst and can leach by water after disposal and pollute the environment (Cho, Kwang, and Woo, 2001). As a result, in many countries the refiners are experiencing pressure from environmental authorities for the safe handling of spent catalysts.

Several alternative methods are available for the disposal of spent catalysts:

1. Disposal as landfill. Spent catalyst have been disposed off as landfill in approved dump-sites. However, the disposal and treatment of spent refinery catalysts not only be act an approved dump-site but current regulations require landfills to be built with double liners as well as leachate collection and groundwater monitoring facilities. Therefore, the landfill option is becoming expensive today (Minocha, Jsin, and Verma, 2003).

2. The encapsulation and chemical fixation/stabilization process. Encapsulation involves surrounding the catalyst particles with an impervious layer of sealed in the thermoplastic agent. It is important that this method has to be stable over long period of time. In the stabilization process, the toxic metals in the spent catalyst are converted to environmentally safe products by reaction with certain chemical or materials such as cement and various glasses. After solidification, the products are converted into a non-leachable form (Choon-Keun, 2000)

3. Recovery of metals with the subsequent reuse of the recovered metals. Spent catalysts containing precious metals, such as platinum and palladium, in the metals recovery processes are highly beneficial. For spent FCC catalysts that contain Ni, V, Co and Al_2O_3, the process economics for metal recovery of metals are influence by metal prices, metal content, and the purify of the recovery metal (Jung-Hsiu, Wan-Lung, and Kung-Chung, 2003).

4. Reactivation/rejuvenation and reuse of spent catalyst. This option is not always possible. Because the application of this option to spent catalyst depends large on the cause of deactivation of the catalysts. For example, if spent catalyst is deactivated by coke deposition are usually regenerated by combustion coke under controlled temperature (Marafi, and Stanislaus, 2003; and Jin, 1998).

5. Utilization in cement production as cement kilns dust. Spent FCC catalyst has been successfully utilized in cement kiln dust as a source of alumina. (Furimsky, 1996).

6. Utilization of spent catalysts as raw material to produce valuable products. It is an attractive option from the environmental and economical points of view. However, this method is not available for many types of spent catalyst such as spent hydroprocessing catalyst, however spent FCC catalyst have been successfully utilized in cement production.

2.2.2 Fly Ash

Fly ash is a solid, fine-grained material that results from the combustion of pulverized coal in power station furnaces. The material is collected in mechanical or electrostatic separators. The characteristic of fly ash vary due to the influence of combustion conditions, coal properties, and collection processes (Sinsiri, Jaturapitakkul, and Jindaprasert, 2003). Three different process are employed for the combustion of the pulverized coal in power station furnaces: high temperature combustion, dry combustion, and fludized-bed combustion. Figure 2.3 shows the process for producing electricity of coal power plant.

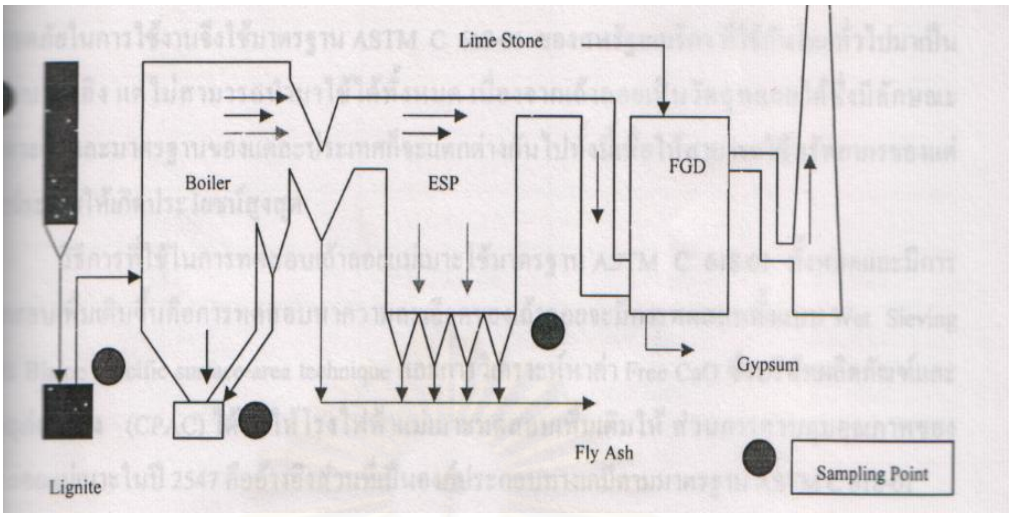

Figure 2.3 Coal Power Plant Diagrams (Nukulkan, 2003)

Normally fly ash is particularly rich in SiO_2 (25-60%), Al_2O_3 (10-30%) and Fe_2O_3 (5-25%). Fly ash is capable of reacting with $Ca(OH)_2$ at room temperature and can act as a pozzolanic materials. This pozzolanic activity is attributable to the presence of SiO_2 and Al_2O_3 in their amorphous form. According to ASTM C618, fly ash can be classified into two classes (Poon, Qiao, and Lin, 2003).

Class C: High calcium fly ash (>10%) is normally produced by burning sub-bitominous coal or lignite; the amounts of the three principal constituents exist in wide ranges that consist of SiO_2, Al_2O_3 and Fe_2O_3 in an amount that is greater than 50%. In addition to the pozzolanic properties, Class C fly ash posses some cementitious properties. This fly ash often reacts directly with water to form the cementitious phase such as C-S-H (calcium-silicate-hydrate) and $Ca(OH)_2$. Since a large proportion of silicate glass, they gain more strength than low-calcium fly ashes.

Class F: Low calcium fly ash (<10%) is usually produced by burning anthracite or bituminous coal and the sum of the three constituents, just mention in Class C fly ash, is greater than 70%. Class F fly ash has pozzolan properties.

Fly ash is used in concrete because of its economics, workability, improvement of concrete durability, reducing the temperature rise in fresh concrete,

and contribution to the long-term strength of hardened concrete (Xu and Sarker, 1994). In addition, it makes efficient use of the hydrated Portland cement as follows:

1. Solution of calcium and alkali hydroxide which exist in the pore structure of the cement pastes and

2. Is heat generated by the hydration of Portland cement, which is an important factor in initial reduction of cement. When fly ash mixing in cement paste is cured, the products of the fly ash reaction help to fill in spaced between the hydrating cement particles in the cement pastes fraction of cement. Thus, it has a lower permeability to water and aggressive heavy metals, i.e., reducing the leachate of heavy metals. Because of the slow reaction rate of fly ash, it helps in limiting the amount of early heat generation and the detrimental early temperature rise in massive structures.

Using fly ash in cement pastes also saves energy by reducing the amount of Portland cement and the quantity of mixing water in the cement mixture that is required to achieve the desired cement properties (Corner, 1993).

2.2.3 Portland Cement

Portland cement is a very important material in construction. The product obtained by pulverizing clinker consists essentially of hydraulic calcium silicate and aluminates, usually containing one or more forms of calcium sulfate as an interground addition.

The major compounds of Portland cement are shown in Table 2.1.

Table 2.1 Major Compounds of Portland Cement

Name	Oxide Composition	Quantity	Symbol
Tricalcium silicate	$3CaO•SiO_2$	50 to 70%	C_3S
Dicalcium silicate	$2CaO•SiO_2$	20 to 30%	C_2S
Tricalcium aluminate	$3CaO•Al_2O_3$	5 to 12%	C_3A
Tetracalcium aluminoferrite	$4CaO•Al_2O_3•Fe_2O_3$	5 to 12%	C_4AF

Note: This shortened notation is used to describe each oxide: C = CaO, S = SiO_2, A = Al_2O_3, F = Fe_2O_3.

It can be found that C_3S and C_2S are the most reactive compound in the system, whereas C_2S reacts much more slowly (Wesche, 1991). C_3S phases gives the essential properties of Portland cement and reacts with water to produces calcium silicate hydrate (C-S-H) during the hydration reaction of cement. Calcium silicate provides most of the strength developed by the Portland cement, C_3S provides most of the early strength (in the first 3 to 4 weeks) and both C_3S and C_2S contribute equally to ultimate strength (Lea, 1971). Another significant phase was gypsum, $CaSO_4•H_2O$, this phases also forms a strength phase by react with C_3S to form ettringite. However, the presence of gypsum also slows the early rate of setting of C_3S.

2.2 The Solidification and Stabilization (S/S) Process

The solidification and stabilization (S/S) process is known as one of the most popular technologies for treating a wide range of waste, most of which are inorganic (e.g., aqueous wastes, slages, and ashes containing hazardous metals) and disposing of hazardous wastes (Marafi, and Stanislaus, 2003). The S/S technologies using cementitious material have been used for decades as a final treatment step prior to the disposal of both radioactive and chemically hazardous waste, thus making them less susceptible of leaching. Not only is the solidified matrix considered as stable and safe for public and environmental health but also its physical property are suitable for application in the field of civil engineering.

Stabilization is a process employing additives (reagents) to reduce the hazardous nature of a waste by converting the waste and its hazardous constituents into a form that minimizes the rate of contaminant migration into the environment, or reduces the level of toxicity. This process alters hazardous wastes to more physical and chemical forms. Physical stabilization refers to the process of solidification and improves engineering properties, such as the bearing capacity, trafficability, and permeability of stabilized waste. Chemical stabilization is an alternation of the contaminants chemical form so that leachability is eliminated or substantially reduced. On the other hand, Solidification is the process of eliminating free water by hydration of a setting agent, or is described as the process by which sufficient quantities of solidified materials are added to a hazardous material resulting in a solidified mass of material (Lappas, Nalbandian, Iatridis, Voutetakis, and Vasalos, 2001). A Solidified dose not involve a chemical interaction between the waste and the solidified reagents, but it may be mechanically binded to the waste in the monolith. Contaminant migration is restricted by vastly decreasing the surface that is exposed to leaching and/or by isolating the wastes within an impervious capsule.

The difference between two terms of the treatment of hazardous wastes is that the solidification process may not necessarily decrease leachability, and stabilization generally refers to a purposeful chemical reaction that has occurred to make the waste constituents less than leachable. Portland cement is the most widely used for S/S as a binding material, it was originally used for the solidification of nuclear wastes in the 1950s. Portland cement is not used alone but is used as major ingredient in a number of S/S process systems. Many formulations have been developed for the S/S process according to the kinds of wastes including cement-based, lime-based, thermoplastic, organic polymer, encapsulation, glassification and self-cementing technique. These processes vary widely in their applicability to certain waste types, but the most are suitable only for primarily inorganic waste. The more commonly used in the fixation process are cement, fly ash, lime, slag, soluble silicates, clay or combination of these, to effect pozzolanic reactions which result in heavy metal binding and conversion of liquid waste into solid waste forms (Bishop, 1988).

Poon, Peters, and Perry (1985) conducted a solution (200 ml of 2000 ppm) of Zn, Hg which was solidified by 50 g of ordinary Portland cement (OPC) and 12 ml. of 40% Na_2SiO_3., where the pH value from the leaching was between 11.3-11.9. The leachate concentration of the heavy metal remained at a constant low concentration (<0.5 ppm) throughout. They conclude that at the addition of sodium silicate to cement, Zn^{2+} reacted with calcium hydroxide to produce insoluble compounds and hence there wasn't unfavorable effect on leachability and it minimized metal mobilization. This mechanism led to chemical stabilization.

Unlike Hg^{2+}, from the Scanning Electron Microscope (SEM), X-ray diffraction (XRD) analysis showed the interaction between the calcium in cement and the added sodium silicate resulted in massive deposits of calcium-silicate gel that absence in Zn added. Because Hg and some heavy metals which do not form insoluble compounds during the S/S process but rely on physical encapsulation to retain heavy metals in order to reduce porosity and hence lower the permeability. This mechanism means physical entrapment.

Some heavy metals do not form insoluble compounds, but they are retained in the structure by physical encapsulation. By adding sodium silicate into the mix, the interaction between the calcium in cement and the added sodium silicate can add the massive deposits of calcium-silicate gel reducing the porosity of the structure (Kulyakorn, 2002). Moreover, if the metals were bound to a solid through the pores or adsorbed in the pore surfaces, they should be released along with the alkalinity. This was confirmed by Bishop (1988) who showed that little metal leaching occurred when the pH value of the leachate was higher than 6.0. However, the presence of heavy metal in cement paste can increase the porosity of the structure resulting in an adverse effect. Poon et al. (1985) studied the effect of heavy metal on the porosity by using the Mercury Intrusion Porosimetry (MIP) test. They found that the addition of heavy metal significantly increased the porosity and shifted the pore size distribution toward a larger pore radius.

To ensure that heavy metal is encapsulated inside the structure, the admixture has been used to reduce the porosity of the matrix. The widely used admixture is pozzolan. Since pozzolan is composed of SiO_2 and Al_2O_3, it can react with calcium hydroxide from cement paste to form a calcium-silicate hydrate gel (C-S-H). The porosity of structure is reduced by an additional C-S-H product from this reaction. Among pozzolan, fly ash is one of the most common binders in waste stabilization and solidification (Constantino, Miguel, and Jose, 2001). The glassy phase in fly ash breaks down and releases SiO_2 and Al_2O_3 to react with calcium hydroxide in the cement paste system.

Consequently, factors that control the pozzolanic activity of pozzolan also control the porosity of the structure. These include particle size, percent replacement of pozzolan material, water-to-cement ratio etc. Paya, Monzo, and Borrachero (1999) investigated the effect of particles size through the grinding on the properties of the fluid catalytic cracking residue (FCC). The results showed that using a spent catalyst smaller than 2 μm in diameter enhanced the pozzolanic properties of spent FCC catalyst as the compressive strength increased with finer particle. This indicates that particles size plays an important role in pozzolanic action. Another benefit of using fine particles is the adsorption process. Bishop (1988) showed that metal leaching rate decreased as particle size decreased. They explained that the heavy metals were bound onto the particle by a sorption mechanism. The smaller particles would cause greater sorption and thus a lower leaching metal concentration. However, an adverse effect of using fine particle size is that the fine particles can increase the absorption/adsorption characteristics of the spent FCC catalyst (Chen, Tseng, and Hsu, 2003). As a result, they require more water to achieve workability.

Moreover, percent replacement of a spent FCC catalyst is another factor that is of concern. Paya, Monzo, and Borrachero (2001) studied the optimal ratio in percent replacement of spent FCC catalyst in Portland cement. They found that the optimal replacing percentage in Portland cement by spent FCC catalyst content is in the 15-20 % range without decreasing another factor. When spent FCC catalyst content in cement increases, the concentrations of calcium cation (Ca^{2+}) and hydroxyl anion (OH^-) decrease.

Similarly, Su et al. (2001) showed that spent catalyst can replace up to 10% of fine aggregate without decreasing strength. On the contrary, Su et al. (2000) found that spent FCC catalyst can substitute up to 15% of the cement content without sacrificing the quality of concrete. Paya, Monzo, Borrachero, and Velazquez (2003) showed that when the percent replacement of spent FCC catalyst increased, the amount of hydration products calcium silicate hydrates (CSH), calcium aluminate (CAH), calcium aluminosilicate hydrates (CASH) and ettringite (Af_t) also increased. CAH and CASH become more important when the percent replacement of spent FCC catalyst was 15-20% because pozzolans are an extra source of aluminates, in addition to the lower CSH production since there were 15% less cement. It can be ascribed that when there is less liquid phase, the transport of ions to form new hydrate products is obstructed, this effect is more marked for the pozzolan pastes than for the control paste (0% replacement of spent FCC catalyst), due to the pozzolanic behavior of the additions.

Another important factor for pozzolanic action in the S/S process is the water-to-binder ratio, especially concerning the hydration reaction and strength of the solidified and stabilized sample. Su et al. (2001) concluded that the flowabilty and bleeding of mortar increased with a higher water-to-cement (W/C) ratio. In general, when W/C ratio was 0.55 or 0.485, the mortars with 5% or 10% replacement of spent FCC catalyst showed higher compressive strength than the control. This is attributed to the pozzolanic activity of the spent catalyst. However, at 15% replacement, the compressive strength was much lower than of the control due to poor compaction of the substituted mortars. In addition, they suggested that 5% of sand substitution should be added when W/C ratio is low to maintain good workability.

A previous study by Su et al. (2000) revealed that these spent FCC catalyst can absorb water easily, thus reducing the W/C ratio in the liquid phase of the mortar. As a result, the W/C ratio of hardened mortar is lower than the apparent the W/C ratio. They also concluded that a decrease in the W/C ratio was advantageous to the concrete strength at the later stage. Likewise, Poon et al. (1984) identified that when W/C ratio more than 0.6, it saved material cost as a larger volume of waste could be treated for the same amount of cement. However, the penalty of increasing the W/C

ratio is increasing porosity in the solidified material, resulting in reduced physical strength and higher permeability (Tsivilis, Tsantilas, Kakali, Chaniotakis, and Sakellariou, 2003). Thus, the solidification process should be adjusted according to the type of heavy metal being stabilized.

It should be noted that all the literature reviewed above were investigated in view of the macroscopic scale, which was effective enough to provide a reliable answer regarding the utilization potential issue. On the other hand, to investigate mechanisms or phenomena taking place in the solidified/stabilized matrices, experiments performed on the microscopic scale are required.

Despite the fact that solidified/stabilized materials has emerged and been applied to cope with various types of waste, ranking from radioactive waste to biological organism for several decades, the physical and chemical phenomena as a result of the interaction between metal pollutants with cement components have not been fully characterized. Figure 2.4 illustrates the various possibilities for the interaction of the hazardous substance. Based on the scientific knowledge, these interactions can be categorized under four headings; the waste chemical component may go through chemisorption, precipitate, lattice inclusion, and form a surface compound to any of several components. However, there may be other possibilities interactions occurring in the system which are still regarded as “Unknows” (Coke and Mallas, 1993). Owing the fact that the complexity of the blending of dynamic cement chemistry with solution equilibrium and kinetic process coupled with the surface and near-surface phenomena, our knowledge of these four important mechanisms is still far from complete in a dynamically reacting system.

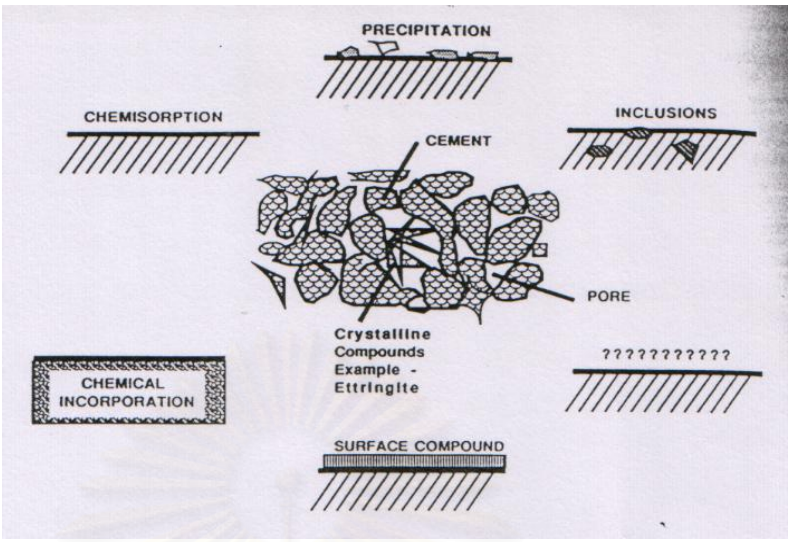

Figure 2.4 Various Possibilities for the Interaction of the Hazardous Substance with Cement (Coke and Mallas, 1993)

2.3 Hydration Reaction and Pozzolanic Activity of the Cementitious Materials

The hydration reaction of the all compound in Portland cement that are composed of tricalcium silicate (C_3S), dicalcium silicate (C_2S), tricalcium aluminate (C_3A) , and tetracalcium aluminoferrite (C_4AF) with water. When brought into contact with water, these compounds are attracted or decomposed and form hydrated compounds. However, the hydration of C_3S and C_2S, which are the key components in cement, generally react with water to produce calcium hydroxide,$Ca(OH)_2$, and calcium silicate hydrate (C-S-H). The formula of calcium silicate hydrate (C-S-H) is only approximate since the composition of this compound varies over a wide range. The equation describing hydration of key components are as follow:

$$2C_3S + 6\,H_2O \longrightarrow C_3S_2H_3 + 3\,Ca(OH)_2$$

$$2C_2S + 6\,H_2O \longrightarrow C_3S_2H_3 + 3\,Ca(OH)_2$$

Where: $C_3S_2H_3$ = C-S-H.

C_3A is known to react very rapidly with water followed by precipitation of calcium aluminate hydrates with consider evolution of heat.

Pozzolan materials have been widely used as substitutes for Portland cement in many applications because they have several advantageous properties that result in cost reduction, reduction in heat development, decrease permeability, alkali-aggregate expansion control, increase chemical resistance, reduce concrete drying shrinkage, and the improvement of the properties of fresh concrete (Roy, A., Eaton, Cartedge, and Tittlebeam, 1998). Based on spent FCC catalyst and fly ash properties, they are commonly classified as pozzolan because their sums of SiO_2, Al_2O_3, and Fe_2O_3 are greater than 70%.

Pozzolan are materials, which in itself possesses non-cementitious properties, and contain constituents that will combine with alkali reagent or lime in the presence of water at normal temperatures to produce stable insoluble compounds with cementitious properties. It is know that the pozzolanic reaction of spent FCC catalyst and fly ash are significant after two or three of weeks.

The first step of a pozzolnic reaction of pozzolan materials is believed to breaking down its glassy phases to release alumina and silica at a pH of about 13.3 or higher in the presence of lime and dissolve to a pore solution; however, that may reduce the solubility of $Ca(OH)_2$ due to the common ion effect. Pozzolanic reaction involve the depolymerization of a glassy matrix by OH^- of alkaline in the pore solution at a high pH. $Ca(OH)_2$ in the pore water combines with these compounds that result in the precipitation of various calcium silicates, calcium aluminates, and calcium aluminosilicates as the reaction is shown below (Plowman, 1991):

$$SiO_2 + 2Na + (\text{or } 2K^+) + 2\ OH^- \longrightarrow Na_2(K_2)\ SiO_3\ H_2O$$

$$Ca^{2+} + SiO_2 + H_2O \longrightarrow xCaO{\bullet}ySiO_2{\bullet}zH_2O$$

$$Ca^{2+} + Al_2O_3 + H_2O \longrightarrow xCaO{\bullet}yAl_2O_3{\bullet}zH_2O$$

$$Ca^{2+} + SiO_2 / Al_2O_3 + H_2O \longrightarrow xCaO{\bullet}\ yAl_2O_3{\bullet}zSiO_2{\bullet}wH_2O$$

$$Ca^{2+} + SO_4^{2-} + Al_2O_3 + H_2O \longrightarrow xCaO{\bullet}\ yAl_2O_3{\bullet}zCaSO_4{\bullet}wH_2O$$

Pozzolanic reactions do not proceed independently. These reactions depend on the amount of calcium, alkali, sulphate, silicate, and aluminate ions that are released into the liquid phase from both cement and cementitious materials. As a

consequence of the decomposition of the glassy structure, silica and alumina are forced into pore water. This process is hindered by the hydration of cement. At the beginner, the dissolution of the pozzolan material is a slow process. Due to the high calcium content in pore water in the early state of hydration, the C-S-H gel will precipitate in the vacant space. It causes any future decomposition of the glassy network to slow down. The pozolan reaction is slow; hence, the rate of strength development and the heat of hydration associated with its reaction is relatively minimal. Latter, when the pH increase and the calcium ion concentration decreases, the rate of the pozzolan material dissolution will increase. Poon et al., (2003) reported that the addition of Na_2SO_4 and K_2SO_4 in the cement pastes is very efficient in accelerating the hydration reaction in the system. This may be because Na^+ and K^+ can increase the pH value of the solution in the pastes and accelerate the dissolution of glassy phase. With an increase in the hydration products, the compressive strength increased as well (Pacewska, Wilinska, and Kubissa, 1998).

In addition, the characteristics, environment, and elevated temperature of cement paste containing a pozzolan also affect the pozzolanic activity of pozzolan nature of concrete (Constantino et al., 2001). The characteristics that affected this reaction are the reactivity of the glassy phases, the quantity of alumina and silica.

2.4 Leaching of Heavy Metals from Stabilized/Solidified Products

Many research was shown that metal leaching from the stabilized/solidified hazardous waste is affected by many important factors, including the type and speciation of the metal, cement paste formulation, particle size, leachant type, acid flux through the waste and time of contact with the leachant. Leaching is also a function of porosity, the degree of hydration or water to cement ratio. When the water contacts or passes through a material like solidified waste, each constituent dissolves and the rate of dissolution can be measured. This process called “leaching”, the water with which start the “leachant,” and the contaminated water that passed through a solidified waste is the “leachate.” The capacity of the solidified waste material to leach called its “leachability” (Lagrega et al., 2001).

The environmental acceptability of a hazardous waste for land disposal in the United State is large based on the results obtained from running the U.S. Environmental Protection Agency Toxicity Characteristic Leaching Procedure (TCLP) test, which has replaced the Extraction Procedure (EP) test. The TCLP test is designed to address the mobility of both organic and inorganic compounds (heavy metal) and to apply a compound-specific dilution/attenuation factor. The purpose of the TCLP test is to simulate the potential for leaching which would occur if the waste is disposed to a municipal landfill along with other general refuse (Bishop, 1988). Like the TCLP, the Notification of Thailand Ministry of Industry No.6, B.E. 2540 (1997), abbreviated as LP-No.6, could be used as the primary indicator as to whether a sludge is a hazardous material or not. Except the extraction fluid made from 80% of sulfuric acid and 20% of nitric acid in deionized (DI) water to a pH of 5.00 is selected to mimic conditions in a municipal landfill for LP-No.6 (Ministry of Industry, 2002).

Both extraction tests, requires that stabilized material be crushed to a particle size smaller than 9.5 mm, if necessary. About 100 grams of the crushed samples was added with extraction fluid. The ratio of the liquid-to-solid weight is 20:1, then it is agitated with a rotary the extraction for 18 hours at 30 rpm at normal temperature. After 18 hours of agitation, the extraction solution is filtered through a 0.6-0.8 μm glass fiber filter, and the filtrates are defined as the extract. This extract is analyzed for a variety of hazardous waste constitutes including volatile and semi-volatile, organic, metals, nd pesticides so that the results are compared to the regular levels. If waste leaches one or more contaminants in excess of specified level, it is classified as a hazardous waste. Until now, there are only eight metals addressed in the TCLP limits; they are silver (Ag), arsenic (As), barium (Ba), cadmium (Cd), chromium (Cr), mercury (Hg), lead (Pb), and selenium (Se). These metals limit are similar to the Thailand regulation limit. Table 2.2 shows the Thailand regulation; their recommended maximum concentration of trace metal and their limits are exactly the same as that of the TCLP limits.

Table 2.2 Recommended Maximum Concentrations of Trace Metals in Leaching Water.

Element	Recommended Maximum Concentration (ppm)
Ag	5
As	5
Ba	100
Cd	1
Cr	5
Hg	2
Pb	5
Se	1

Factors affecting to the leachability can be divided into two sets: (1) those which originate with the waste material itself and (2) those which a the function of the leaching test. The combination of the two sets determines the leachability of the waste material (Cocke and Mollah, 1993). However, the surface area of the waste, the nature of the extraction vessel, the agitation technique, the nature of the leachant, the ratio of the leachant to waste, to number of the elution used, the time of contact, temperature, pH of the leachant, and the method used to separate extract from the solid also affects the leachability of the waste materials.

Bishop(1988) used the sequential batch extraction technique to demonstrate that even after the alkali had been leached from cement–based waste forms, lead and chromium leaching was much lower than that would be expected from metal hydroxide solubilities. Therefore, pH control is necessary for metal fixation in most system. In addition, Wang, and Vipulanandan (2000) reported that the heavy metal leaching rate was greatly affected by the composition of the cement, especially the amount of $Ca(OH)_2$ present. An optimum $Ca(OH)_2$ content would show the maximum inhibition of heavy metal leaching. When pollutants were released from acidic water, the presence of $Ca(OH)_2$ would slow down the release rate. On the other hand, if dissolved, it would leave extra pores on the body that would speed up the dissolution of the main body.

Li, Poon, Sun, Lo, and Kirk (2001) revealed that the leaching behaviors of metals in S/S waste matrix were mainly controlled by the alkaline nature and acid buffering capacity of the S/S matrix. During the leaching process, with the dissolution $Ca(OH)_2$ and CSH, the pH value and buffering capacity of the matrix decreased and the leachability of heavy metal in S/S waste material increased. Bishop (1988) found that the amount of heavy metal leaching from a 42-day-old sample was essentially the same as from a two-year-old one. Consequently, all future leach testing was done using samples which were at least six weeks old. In addition, leaching occurs under highly alkaline conditions, rather than the acidic conditions intended in the TCLP test.

From the literature survey, it was found that the major chemical composition of spent FCC catalyst consists of SiO_2 and Al_2O_3. The reaction between these compound, cement, and water results in the formation of a cement-like product. In addition, the permeability and leachability of cement mixing with these materials were less than the control sample.

If the experimental data goes along with the expected results, reusing spent FCC catalyst and fly ash as cementitious materials is feasible and will not result in pollution due to the leaching to heavy metals.

CHAPTER III

METHODOLOGY

3.1 Materials

3.1.1 Spent Catalyst

The spent catalyst in fluid catalytic cracking (FCC) plant was used in this experiment obtained from the Star Petroleum Oil Refinery, Rayong Province, Thailand. The spent FCC catalyst was ground to a very small particle size by disc mill and pass though a standard sieve No.325 (45 micrometer openings).

3.1.2 Fly Ash

The fly ash used in this experiment was a by-product from Mae Moh Power Plant, Lampang Province, Thailand. The fly ash sample was sieved through a standard sieve No.200 (75 micrometer opening) before carried out any tests.

3.1.3 Portland Cement

The Diamond brand ASTM Type-I Portland cement according to ASTM C150-95 manufactured by Siam City Cement Public Company Ltd. (SCCC), Bangkok, Thailand is used throughout the experiments.

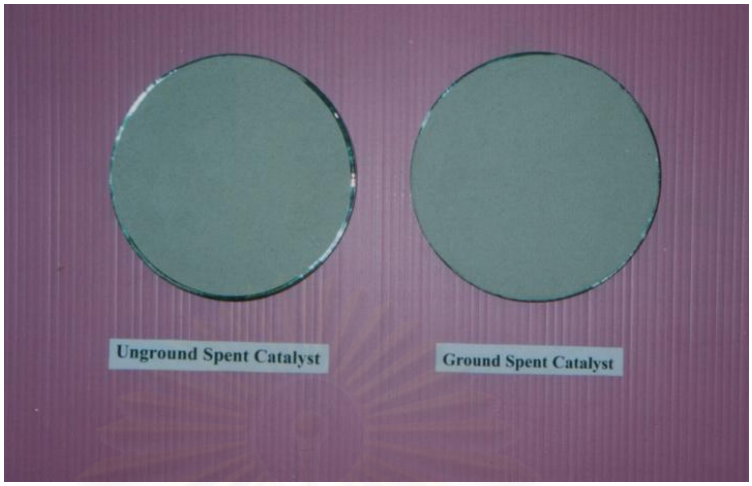

Figure 3.1 Unground Spent FCC Catalyst and Ground Spent Catalyst

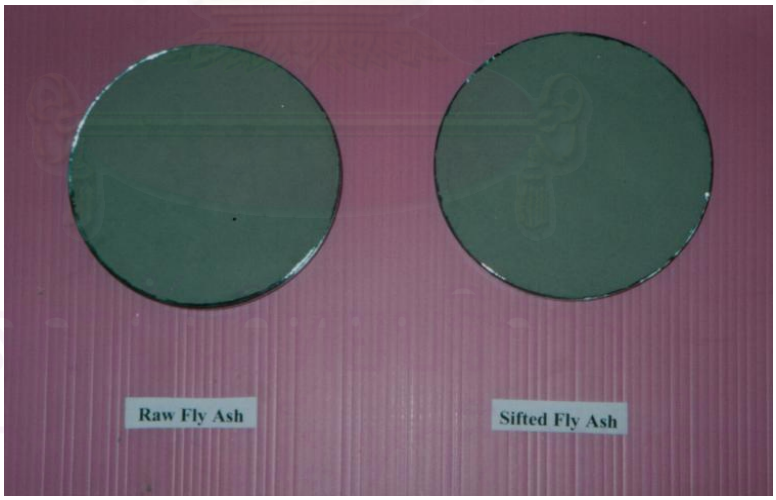

Figure 3.2 Raw Fly ash and Sifted Fly Ash

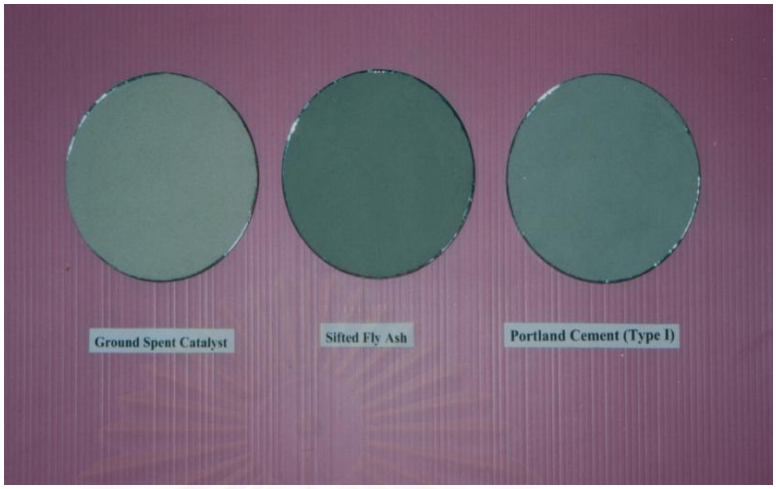

Figure 3.3 Ground Spent FCC Catalyst**,** Sifted Fly Ash, and Portland Cement

3.1.4 Sand

The river sand used for making specimens was natural silica sand that conforms graded sand as specified by ASTM C778-92.

3.1.5 Water

Ordinary tap water was used for all mixtures.

3.1.6 Reagents and Glassware

All chemicals used in this study were reagent grade and were used without future purification. All glassware was cleaned by soaking in 10% HNO_3 and rinsed four times with deionized (DI) water.

3.2 Experimental Programs

3.2.1 Characterization of Raw Materials

3.2.1.1 Particle Size and Specific Surface Area

Raw materials consisted of spent FCC catalyst, fly ash, Portland cement, and sand were subjected to particle size analysis by Malvern Particle Size Analyzer Model Mastersizer S that can measure particle size ranging from 0.05 to 880 microns. In this study, water was used as a medium with dispersing refractive index of 1.33.

According to ASTM C204-96, the standard test method was used to determine fineness of spent FCC catalyst, fly ash, and Portland cement by Blaine air-permeability apparatus in view of specific surface. Specific surface is expressed as total surface area in terms square centimeters per gram of sample by measuring the consuming time for fixed quantity of air flows through a compacted bed of specified dimensions and porosity. This method generally requires calibration of apparatus with standard cement. The weight of sample used for test was the same as that used in the calibration test, in this test, 2.14 grams. The weighted sample was placed and compacted in a permeability cell, to which the manometer tube for airflow measurement was attracted (Podjanee, 2002).

3.2.1.2 Bulk Specific Gravity and Water Absorption

Bulk specific gravity is defined as the ratio of the weight of a given volume of sample, including voids between the grains, to the weight of an equal volume of water. According to ASTM C188-95 that described the procedure to determine bulk specific gravity of Portland cement and adapted to calculate that of spent FCC catalyst and fly ash. About 50 grams of these samples were used instead of 64 grams of cement as recommended in ASTM C311-96. In this study, kerosene was used in place of water to ensure that all grains of spent FCC catalyst and fly ash were wetted by the liquid and hydration of the samples were minimized.

The method was used to determine the water absorption as described in ASTM C645. The mass “A” was measured after dying at 110±5 °C for sufficient time to remove all uncombined water. Then, these samples were immersed in water at 23±1.7 °C. The sample was removed and surface-dried using a moist cloth. Care was taken to remove only surface water and to ensure that no fragments were lost. The mass of the surface-dried sample was “B”

$$\text{Water absorption (\%)} = \frac{(B-A)}{A} \times 100\ \%$$

3.2.1.3 pH

The guidance described in the U.S. EPA SW-846 Method 9045C was used to determine pH of spent FCC catalyst and fly ash. The aqueous phase sample was prepared by adding 100 ml of deionized (DI) water in a 150-ml beaker, in which approximately 5 grams of sample was first placed. The sample was regularly stirred at least 5 minutes and let to gradually stand and settle out for about 15 minutes from the suspension. After complete segregation, the HACH SensIon-3 pH Meter were employed to determine the pH of the sorted aqueous phases of sample.

3.2.1.4 Loss on Ignition (LOI)

The method to determine the Loss on Ignition (LOI) is defined in ASTM C311-96 and ASTM C114-94 as the weight fraction of material that is lost by heating in a muffle furnace at 750 °C. The residue left from moisture content determination shall be ignited to a constant weight in an uncovered porcelain crucible at 750±50 °C. LOI is measurement of unburned carbon remaining in the ash. This value is perhaps the single most critical characteristics of sample. LOI can also be used as an indicator of the degree of burnout or defined the combustion efficiency.

3.2.1.5 Bulk Chemical Compositions

X-ray fluorescence (XRF) spectroscopy was carried out to measured bulk chemical compositions of spent FCC catalyst fly ash and Portland cement. The Philips XRF Spectrometer Model 2400 was used in this study. XRF provides useful information on the overall compositions of the analyzed materials. To obtain a good representative, the sample was initially ground in a ceramic mortar to achieve a homogeneous size of below 45 microns since the XRF only penetrated up to a few millimeter from the surface of a sample. About 1.5 grams of H_3BO_3 (2.5% by weight) binder, around 4.5 grams of ground sample was pressed into a pellet for convenient handling and measurement. Before running, the pilled sample was put in a sample cup and loaded on a feeder tray.

3.2.1.6 Morphology

The microstructure of spent FCC catalyst, fly ash, and Portland cement were observed by JSM 6400 Scanning Electron Microscopy (SEM) equipped with Energy dispersive Analysis of X-ray (EDS) Link^{isis} Series. These materials were initially glued on an aluminum stub and coated with goal palladium alloy. This method examines only a tiny area of these particles. Each sample will be taken at different magnifications and different location in order to obtain the representative image.

3.2.1.7 Mineralogical Compositions

The power X-ray diffraction (XRD) spectrometer, Bruker Model D8 Advance, was used to identify mineralogical compositions of spent FCC catalyst, fly ash, and Portland cement. XRD patterns were obtained with a computer controlled diffractometer equipped with a copper X-ray tube and a scintillation detector. A graphite monochromator was used to produce diffracted lines according to a single X-ray wavelength with low background. Each sample was pulverized in a ceramic mortar until homogeneous with particle size of below 45 microns and grinding with acetone to stop hydration by dewatering. All samples were analyze at 40 kV accelerating voltage, 40 mA current, 0.015 step time and 10° to 70° 2θ scanning range.

3.2.1.8 Heavy Metals Concentration

The U.S. EPA Method 3051, microwave assisted acid digestion, was used to destructed sample and conducted to analyze the concentration of heavy metals; cupper (Cu), iron (Fe), nickel (Ni), vanadium (V), and zinc (Zn) by Inductive Couple Plasma-Optical Emission Spectroscopy (ICP-OES). In each sample, three replicates of each samples were chosen.

3.2.1.9 Leaching Behaviors

To identify the leachability of spent FCC catalyst and fly ash under different simulated condition, in this study, not only the TCLP test but also the Notification of Ministry of Industry No.6, B.E. 2540 (1997) extraction test were used to simulate these wastes before solidification and stabilization. This test does not determine the total elemental contents of the samples, but indicates the leaching potential of some elements.

Under the TCLP test, one of the universal extraction test procedures, issued by the U.S.EPA under the Hazardous and Solid Waste Amendments of 1984 (HSWA), to follow this procedure, the tested materials were crushed to a particle size smaller than 9.5 mm, if necessary. About 100 grams of the crushed samples was added with extraction fluid, which made from water and acetic acid to a pH of 4.93±0.05, these condition was selected to mimic conditions in municipal landfill. Ratio in a liquid-to-solid weight is 20:1, then agitated with a rotary extraction for 18 hours at 30 rpm at normal temperature. After 18 hours of agitation, the samples were filtered through a 0.6-0.8 μm glass fiber filter, and the filtrates were defined as the TCLP extract (Method 3011, 1992). In this study, the filtrates were analyzed by ICP-OES and pH of leachate samples were measured by the HACH SensIon 3 pH Meter.

On the other hand, according to the leaching procedure described in the Notification of Ministry of Industry No.6, B.E. 2540 (1997) which Thailand has developed its own leaching proceduce. This leaching procedure is almost similar to

the TCLP except the extraction fluid made from 80% of sulfuric acid and 20% of nitric acid in deionized (DI) water to pH of 5.00 (Podjanee, 2002).

3.2.2 Chemical and Physical Properties of the Solidification/Stabilization Materials

Spent FCC catalyst and fly ash were directly replaced cement in the mixed with different replacement (0%, 5%, 10%, 15%, and 20% by weight). According to the requirement in ASTM C109-95, the weight ratio of cement to sand is 1.00:2.75. The ratio of water to binder was 0.55 through experiment. In each experiment programs consist of 13 samples for testing. Each mix proportion of cement pastes in this experiment were shown in Table 3.1

Table 3.1 Mix Proportion of Cement Pastes for w/(binders) = 0.55

Symbol	Mix Proportion by Weight			
	Cement	Spent Catalyst	Fly Ash	Sand
Control	1.00	-	-	2.75
CSP 5	0.95	0.050	-	2.75
CSP 10	0.90	0.100	-	2.75
CSP 15	0.85	0.150	-	2.75
CSP 20	0.80	0.200	-	2.75
CFA 5	0.95	-	0.050	2.75
CFA 10	0.90	-	0.100	2.75
CFA 15	0.85	-	0.150	2.75
CFA 20	0.80	-	0.200	2.75
CSFA 5	0.95	0.025	0.025	2.75
CSFA 10	0.90	0.050	0.050	2.75
CSFA 15	0.85	0.075	0.075	2.75
CSFA 20	0.80	0.100	0.100	2.75

3.2.2.1 XRD Application for Investigate Hydration Reaction and Pozzolanic Activity of the Solidified/ Stabilized Materials

All of solidified/stabilized materials, 13 samples, were used in this study as the same component as Table 3.1. To study phases analysis and process of hydration

reaction and pozzolanic activity formed in the spent FCC catalyst-cement pastes (CSP), fly ash-cement pastes (CFA), and (spent FCC catalyst + fly ash)-cement pastes (CSFA), XRD analysis was performed on CSP pastes, CFA pastes, and CSFA pastes to eliminate interference peaks originated from sand by without addition of sand. The mixtures were cured in airlight plastic bags at normal temperature to minimize their carbonation until tested. At the curing time 3, 7, 14, 28, 56, and 90 days, conduct to tested by XRD. All samples were analyzed at each by Bruker Model D8 Advance, at 40 kV accelerating voltage, 40 mA current, 0.015 step time and 10° to 70° 2θ scanning range Before testing, the sample was first was first pulverized by grinding it with acetone for 5 minutes to stop its hydration reaction. The soaked sample was dried in an oven at 60 °C for about 4 hours and again pulverized in ceramic mortar to obtain homogeneous size of approximate 45 microns.

3.2.2.2 SEM Application for Examining Macroencapsulation of Solidified/ Stabilized Materials

To obtain a better understanding of CSP pastes, CFA pastes, and CSFA pastes on the microstructure of cement paste, 13 samples of cement pasts at the same component as Table 3.1, were cast into 5 mm-diameter plastic tubes. The samples were vibrated to remove include air and sealed with parafilm and were cured in airlight plastic bags at normal temperature. By the age of 3, 7, 14, 28, 56, and 90 days of curing time, the samples were crossectionally cracked, coated with goal, and their microstructures were observed by JSM 6400 Scanning Electron Microscopy.

3.2.2.3 Permeability of Solidified/ Stabilized Materials

Mercury intrusion porosimetry (MIP), Poresizer 9320, was used to study the porosity of CSP pastes, CFA pastes, and CSFA pastes in this study. This instrument can measure particle size ranging from 0.006 to 360 um. The sample that used in this study as the same component as Table 3.1. After 28 days and 90 days of curing time, all the sample was first pulverized in ceramic mortar to obtain homogeneous size. About 3 grams of sample were put in penetrometer at the low pressure port of MIP. Waiting until pressure below 50 μmHg and press liquid mercury. Increased pressure

until 24-25 Psi., record the relation between pressure and mercury volume. After that, put the penetrometer into high pressure port until pressure 30,000 Psi., the relation between pressure and mercury volume were recorded also. Finally, adjust pressure to atmosphere pressure and recorded.

3.2.2.4 Leaching Characteristics of the Solidified/Stabilized Materials

To examine the influence of CSP paste, CFA pastes, and CSFA pastes on the lechability of the solidified/ stabilized products and the ability of cement fixation, after 28 days and 90 days of curing time, all of solidified/stabilized samples cast as the same component as Table 3.1 were crushed to particle size smaller than 9.5 mm and next process of both the TCLP and the Notification of Ministry of Industry No.6, B.E. 2540 (1997) extraction test as described in 3.2.1.8.

According to U.S. EPA SW-846 Method 3015, microwave assisted acid digestion of aqueous samples and extracts, used to reduce the interference by organic matters and to convert metal associated with particulate to a form (usually the free metal) that can be determined by ICP-OES. The procedure following, a 45 ml of extract in 5 ml of concentrated nitric acid in digestion vessel. The temperature of the extraction was brought to 170±5 °C in 10 minutes, and maintained at 170±5 °C for 10 minutes to accelerate the leaching process. After the digestion process, the digested solution was cooled to room temperature and kept in a HDPE bottle before analysis.

CHATER IV

RESULTS AND DISSUSSION

4.1 Characterization of Raw Materials

4.1.1 Particle Size

The influence of the particles size distribution is one of the main parameter to study. Figures 4.1-4.3 show the particle size distribution with its cumulative passing of spent FCC catalyst, fly ash and Portland cement.

4.1.1.1 Particle Size Analyses of Spent FCC Catalyst

Particle size distribution of ground spent FCC catalyst, unground spent FCC catalyst, and Portland cement are shown graphically in Figure 4.1. The particle size distribution of ground spent FCC catalyst has range from 0.1 to 50.2 microns while that of unground spent FCC catalyst has range from 14.1 to 224.4 microns that of Portland cement has range from 0.2 to 224.4 microns. This is in agreement with Hsu, Chang, Hwange, and Liao (1996) which reported that 85% of spent FCC catalyst particle size was less than 100 microns.

It can be seen that particle size of ground spent FCC catalyst is much finer than unground spent FCC catalyst because it was subjected to grinding several times and pass though a standard sieve No.325 (45 micrometer openings). This is confirmed by results in Table 4.1. The median particle size ($d_{50\%}$) of ground spent FCC catalyst is about 15.7 microns while those of unground spent FCC catalyst and Portland cement are 70.6 microns and 20.3 microns, respectively. Moreover, the 90-percentile size ($d_{90\%}$) of ground spent FCC catalyst is 49.6 microns compared with 70.6 microns of unground spent FCC catalyst and 55.3 microns of Portland cement.

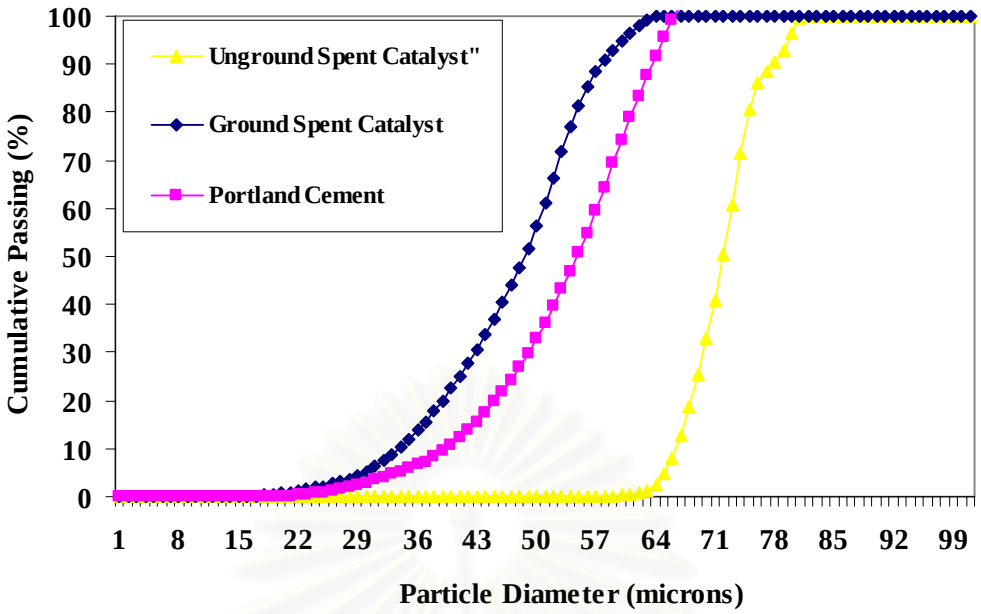

Figure 4.1 Particle Size Distribution Curves of Unground Spent FCC Catalyst, Ground Spent FCC Catalyst, and Portland Cement

By comparing at different percentiles, $d_{10\%}$, $d_{50\%}$ and $d_{90\%}$, it can be seen that ground spent FCC catalyst is the finest particle size of all sample while unground spent FCC catalyst is the coarsest of all samples.

Table 4.1 Particle Size Analysis Result of Spent FCC Catalyst, Fly Ash, and Portland Cement

Sample	Conditions	Particle Size (microns)		
		$d_{10\%}$	$d_{50\%}$	$d_{90\%}$
Spent FCC Catalyst	Unground	37.4	70.6	139.5
	Ground	5.5	15.7	49.6
Fly Ash	Raw	7.2	23.4	118.4
	Sifted	5.6	19.8	65.8
Portland Cement	-	8.9	20.3	55.3

4.1.1.2 Particle Size Analyses of Fly Ash

Figure 4.2 shows the particle size distribution of raw fly ash, sifted fly ash, and Portland cement. The cumulative passing curve of raw fly ash at the smaller particle diameter is much lower than sifted fly ash and Portland cement which means that raw fly ash is much coarser than sifted fly ash and Portland cement. The median particle size ($d_{50\%}$) of raw fly ash is 23.4 microns compared with 19.8 microns for sifted fly ash. This is evident to noted that the particle size between raw fly ash and sifted fly ash are insignificantly different. Even though, sifted fly ash was sifted through a standard sieve No.200 (75 micrometer opening). It can be seen that sifting process has no effect on the particle size of raw fly ash. This is because an average particle size of raw fly ash is 10 μm diameters (Malhotra, 1987).

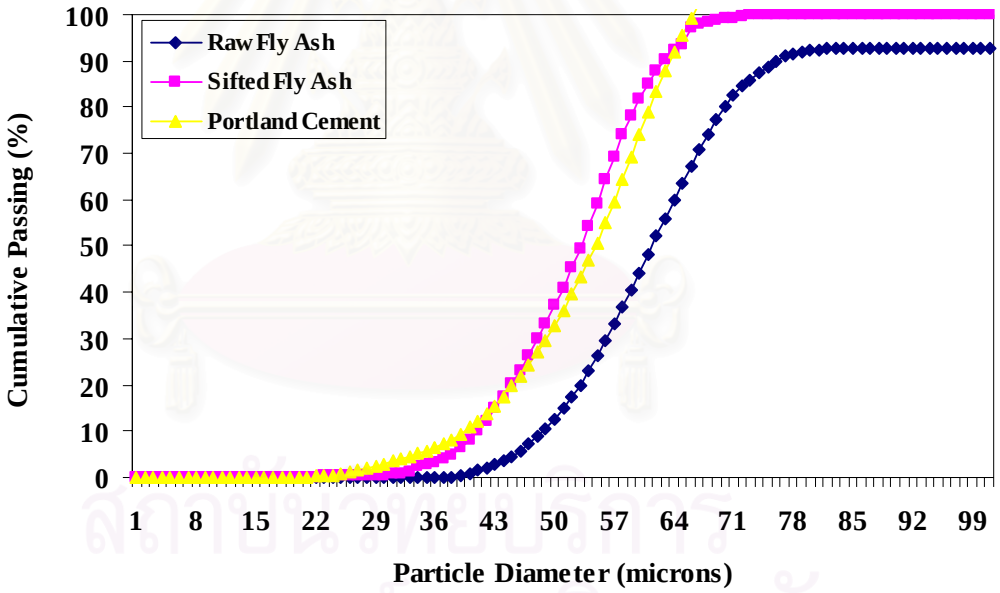

Figure 4.2 Particle Size Distribution Curves of Raw Fly Ash, Sifted Fly Ash, and Portland Cement

4.1.1.3 Particle Size Analyses of Ground Spent FCC Catalyst, Sifted Fly Ash, and Portland Cement

Figure 4.3 shows the particle size distribution of ground FCC spent catalyst, sifted fly ash and Portland cement. It can be seen that these particles are not significantly different. This is agreed with particle size analyses result at different percentiles listed in Table 4.1.

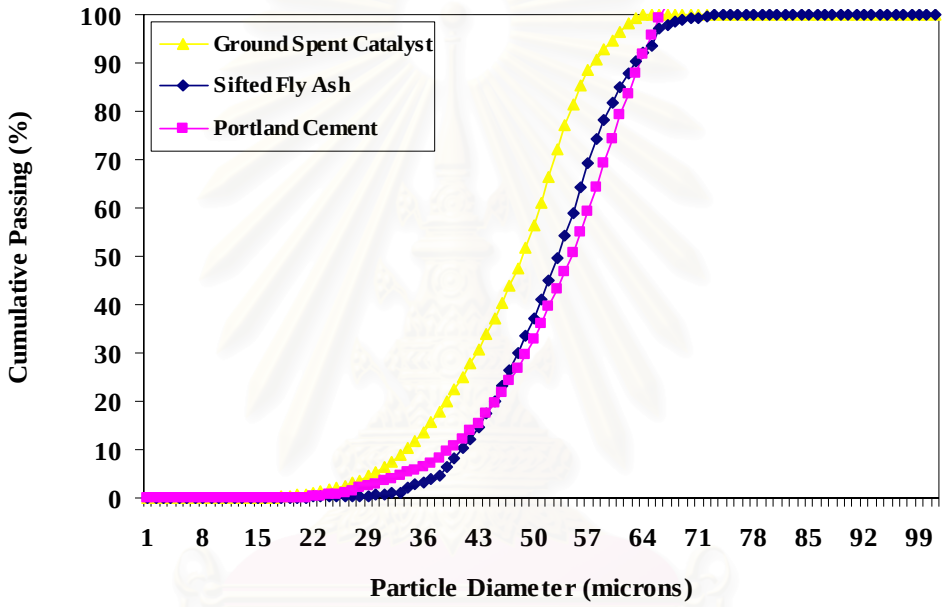

Figure 4.3 Comparison of Particle Size Distribution Curves of Ground FCC Spent Catalyst, Sifted Fly Ash, and Portland Cement

In addition, it is also seen that there is not much different between the size distributions of ground spent FCC catalyst and sifted fly ash. These fine particles size of ground spent FCC catalyst, sifted fly ash, and Portland cement will be consistent with water demand and workability in concrete. When workability kept constant, water demand decreases with the increase of fineness (Lea, 1971). Another advantage of having finer particle size of ground spent FCC catalyst and sifted fly ash is that it may improve the properties of spent FCC catalyst pastes and fly ash paste by enhancing the hydration process. It increases the rate of hydration because there will be small amount of unreacted cement developed inside the grain. Moreover, it can modify the pore size of cement paste also (Mattle and Moranville, 1999).

4.1.2 Specific Surface Area

Specific surface area, was used to determine fineness of spent FCC catalyst and fly ash, was defined as a number of units of surface area contained in a unit of mass. Table 4.2 shows the specific surface area of raw materials in this experiment.

Table 4.2 Specific Surface Area Results of Spent FCC Catalyst, Fly Ash, and Portland Cement

Sample	Conditions	Specific Surface Area (cm^2/g)
Spent FCC Catalyst	**Unground**	3040
	Ground	4328
Fly Ash	**Raw**	2310
	Sifted	3273
Portland Cement	**-**	3580

From Table 4.2, the specific surface areas of ground spent FCC catalyst is about 4328 cm^2/g compared with 3273 cm^2/g of sifted fly ash and 3580 cm^2/g of Portland cement. Spent FCC catalyst has the highest value of specific surface area because its structure like porous structure that may be caused allow air to flow rapidly through them, thereby leading to high specific surface area of the spent FCC catalyst.

Fly ash is fine-grained materials that consist of spherical particle, rounded particle, and spheres particle with irregular shape or having surface precipitation. As a result, the specific surface area of raw fly ash is high. It is about 2310 cm^2/g for raw fly ash and 3273 cm^2/g for sifted fly ash. The resistance of fly ash to air flow through fly ash particle is lower, thus resulting in misleading high air flow.

The factors governing the specific surface areas value are morphology, particle shapes, carbon content and its environment. Because, in the Blain-air permeability equipment, air can rapidly flow through porous and irregular. As a result, spent FCC catalyst has higher specific surface areas value. The higher specific surface areas value, the better workability and higher reactivity than smaller specific area (Lea, 1971).

4.1.3 Bulk Specific Gravity and Absorption

Bulk specific gravity, absorption and other physical properties of spent FCC catalyst and fly ash are tabulated in Table 4.3

Table 4.3 Physical Properties of Spent FCC Catalyst and Fly Ash

Physical Properties	Spent FCC Catalyst	Fly Ash
Appearance	Very slightly gray spheroid	Brown dust
Odor	Odorless	Odorless
Bulk Specific Gravity	2.45	2.32
Absorption, %	34	ND
pH	4.30	12.26

Note: ND means Not Detected

The spent FCC catalyst is micro-spheroidal particles and slightly gray in color. The spent FCC catalyst does not have organic smell although it came from oil refinery process. This may be because the spent FCC catalyst has come to contact with crude oil at very short contact time in feedstock and the original conventional feedstock. The spent FCC catalyst is insoluble and has high specific gravity. Bulk specific gravity of spent FCC catalyst is 2.45 that is higher than water. The specific gravity of spent FCC catalyst depends on the specific gravity of its minerals its fineness and its porosity. The absorption of spent FCC catalyst is very high, 34%. As a result it has higher water consumption than regular cement mortar.

Fly ash had brown color and the particle was the form of dust or powder. Another investigator suggested that the characteristics and properties of fly ash are dependent upon the location, waste feed composition, and operating conditions which they are sampled (Rachakornkij, 2000)

4.1.4 pH

As describe in Table 4.3, spent FCC catalyst is acidic and fly ash is base. pH of spent FCC catalyst is 4.30. This is because spent FCC catalyst containing sulfur which can interact with water to form sulfuric acid Moreover, acid such as HF, H_2SO_4, and H_3PO_4 is being used as a catalysts for alkylation in polymerization process of crude oil.

However, it can be seen in Table 4.3 that the pH of 12.26 of fly ash from Mae Moh coal power plan is the highest. This may be because this plant used lignite as raw material to produce electric power and contains high amounts of lime in the fly ash particle.

Moreover, pH of fly ash can be used as an indicator to evaluate the effectiveness of stabilized materials particularly in cement-base stabilization. Most trace elements such as heavy metals can be stabilized as insoluble metal hydroxides in high pH pore water in fly ash concrete.

4.1.5 Loss on Ignition (LOI)

It is confirmed that carbon is the most important component of ignition loss. Therefore, carbon content is often assumed to be approximately equal to the loss on ignition (LOI). The LOI value of fly ash indicated that the amount of unburned carbon or charred particles in the fly ash. It is related to the presence of carbonates, combined water in residual clay minerals, and combustion of free carbon. The result shows that LOI value of fly ash is quite low because Class F fly ash contain smaller amount of unburned carbon (<1%). This unburned coal chemically contributes strength to cement paste since it is also composed of silica and alumina oxides to form pozzolanic product (Wesche, 1991).

The carbon content in spent FCC catalyst and fly ash are decisive in determining the water requirement for mortar and concrete applications. The amount of water necessary to obtain a paste with normal consistency is greater when the

carbon content is high. In general, the lower the carbon percentage, the better of the cement pastes.

Table 4.4 shows the value of LOI of spent FCC catalyst is about 1.85% for ground spent FCC catalyst and 2.03% for unground spent FCC catalyst which is higher than the LOI of fly ash both raw fly ash (0.28%) and sifted fly ash (0.22%). From this result, it can be explained that spent FCC catalyst contains high amount of carbon that came from crude oil (about 84%) and the fluidized catalytic cracking process of refinery process.

4.1.6 Bulk Chemical Compositions

Table 4.4 Chemical Compositions of Spent FCC Catalyst, Fly Ash, and Portland Cement

Chemical Compositions	Spent FCC Catalyst		Fly Ash		Portland Cement (Type I)
	Unground	Ground	Raw	Sifted	
Al_2O_3	41.5	42.03	28.21	28.41	5.42
CaO	0.01	0.01	14.70	14.02	63.82
Fe_2O_3	0.43	0.52	4.50	4.65	2.97
K_2O	0.15	0.08	0.58	0.64	0.54
La_2O_3	0.50	0.46	-	-	-
MgO	0.13	0.20	0.54	1.09	1.57
Na_2O	0.54	0.67	0.62	0.64	0.26
NiO	0.27	0.18	-	-	-
P_2O_5	1.37	1.04	0.32	0.23	-
SiO_2	51.05	51.35	40.43	41.16	20.34
SO_3	0.26	0.14	5.78	5.11	2.55
TiO_2	0.87	0.83	2.46	2.23	-
V_2O_5	0.89	0.64	-	-	-
LOI[a]	2.03	1.85	0.28	0.22	-
Total	100.00	100.00	98.42	98.40	97.47

Note: LOI[a] means Loss on ignition

Table 4.4 shows the chemical compositions of ground spent FCC catalyst, sifted fly ash in comparison with unground spent FCC catalyst and raw fly ash. All of the elemental compositions analyzed by the XRF. The result will be used to study the possibility to using this waste as cementitious material. All elemental compositions of these materials were reported in oxide form.

For beginning, it should be noted that there is no significant difference between chemical compositions of ground and raw spent FCC catalyst or sifted and raw fly ash. Thus, the processing does not have influence on the chemical compositions of these wastes. This is agreement with other investigators Malhotra (1987) and Rachakornkij (2000) also reported that no apparent influence on the particle size changed because fractionation did not drastically alter particle size distribution. However, their chemical forms and behaviors in cement pastes may not be similar.

It is revealed from this table that spent catalyst from fluid catalytic cracking (FCC) units are mainly made up of SiO_2 and Al_2O_3. As can be seen, these two components account for over 90% of the total weight. In addition, the main elements were found via XRF to be Si, Al and O with small amount of Fe, Mg, K, Ni, V and S. Normally, the crude oil contains metal less than 1% and the principal metal contaminants in crude oil are Ni, V and alkali metal. Chen et al. (2003) also reported that 80% of spent FCC catalyst was SiO_2 and Al_2O_3 together with some impurities of minute quantities.

Fly ash used in this experiment is by product of pulverized coal in thermal power plants. Therefore, the chemical compositions of fly ash depends on the characteristics and the composition of the coal burned in power stations. The chemical composition analysis of fly ash by means of XRF shows that SiO_2, Al_2O_3, Fe_2O_3 and CaO are the major constituents of fly ash. Other oxides, K_2O, MgO, Na_2O, P_2O_5, TiO_2 and SO_3 are the minor constituents. As shows in Table 4.5, the summation of three ingredients of SiO_2, Al_2O_3 and Fe_2O_3 equals to 73.14% for raw fly ash and 74.22% for sifted fly ash. Hence, both types of fly ash were classified to be Class F or low calcium fly ash. The presence of Fe_2O_3 in the fly ash was quite high and about 4.50% for raw fly ash and 4.65% for sifted fly ash.

Table 4.5 Some Properties of Fly Ash Compare with the ASTM C618 Requirements for Class C and Class F Pozzolan

Properties	Class C	Class F	Raw Fly Ash	Sifted Fly Ash
$SiO_2+Al_2O_3+Fe_2O_3$ (% Min.)	50.0	70.0	73.14	74.22
SO_3 (% Max.)	5.0	5.0	5.78	5.11
CaO (% Max.)	>10.0	≤10.0	14.70	14.02
LOI (% Max.)	6.0	6.0	0.28	0.22
Available alkalines as Na_2O (% Max.)	1.5	1.5	0.96	1.06

Note: Available alkalines as Na_2O (%) = Na_2O (%) + 0.658 K_2O (%)

4.1.7 Morphology of Raw Materials

4.1.7.1 Morphology of Unground Spent FCC Catalyst

The Microstructure of spent FCC catalyst was studied by scanning electron microscope (SEM). Figures 4.4 (a) and (b) show the scanning electron micrographs of unground spent FCC catalyst at the 350x and 1500x magnification.

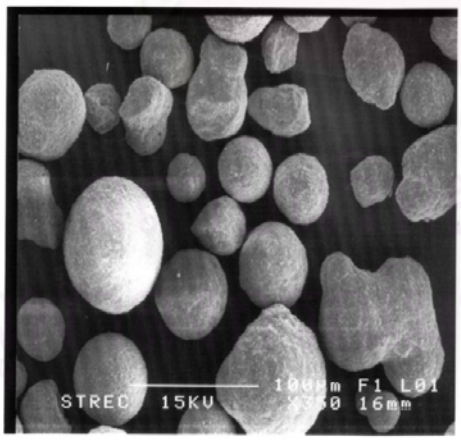

(a) 350x **(b) 1500x**

Figure 4.4 Micrographs of Unground Spent FCC Catalyst under SEM-EDS, (a) 350x and (b) 1500x

The particles size of spent FCC catalyst is depend on the source. Figure 4.4(a) shows a typical spherical of unground spent FCC catalyst particle. However, particle with an irregular shape can also be used in the cracking process. High magnified image is shown in Figure 4.4 (b). It can be seen that unground spent FCC catalyst is coarse, porous, and spherical, hence it leads to highly porous surface structure and it possess high water absorption (34%). Liu (1995) reported that spent FCC catalyst is made up of many tiny particles sintered or agglomerated together. This implies that granulation involves in the formation of spent FCC catalyst. The catalyst particles consist of a porous refractory material and smaller metal dispersed throughout the particle (Stuff works, 1998).

4.1.7.2 Morphology and Element Mapping Analysis of Ground Spent FCC Catalyst

Figures 4.5 (a) and (b) show the image of ground spent FCC catalyst, which was subjected to grinding several time and was sieved though a standard sieve No.325 (45 micrometer openings) at the 300x and 1500x magnification.

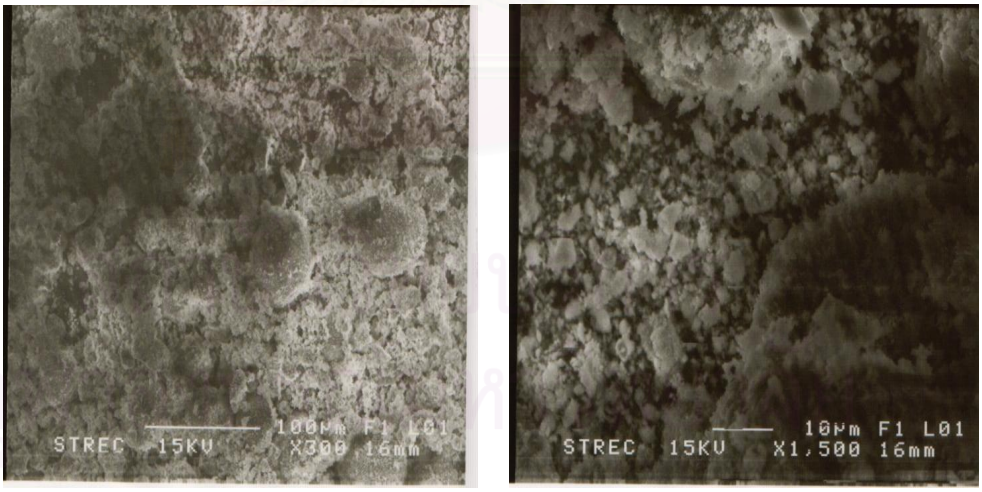

(a) 300x **(b) 1500x**

Figure 4.5 Micrographs of Ground Spent FCC Catalyst under SEM-EDS, (a) 300x and (b) 1500x

Observation at lower magnification (300X) is shown in Figure 4.5(a). It reveals that particle of ground spent FCC catalyst can be separated into three categories, irregular sharp, spherical particle and some angular particle. This may be because the irregular shape that mostly contains spherical particle is crushed during the grinding process. As a result, the particle has irregular shape. However, the spherical particles and angular shape that are very fine still exist because the media of disc mill is too big to grind the fine particle.

The microstructure of ground spent FCC catalyst with the X-ray dot mapping of the ground spent FCC catalyst is shown in Figure 4.6, respectively. Their element mapping reveals only the information regarding distribution of their components such as Al, Ca, Cu, Fe, Ni, Si, V, and Zn within 10 μm below the surface and averaged into the bulk material. The area that has the element is shown as white dot while the area that does not have the element is shown in dark.

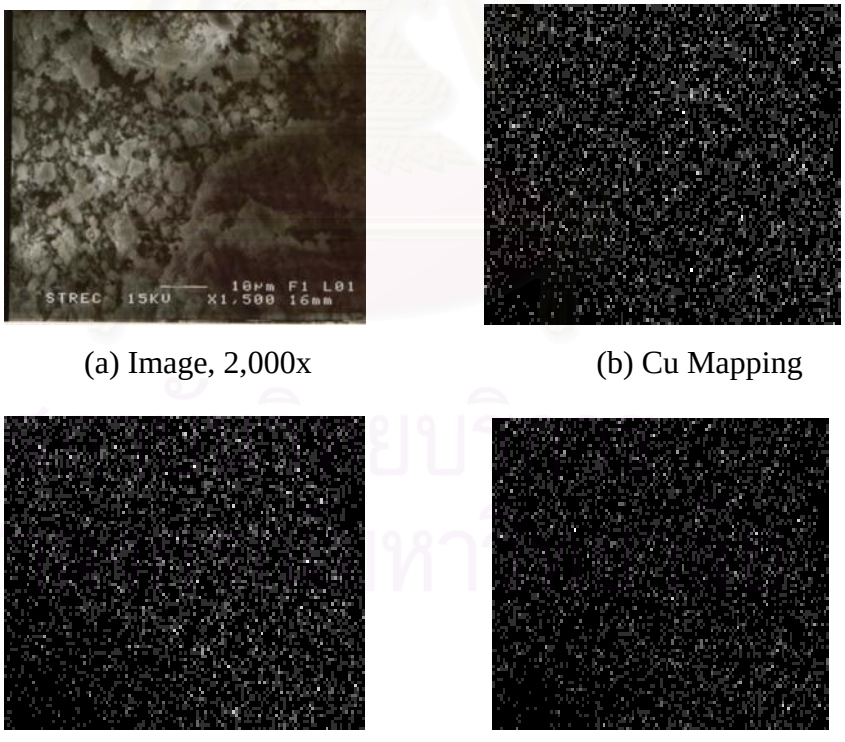

(a) Image, 2,000x (b) Cu Mapping

(c) Fe Mapping (d) Ni Mapping

Figure 4.6 Element Mapping of Ground Spent FCC Catalyst

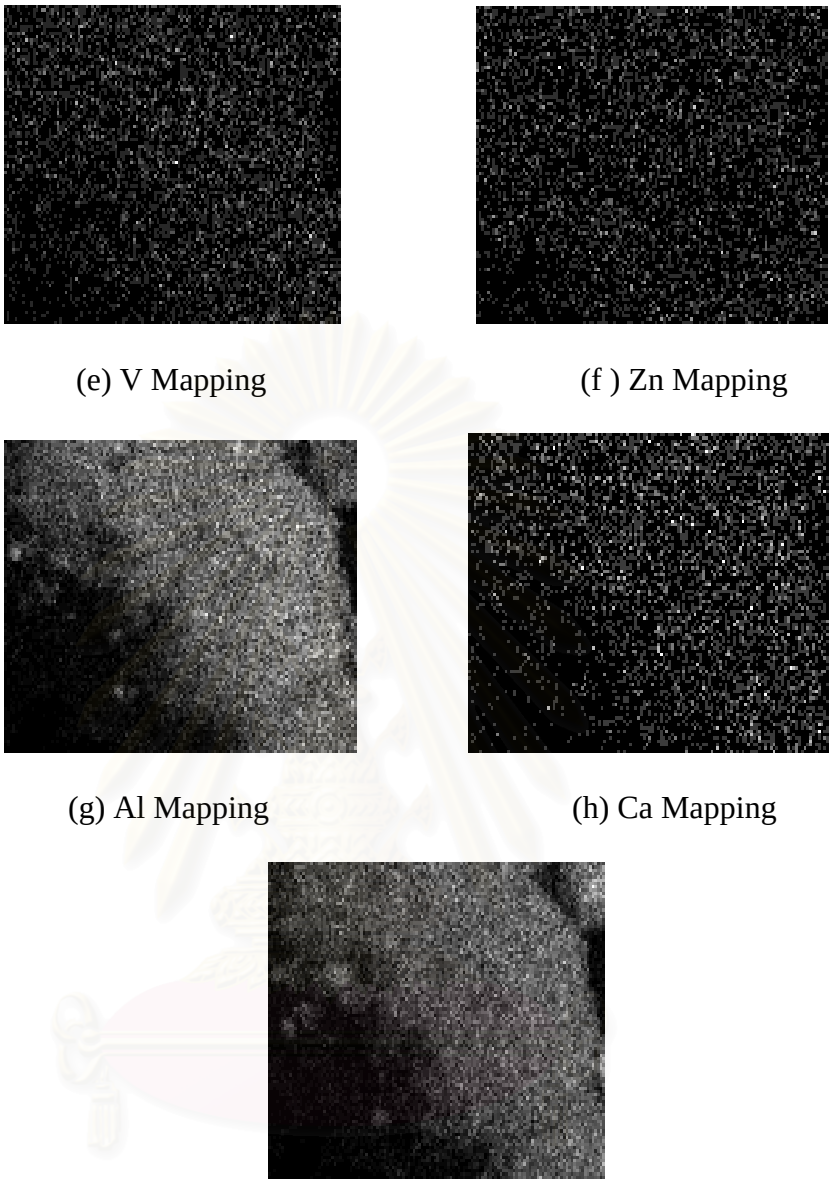

(e) V Mapping (f) Zn Mapping

(g) Al Mapping (h) Ca Mapping

(i) Si Mapping

Figure 4.6 X-ray Dot Mapping of Ground Spent FCC Catalyst (Continued)

According to the element mapping that focusing on the spheres particle, white sports representing high concentration of Al and Si were found on this spherical particle of ground spent FCC catalyst particle. Other area has low concentration of Al and Si. Other element, including Ca, Cu, Fe, Ni, V, and Zn appear to scatter around the area. Even through, there is low concentration of these metals on the surface of ground spent FCC catalyst particle, it shows in the results in Section 4.1.9 that there is high concentration of these elements inside the structure. This can be because metal

cluster and coke had deposited on the surface and then absorb inside the spent FCC catalyst structure suddenly because it had the porous structure. This leads to the concentration of heavy metals inside structure of ground spent FCC catalyst higher than on the surface.

Table 4.6 Semi-quantitative Surface Compositions of Spent FCC Catalyst Shown in Figure 4.4(b) and Figure 4.5(b) by EDS(%)

Element	Weight (%)	
	Figure 4.4 (b)	**Figure 4.5 (b)**
Oxygen (O)	61.19	63.28
Carbon (C)	18.34	18.29
Aluminum (Al)	8.80	9.20
Silica (Si)	10.65	8.68
Magnesium (Mg)	0.25	0.10
Phosphorus (P)	0.18	0.18
Iron (Fe)	0.12	0.09
Titanium (Ti)	0.07	0.05
Vanadium (V)	0.16	0.09
Nickel (Ni)	0.24	0.04
Total	100.00	100.00

Surface element analysis result in Table 4.6 shows the comparison level of the major elements are C, Al, Si, Mg, P, Fe, Ti, V, and Ni of unground spent FCC catalyst (Figure 4.4(b)) and ground spent FCC catalyst (Figure 4.5(b)). It is show high level of Al and Si on the surface of particles which confirm to the X-ray dot mapping result. Other elements present in the major amount are Mg, P, Fe, Ti, V, and Ni. However, phase of these elements could not be detected by XRD (except Fe). This may be because these elements are amorphous form (glassy phases).

4.1.7.3 Morphology of Raw Fly Ash

Figures 4.7(a) and (b) show the scanning electron micrograph of raw fly ash at the 1500x and 5000x magnification. This figure shows that fly ash has significantly percentage of spheres particle with irregular surface or surface precipitation. Some fly ash also contains irregular or angular particles that usually smaller than spherical particle. With high magnification in Figure 4.7(b), the morphology shows that the surface of fly ash has unknown particles depositing on it.

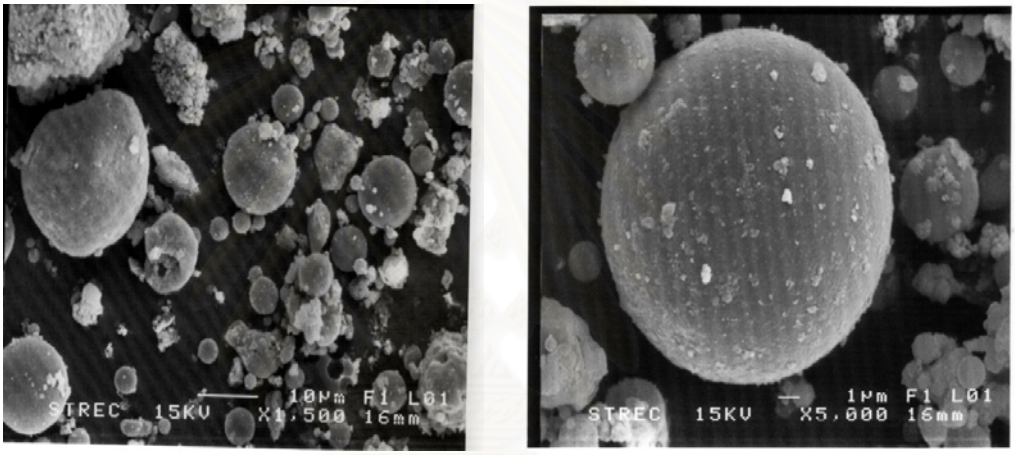

(a) 1500x **(b) 5000x**

Figure 4.7 Micrographs of Raw Fly Ash under SEM-EDS, (a) 1500x and (b) 5000x

The particles size of fly ash depends on the nature, the granulometry of the coal and the combustion conditions in the power plant. If the combustion temperature is not above the melting point, the mineral ash fails to melt in this process. The clusters that found in the fly ash should be the clusters formed. On the other hand, at high combustion temperature, the mineral matter in the coal melts and forms larger spheres which contains a number of smaller spheres. At a combustion temperature of roughly 1500 °C, the majority of the particles are round shape and hollow, with smooth or rough surface (Wesche, 1987). Round particles appear to be ideal with respect to workability of cement since they act as a lubricant between the angular and irregular particle of cement and aggregates. Therefore, the more round particles in fly ash, the better the fly ash cement performance will be.

4.1.7.4 Morphology and Element Mapping Analysis of Sifted Fly Ash

The micrograph of sifted fly ash is shown in Figures 4.8(a) and (b).

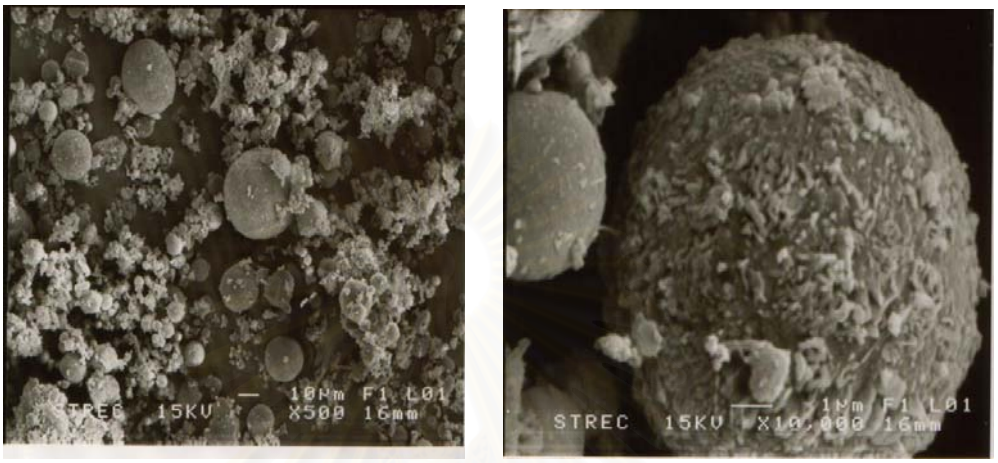

(a) 500x **(b) 10000x**

Figure 4.8 Micrographs of Sifted Fly Ash under SEM-EDS, (a) 350x and (b) 1500x

Figure 4.8(a) shows the morphology of sifted fly ash at the low magnification. There are several features that can be distinguished from picture, which included spheres, irregular, angular particle. High magnification is shown in Figure 4.8(b), the micrograph shows the surface of fly ash is covered with unknown particle.

Element mapping of sifted fly ash in Figure 4.9 reveals that the surface of the particle is enriched with Al, Fe, and Si. The element maps confirm the XRF result in Section 4.1.6 that show Al, Si, and Fe are the major constitutions of the surface of the particles. This may be because these fly ash are classified to be Class F of fly ash. From the mapping of Al and Si, they can be found on the particle itself more than on the boundary. The area that these two elements present corresponds with the area that spherical fly ash present. In some area of the center particle, Si is found without Al and other elements. The mineral phases in that area could be quartz or SiO_2. The area that has quartz phase does not participate in pozzolanic reaction. If more number of quartz is found on the surface of fly ash, the lower pozzolanic activity it has. In addition, it can be seen that Ca is found in high concentration in the fly ash particle

like Al and Si. However, Cu, Ni, V, and Zn are found to scatting all over the surface but in low concentration. From this evidences, it can relate to the result of heavy metal of sifted fly ash in Section 4.1.9 that showed that high concentration of metals absorbed inside the structure of sifted fly ash.

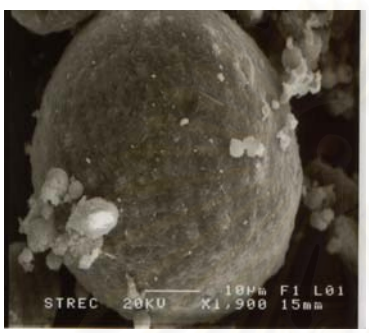

(a) Image, 1900x

(b) Cu Mapping

(c) Fe Mapping

(d) Ni Mapping

(e) V Mapping

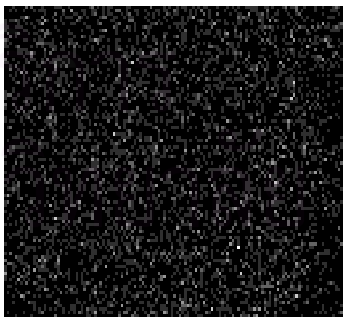

(f) Zn Mapping

Figure 4.9 Element Mapping of Sifted Fly Ash

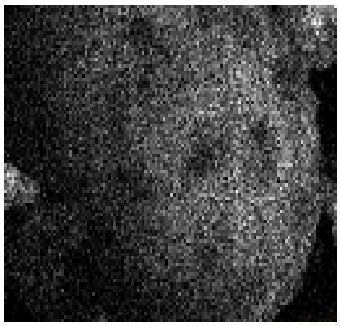

(g) Al Mapping

(h) Ca Mapping

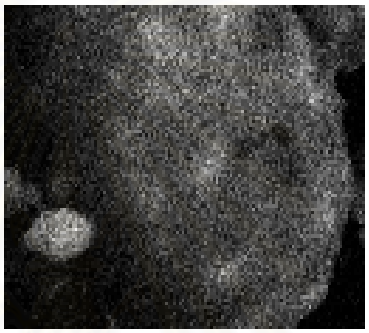

(i) Si Mapping

Figure 4.9 Element Mapping of Sifted Fly Ash (Continued)

Surface element analysis result in Table 4.7 shows the comparison level of the major elements are C, Al, Si, Ca, K, Fe, S, and Ti of raw fly ash (Figure 4.6(b)) and sifted fly ash (Figure 4.7(b)). The major element, Si and Al, is influenced by sifting process more than raw fly ash. This may be beneficial to applications since Al and Si are important elements in hardening of cement.

Table 4.7 Semi-quantitative Surface Compositions of Fly Ash Shown in Figure 4.7(b) and Figure 4.8(b) by EDS(%)

Element	Weight (%)	
	Figure 4.6 (b)	**Figure 4.7 (b)**
Oxygen (O)	56.84	54.03
Carbon (C)	28.88	29.52
Aluminum (Al)	5.31	7.14
Silica (Si)	5.78	6.10
Calcium (Ca)	1.75	1.82
Potassium (K)	0.08	0.03
Iron (Fe)	0.54	0.67
Sulfur (S)	0.50	0.46
Titanium (Ti)	0.32	0.23
Total	100.00	100.00

4.1.7.5 Morphology of Portland Cement

The microstructures of Portland cement are shown in Figures 4.10 (a) and (b).

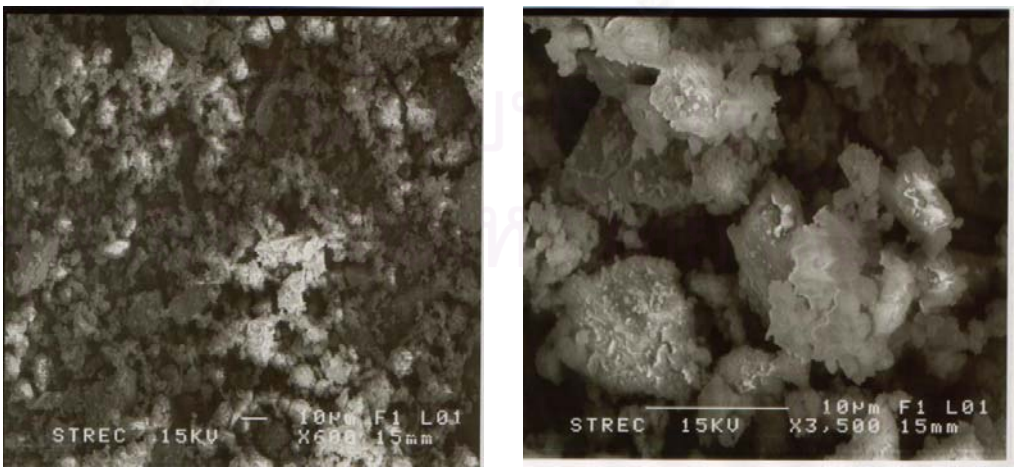

(a) 600x **(b) 3500x**

Figure 4.10 Micrographs of Portland Cement under SEM, (a) 600x and (b) 3500x

Figure 4.10(a) shows the micrograph of Portland cement at low magnification. It can be seen that the fine particle is attached together to form small cluster that is shown in Figure 4.10(b). However, spheres particle and irregular shape can be seen. As might be expected, the surface of Portland cement particles had many fine particles depositing on it. Most of these particle are larger than 10 microns.

4.1.8 Mineralogical Compositions

The information obtains from bulk chemical compositions only give a rough idea as how much each element in sample in oxide form. Therefore, X-ray powder diffraction (XRD) spectrometer is necessary. XRD is powerful tool for determining the crystalline phases and the element constitutes that will occur in cement paste.

The crystalline phase of ground spent FCC catalyst is shown in Figure 4.11. The main components of the crystalline phases that can be detected in ground spent FCC catalyst are $Al•Fe•SiO_2•O$ (chlorite), $Al_2•(SiO_4)•O$ (andalusite), $3Al_2O_3•2SiO_4$ (mullite), $Ca•Mg•SiO_4$ (munticellite), and SiO_2 (quartz). In addition, $Ca_5•Cl•(PO_4)_3$ (chlorapatole), $Fe_2O_3•H_2O$ (lepidogrocite), $(Fe,Mg)_5•Al•(Si_3•Al)O_{10}(OH)_8$ (chamosite), $(Na_2•(Fe,Mg)_3•Fe_2•SiO_{22}•(OH)_2$ (riebeckite), $Na_{7.15}•(Al_{7.2}•Si_{8.8}•O_{32})$ (napheline), $Na•(Al•SiO_8)$ (albite), and $Mg_2•Al_3•(Si_3•Al)•O_{10}•(O)_8$ (chlorite). The result verifies the bulk chemical compositions analysis in the Section 4.1.6 that shows high concentration of Al, Fe, Na, P and Si.

However, there is no crystalline phase which contains P or Ti although they present in high concentration in bulk chemical compositions. This is because the pattern is complexity and has numerous overlapping peaks. As a result it is very difficult to identify.

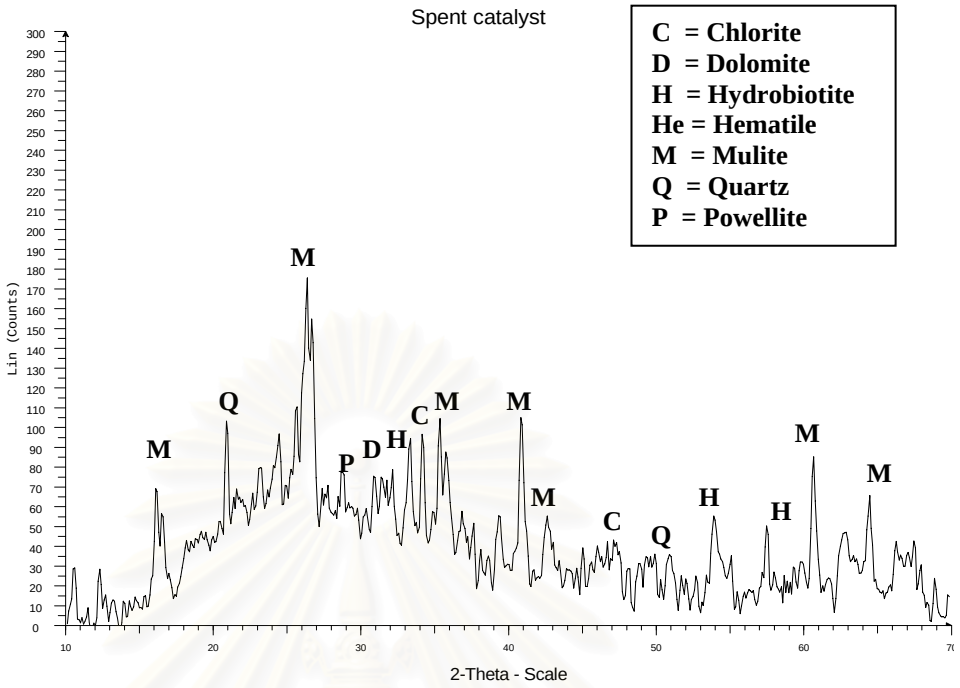

Figure 4.11 X-ray Diffraction Spectrum of Spent FCC Catalyst

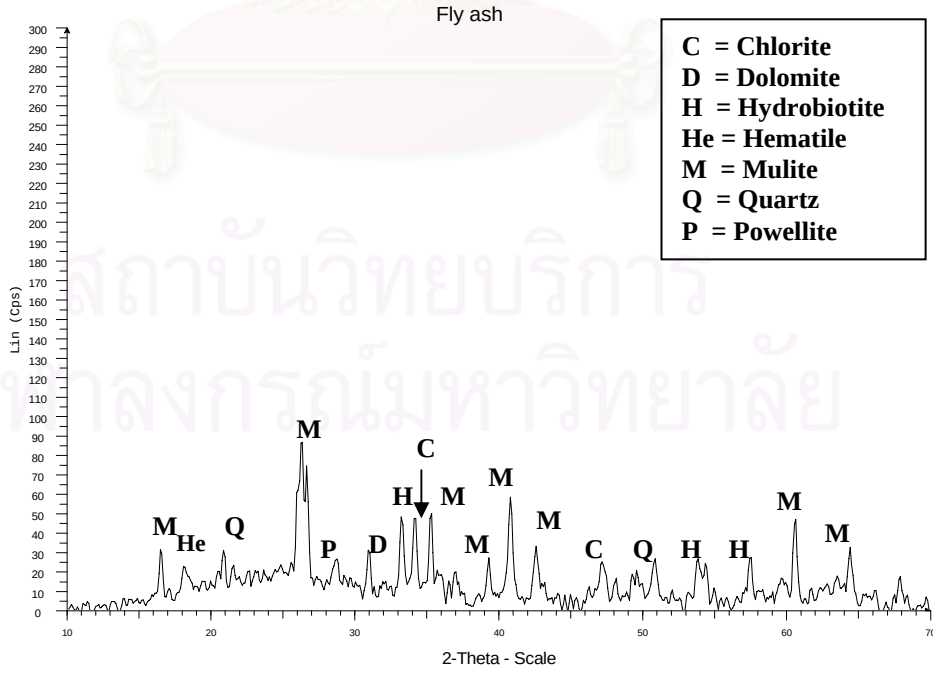

Figure 4.12 X-ray Diffraction Spectrum of Mae Moh Coal Fly Ash

Figure 4.12 shows the XRD diffractogram of sifted fly ash from Mae Moh coal power plant. The crystalline phases of sifted fly ash that can be detected consist of $Al_{4.52}•Si_{1.48}•O_{9.74}$ (mullite), $Ca•Mg•(CO_3)_2$ (dolomite), $Ca•Mo•O_4$ (powellite), $Cu•Fe_2•S_3$ (cubanite), $CuSO4•5H_2O$ (chaleanthite), Fe_2O_3 (hematile), K•Mg•Fe•Al•SiO•(OH) (hydrobiotile), K•Mg•Fe•Al•SiO•(OH) (hyrobiotile), $Mg•SiO_2•(OH)$ (chlorite), $Na_{0.68}•Fe_{0.68}•Si_{0.32}•O_2$ (sodium iron silicon oxide), and SiO_2 (quartz). This is consistent with the bulk chemical compositions result in Section 4.1.6 that shows high concentration of Al, Ca, Fe, K, Mg, Na, and Si.

From sifted fly ash diffractogram, it is important to note that mulite, hematile, hydrobiotile, chlorite, sodium iron silicon oxide, and quartz present as the major crystalline phases. This is similarly to the previous researcher who investigated the mineralogical composition of coal fly ash (Mattle and Moranville, 1999). They reported that the amount of noncrystalline or glass phases in coal fly ash, each fly ash may contained one of more of the four major crystalline phases: quartz, mullite, magnetile, and hematile. In addition, the amount of the most important crystalline phases in ASTM Class F fly ash is shown in Table 4.8 (Wesche, 1987).

Table 4.8 The Amount of Crystalline Phases in ASTM Class F Fly Ash

Crystalline Phases	**Quantity (%)**
Quartz	2.2-8.5
Mullite	6.5-9.0
Magnetile	0.8-6.5
Hematile	1.1-2.7
Free calcium oxide	$\geq$ 3.5
Other minerals	$\leq$ 2.5

Figure 4.13 shows X-ray diffraction pattern of Portland cement used in this study. The main crystalline phases that can be identified is tricalcium silicate, C_3S. This phases is the major component of Portland cement. It reacts with water to produce calcium silicate hydrate (C-S-H) during hydration reaction of cement. Dicalcium silicate, C_2S, is also found in Portland cement pattern. It reacts in

slow late at early age but its rate increases at later curing time. Portland cement contains small amounts of oxides that influences the reactivity. Another significant phase is gypsum, $CaSO_4 \cdot H_2O$. this phase react with C_3S to form ettringite.

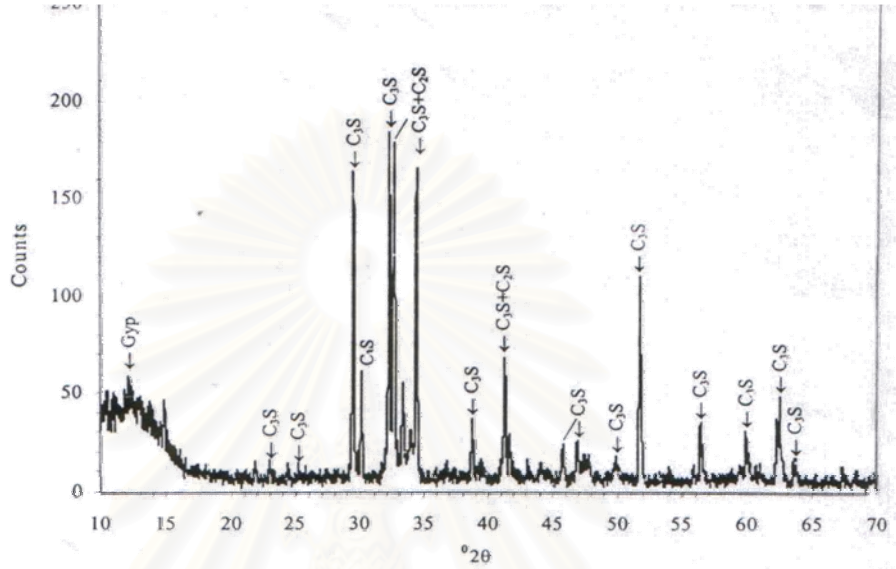

Figure 4.13 X-ray Diffraction Spectrum of Portland Cement

4.1.9 Heavy Metals Concentration

Heavy metals analyzed in this study are consisted of five elements; copper (Cu), iron (Fe), nickel (Ni), vanadium (V), and zinc (Zn). These metals are the major trace elements in the spent FCC catalyst and fly ash. Even through, there is no leaching standard of these metals and they do not serious problem to human, this study attempts to study the mechanism that captures heavy metals in spent FCC catalyst and fly ash cement paste.

The result in Table 4.9 shows that there are high concentration of Cu, Fe, Ni, V, and Zn. For ground spent FCC catalyst, it has higher Ni, V, and Fe concentration than Cu and Zn. These metals have been occurred during the decomposition of hydrocarbons to hydrogen and coke (Hopkins, 1983). Under the FCC operating conditions, almost 100% of these metals decompose and deposit on the FCC catalyst surface.

Table 4.9 Heavy Metals in Spent FCC Catalyst, Fly Ash, and Portland Cement

Materials	Concentration (ppm)				
	Cu	**Fe**	**Ni**	**V**	**Zn**
Ground Spent FCC Catalyst	0.067	15.576	3.147	13.910	0.288
Sifted Fly Ash	0.246	191.290	0.193	0.467	0.749
Portland Cement	0.015	5.035	0.034	<0.007	0.143

By comparing the level of contamination of FCC catalyst with other type of spent catalyst, it shows that spent FCC catalyst is significantly lower because of a much shorter contact time, as well as a less contaminated feedstock. Sifted fly ash has the highest concentration of Fe in this study. This result is similar to XRF results in Section 4.1.6. Since the coal source of fly ash used in this study has high Fe_2O_3 as a result it has high Fe content. However, other metal in fly ash has only trace metal. There is low concentration of heavy metals in Portland cement than spent FCC catalyst and sifted fly ash particle. Therefore, it can be predicted that heavy metals in cement mixture pastes mostly came from waste replacement.

4.1.10 Leaching Behaviors

The heavy metal analyzed in the leachate consist of Cu, Fe, Ni, V, and Zn. As shown in Section 4.1.9 that these metals are the major trace elements in the spent FCC catalyst and fly ash. Leachant from spent FCC catalyst and fly ash are analyzed by Inductive Coupled Plasma Spectroscopy (ICP). To measure the amount of Cu, Fe, Ni, V, and Zn leached from waste and the cement pastes, the Toxicity Characteristic Leaching Procedure (TCLP) and the Notification of Ministry of Industry No.6, 1997 (LP-No.6) extraction test were used in the study. The TCLP test is currently used to decide whether a waste is hazardous based on the EPA toxicity characteristic (TC) criteria. LP-No.6 is used as Thailand leachates extraction procedure. According to method 1311 of U.S. EPA SW-846, the test methods for evaluated solid waste, physical/chemical methods is used to determine whether the waste is necessary to analyze individual heavy metal.

Table 4.10 Leaching Concentration of Cu, Fe, Ni, V, and Zn from Ground Spent FCC Catalyst and Sifted Fly Ash

Heavy metal	Leaching concentration (ppm)				Surface Water Standards (ppm)	Drinking Water Standards (ppm)
	TCLP test		LP-No.6 test			
	Ground Spent FCC Catalyst	Sifted Fly Ash	Ground Spent FCC Catalyst	Sifted Fly Ash		
Cu	<0.007	<0.007	<0.007	<0.007	≤ 0.1	≤ 1.0
Fe	0.090	<0.006	<0.006	<0.006	≤ 0.5	≤ 0.5
Ni	0.213	<0.007	0.198	<0.007	≤ 0.1	-
V	9.660	0.013	10.240	<0.007	-	-
Zn	0.301	0.074	0.289	0.050	≤ 1.0	≤ 5.0

Note: "-" mean Not Report

Source: Ministry of Natural Resource and Environment, Pollution Control Department, Thailand

Table 4.11 shows the leaching concentration of heavy metal in spent FCC catalyst, fly ash and the allowance of these metal in the surface water standard and drinking water standards according to Ministry of Natural Resource and Environment, Pollution Control Department. The result shows that metal concentrations from both types of extraction test are not significantly different. It is found that leaching concentration of Cu, Fe, Ni, and Zn from ground spent FCC catalyst and sifted fly ash were within acceptable value. In spite of, the leaching concentration of vanadium (V) in ground spent FCC catalyst is high, there is no standard of this metal. Even though, most of heavy metals concentration in spent FCC catalyst and fly ash met the regulatory limit but we cannot guarantee that in the future will not be changed. Therefore, solidification and stabilization (S/S) treatment processes were chosen to treat and encapsulate heavy metal in these waste.

Spent FCC catalyst and fly ash were mixed with cement, water, and sand to form cement pastes. After 28 and 90 days of curing period, leaching concentration of Cu, Fe, Ni, V, and Zn from cement pastes was measured by ICP.

4.2 Chemical and Physical Properties of the Solidification/Stabilization Materials

4.2.1 XRD Application for Investigate Hydration Reaction and Pozzolanic Activity of the Solidified/ Stabilized Materials

4.2.1.1 Hydration reaction of Portland cement

The hydration reaction of Portland cement occurs when the major compounds of cement reacts with water to produce reaction products are tricalcium silicate (C_3S), dicalcium silicate (C_2S), tricalcium aluminate (C_3A), and tetracalcium aluminoferrite (C_4AF). The hydration products of two calcium silicates are similar and differ in the amount of calcium hydroxide formed, as show below: (Malhotra, 1987).

$$2C_3S + 6\,H_2O \longrightarrow C_3S_2H_3 + 3\,Ca(OH)_2$$

$$2C_2S + 6\,H_2O \longrightarrow C_3S_2H_3 + 3\,Ca(OH)_2$$

Where: $C_3S_2H_3$ = C-S-H.

The reaction of C_3A with water is very fast and involves reactions with sulfate ion supplied by the dissolution of gypsum. Moreover C_4AF forms hydration products similar to those of C_3A, with iron substituting partially for alumina in the crystal structures of ettringite and monosulphoaluminate hydrate. The reactions can be represented by the following : (Malhotra, 1987)

$$C_3A + 3\,CaSO_4{\bullet}H_2O + 26\,H_2O \longrightarrow C_3A(CS)_3H_{32}$$

$$C_3A + CaSO_4{\bullet}H_2O + 10\,H_2O \longrightarrow C_3ACSH_{12}$$

Where: $CaSO_4{\bullet}H_2O$ = Gypsum

$C_3A(CS)_3H_{32}$ = ettringite

C_3ACSH_{12}= Monosulphoaluminate hydrate

It can be seen that these reactions involve sulfate ion from gypsum. With the presence of sufficient sulfate ion in solution, the ettringite can be formed but if it lacks of sulfate ion, monosulphoaluminate may take place. If sulfate is not available C_3A may form C_3AH_6 or C_4AH_{19}.

4.2.1.2 Pozzolanic Activity

Pozzolanic reaction is the reaction occur after the hydration reaction and the reactions cannot takes place independently because it used $Ca(OH)_2$ from hydration products as initial material. In addition, water soluble alkali, sulfate, lime, and organic from spent FCC catalyst and fly ash may also affect the hydration reaction and pozzolanic activity through the surface reactions, nucleation, and crystallization processes, especially in the early stages of cement hydration.

Spent FCC catalyst and fly ash exhibit pozzolanic activity because silicon oxide and aluminum oxide are the main compositions of spent FCC catalyst and fly ash. Pozzolanic activity is the reaction between the reactive silica and alumina of pozzolan and $Ca(OH)_2$ resulting precipitation of various calcium silicates, aluminates, and aluminosilicates. The reaction is shown below:

$$Ca(OH)_2 + SiO_2 + H_20 \longrightarrow xCaO{\bullet}ySiO_2{\bullet}zH_2O$$

$$Ca(OH)_2 + Al_2O_3 + H_20 \longrightarrow xCaO{\bullet}yAl_2O_3{\bullet}zH_2O$$

The product from these reactions is called the calcium silicate hydrate and x, y, z are the values that depend on the type of calcium silicate hydrate (C-S-H). Both C-S-H and calcium aluminate hydrate (C-A-H) can increase compressive strength in comcrete and also reduce the pore between the cement particles (Mindess et al. 1981). In addition, fly ash will improve the workability of mixes and will lower the total heat of hydration.

4.2.1.3 Influence of Hydration on Tricalcium Silicate

Hydration reaction of spent FCC catalyst and fly ash in cement pastes can be evaluated by the reduction of starting material and the increasing in the hydration products as the one of method to evaluated hydration process of spent FCC catalyst and fly ash in cement pastes. This study used C_3S or $3CaO•SiO_2$, to represent starting material because it is a main compound in cement paste that produces strength upon hydration. C_3S was determined at the strongest peak intensity at ranging from 29.44-29.68 2θ angles (PDF database from ICDD). Although C_2S can represent starting material also it has small relative intensity and interference. The amount of C_3S in the cement paste depended on the amount of cement in the paste. Figure 4.14 through 4.16 illustrate the relationship between the intensity value and the curing time of C_3S.

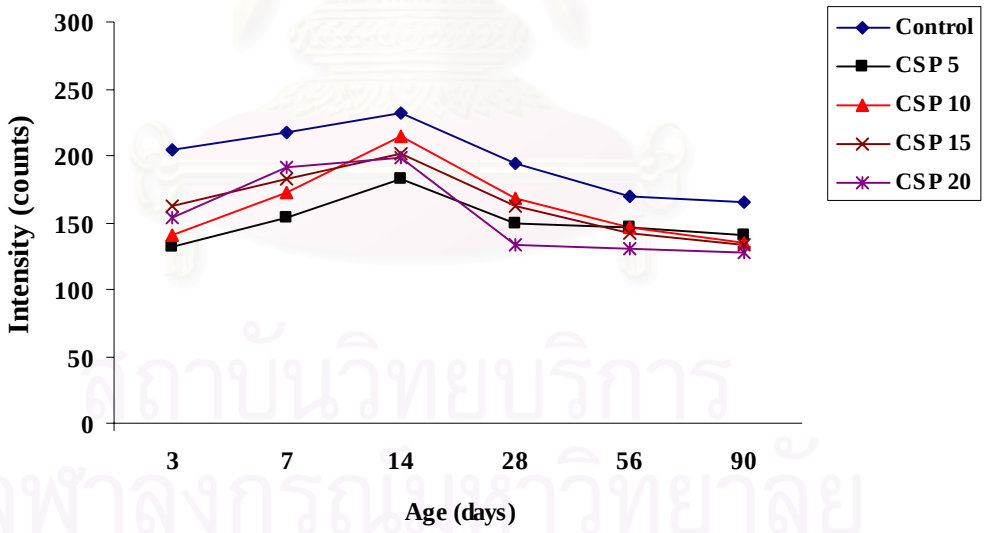

Figure 4.14 Intensity of C_3S of Cement Pastes with Different Percentage of Spent FCC Catalyst Replacements (CSP)

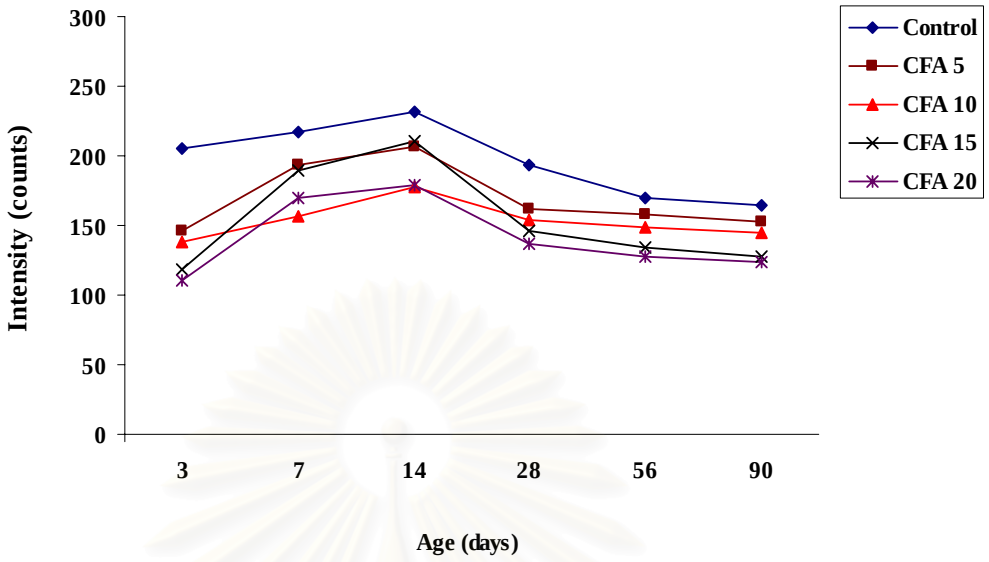

Figure 4.15 Intensity of C_3S of Cement Pastes with Different Percentage of Fly Ash Replacements (CFA)

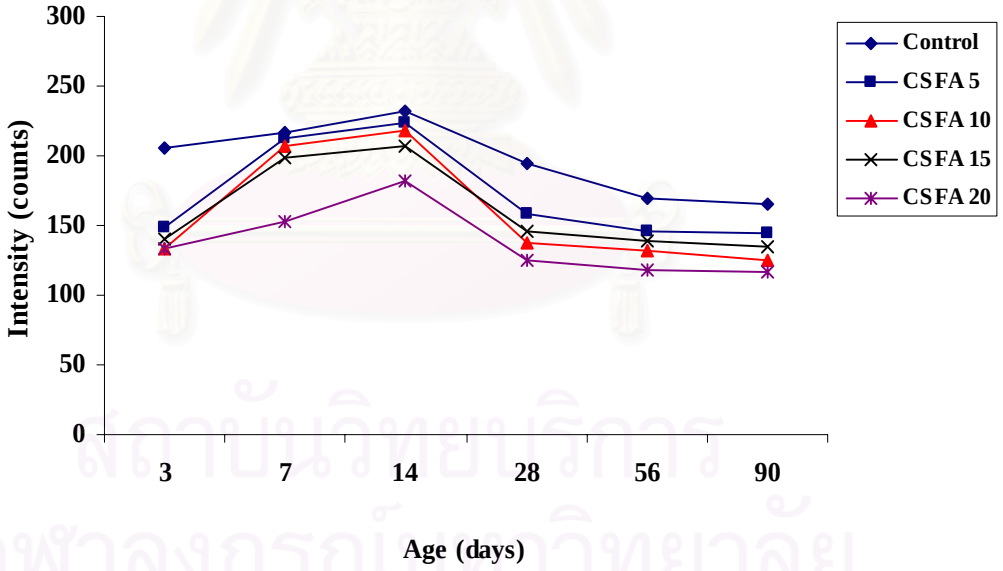

Figure 4.16 Intensity of C_3S of Cement Pastes with Different Percentage of Spent FCC Catalyst and Fly Ash Replacements (CSFA)

As seen from Figures 4.14–4.16, it is clear that C_3S was consumed at a very high at during first week of curing time. The consumption rate was more evident in the control pastes because the initial intensity of C_3S in control paste is higher than

C_3S in CSP pastes, CFA pastes and CSFA pastes. From the beginning to age 14 days, the intensity of C_3S begins to increase and then stared to decrease gradually.

The addition of spent FCC catalyst or fly ash can dilute the cement content. It can be seen that all of cement pastes show the highest of C_3S intensity at 14 days of curing time. This is because the hydration reaction is still not completed at this age and it still has high C_3S in the mixture. However, after 14 days of curing time, the consumption rate of C_3S in all pastes decreases. It seems that the C_3S reaction is close to complete. The C_3S intensity began to decrease at the same time with the formation of C-S-H and $Ca(OH)_2$ in hydration and pozzolan reaction.

The distinguished intensity of C_3S between CSP pastes may be from the nature of spent FCC catalyst and the percent replacement in cement pastes. As known that C_3S compound represent in cement. If higher percent replacement of spent FCC catalyst in cement pastes (CSP 15 and CSP 20) as a result lower amount of C_3S content in cement paste. This is confirmed by Figure 4.4, the intensity of C_3S in CSP 20 was lower than other CSP pastes. This may be because C_3S content in CSP 20 was smaller than other CSP pastes.

Figure 4.15 shows the intensity of C_3S in the CFA pastes. The intensity of C_3S decreases rapidly and the reaction rate of all CFA pastes slowed down after 28 days of curing time. This may be because the hydration reaction is almost completed at 28 days. The effect of percentage of fly ash on the C_3S consumption was clearly shown. Since C_3S compound is the major compound in cement, it will be lower if high percent replacement of fly ash in cement pastes is used. Therefore, CSP 5 has the C_3S content higher than other CSP pastes at all time. On the other hand, the reduction of C_3S in CFA 20 was lower than other CFA pastes.

The pattern of C_3S intensity in CSFA pastes as shown in Figure 4.16. It can be seen that the pattern of C_3S intensity in CSFA pastes was similar to CSP pastes and CFA paste. From the beginning to the end to curing, CSFA 5 shows the higher intensity of C_3S than another CSFA pastes. This is because CSFA 5 has higher amount of C_3S content. On the other hand, CSFA 5 has smaller amount of spent FCC catalyst and fly ash that was replaced in these paste.

Figures 4.14-4.16 showed that the intensity of C_3S in control is higher than other mixing pastes (CSP pastes, CFA pastes, and CSFA pastes) throughout the experiment. This is because the C_3S compound is major compound of Portland cement so it is no doubted that it should be higher in control.

4.2.1.4 Influence of Hydration on Calcium Hydroxide

According to diffraction patterns, the product of $Ca(OH)_2$ from hydration reaction showed the strongest peak intensity at 18.08 2θ angles (PDF database from ICDD). This 2theta is selected since it is free of overlapping peaks and interference from other crystalline phase in the same area. The presence of $Ca(OH)_2$ in the spent FCC catalyst and fly ash in cement pastes is showed in Figures 4.17-4.19

In the first week, the line representing intensity of $Ca(OH)_2$ increased until the maximum intensity was detected at 14 days. Then, the production of $Ca(OH)_2$ continues to decrease gradually. This is because $Ca(OH)_2$ became significant and was used in the pozzolanic action. This activity involve the production of C-S-H and C-A-H at the expense of $Ca(OH)_2$, SiO_2, and Al_2O_3.

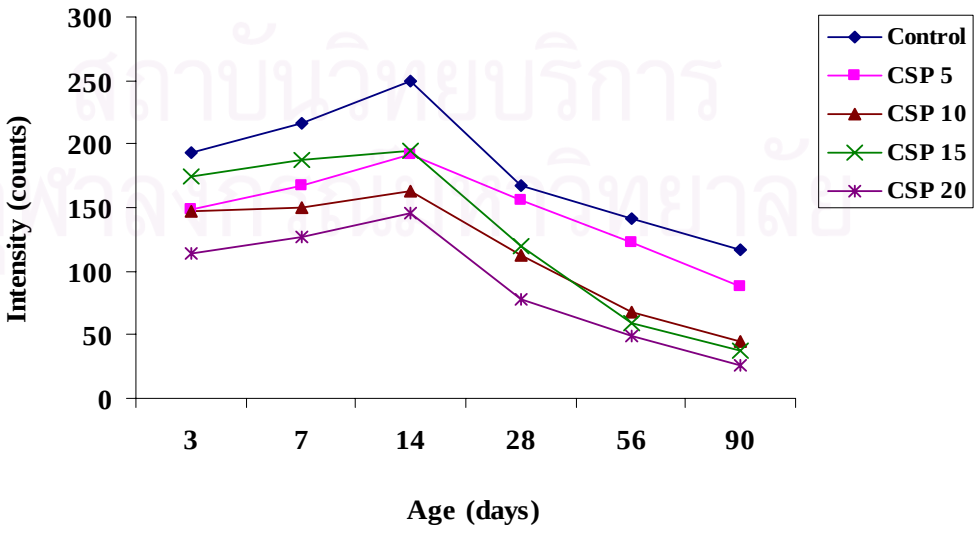

Figure 4.17 Intensity of $Ca(OH)_2$ of Cement Pastes with Different Percentage of Spent FCC Catalyst Replacements (CSP)

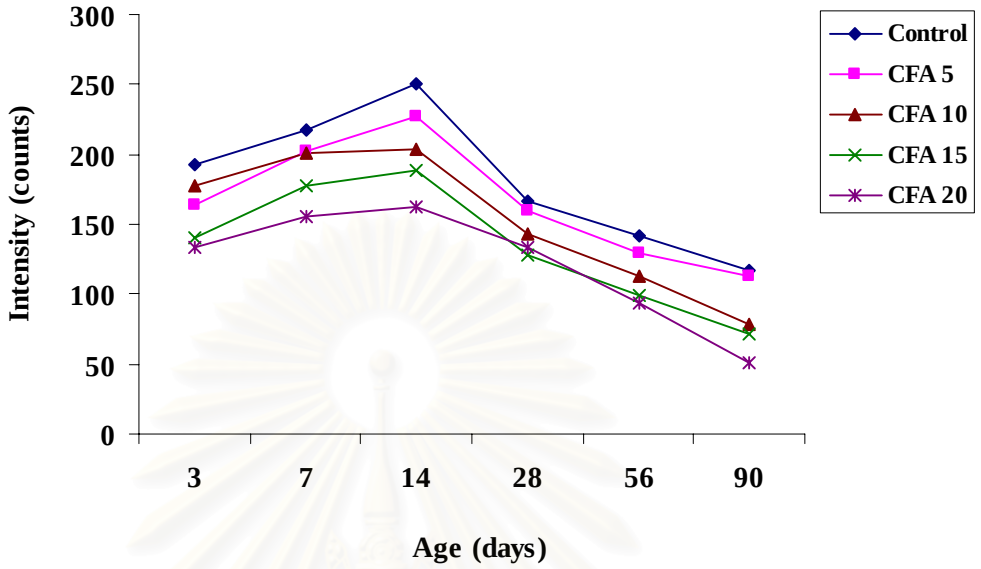

Figure 4.18 Intensity of $Ca(OH)_2$ of Cement Pastes with Different Percentage of Fly Ash Replacements (CFA)

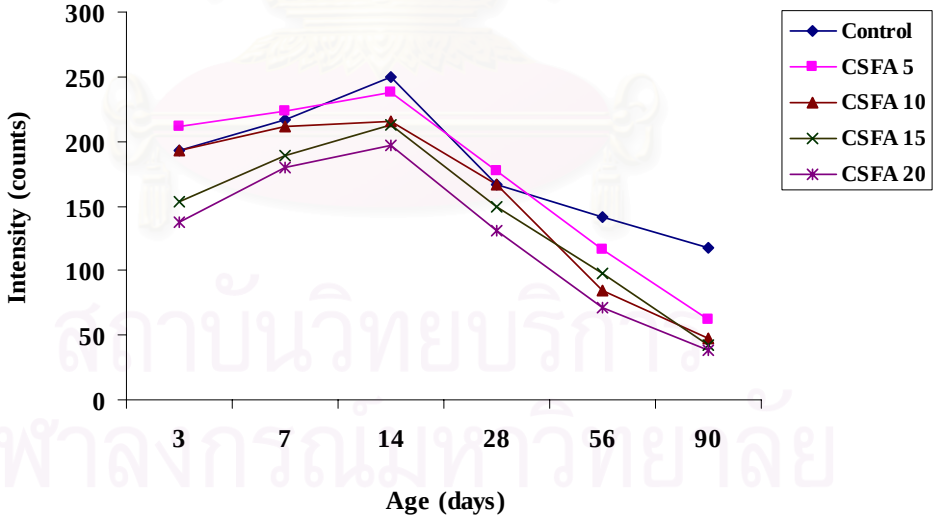

Figure 4.19 Intensity of $Ca(OH)_2$ of Cement Pastes with Different Percentage of Spent FCC Catalyst and Fly Ash Replacements (CSFA)

The intensity of $Ca(OH)_2$ in control was slightly higher than $Ca(OH)_2$ in CSP pastes, CFA pastes and CSFA pastes because these pastes may use $Ca(OH)_2$ in the

pozzolan action in which small amount of $Ca(OH)_2$ was used to react with their silica and alumina compounds in the pozzolanic reaction. Another reasons may be because $Ca(OH)_2$ was produced from the major compound of Portland cement. As a result, the amounts of $Ca(OH)_2$ in control higher than another cement mixture paste.

Upon comparing the effect of percentage variation on $Ca(OH)_2$ in the CSP pastes. It can be seen that the percentage of spent FCC catalyst was associated with the amount of $Ca(OH)_2$ used. As shown in Figure 4.17, after 14 days of curing time CSP 20 had lowest intensity of $Ca(OH)_2$. This may be because CSP 20 contained high amount of SiO_2 and Al_2O_3 than other CSP pastes, thus they react with $Ca(OH)_2$ from hydration reaction resulting in lower $Ca(OH)_2$ amount left in the paste. However, the intensity of $Ca(OH)_2$ in the control show highest intensity after 14 days of curing time. This may be because there was less SiO_2 and Al_2O_3 in the paste.

Figure 4.18 illustrates the production of $Ca(OH)_2$ in CFA pastes. The control and the CFA pastes showed increasing intensity of $Ca(OH)_2$ until 14 days of curing time. Then, the intensity began to decline. After 14 days there is higher amount of $Ca(OH)_2$ in control than CFA pastes. This could be because the pozzolanic reaction occurred in the CFA pastes similar to CSP pastes and it used the $Ca(OH)_2$ from hydration products as the initial material to produces C-S-H and C-A-H in the paste.

The intensity of $Ca(OH)_2$ in CSFA pastes was showed in Figure 4.19. The $Ca(OH)_2$ content in CSFA pastes started to increase until 14 days of curing time. After that, it decreases gradually. It can be seen that, the intensity of $Ca(OH)_2$ in CSFA 20 was lower than other CSFA pastes. This is because about 20% of cement pastes were replaced by spent FCC catalyst and fly ash. So there is less $Ca(OH)_2$ available for hydration reaction and pozzolan action.

As should be expected, Figures 4.17-4.19 show the $Ca(OH)_2$ intensity of each pastes raise within the 14 days of curing time and then the $Ca(OH)_2$ intensity starts to decreased. All of $Ca(OH)_2$ intensity results showed that the CSP pastes, CFA pastes,

and CSFA pastes inhibited the rate of cement reaction and prolonged the hydration. It is interested to note that metal ions in spent FCC catalyst and fly ash have no serious

effect to the degree of hydration although it possesses calcium silicate and less $Ca(OH)_2$. The absence of $Ca(OH)_2$ in the paste may be because it is used as initial material in pozzolan activity or hydroxyl ions from $Ca(OH)_2$ combined with heavy metal ion to form complexes.

From Figures 4.14 through 4.19, it shows that the intensity of C_3S and $Ca(OH)_2$ of the solidified wastes varied due to the type of waste binders and percent replacement variation. The C_3S and $Ca(OH)_2$ content of the CSP pastes, CFA pastes, and CSFA pastes decreased with the increase the amount of these waste in cement. In addition, the hydration reactions are subject to interferences in the degree of hydration and the pore size that will describe in Section 4.2.3. As previously described that the major compositions in spent FCC catalyst and fly ash are SiO_2 and Al_2O_3 which can reacts with $Ca(OH)_2$ to product C-S-H and C-A-H. If high amount of reactive SiO_2 and Al_2O_3 as a result the consumption of $Ca(OH)_2$ from hydration reaction will be high. As a result, percent replacement was concerned. However, both of products have beneficial in cement that is described in previously.

Due to the complexity of solidified/stabilizes material, X-ray diffraction (XRD) is found to be useful applications in characterizing the crystalline phases and structure information of the solidified waste. Figures 4.20-4.32 summarized the diffraction patterns of control and cement pastes with 5%, 10%, 15% and 20% in spent FCC catalyst and fly ash replacements. In each figure, cement pastes were test at the age 3, 7, 14, 28, 56, and 90 days. These diffractograms identified the major phases of control and the paste with spent FCC catalyst and fly ash replacements are $Ca(OH)_2$, C_2S, C_3S and C_3A. In addition, other phases found in spent FCC catalyst and fly ash pastes are the compound of calcium (Ca), silica (Si), alumina (Al) such as ettringite ($3CaO•Al_2O_3•3CaSO_4•32H_2O$), gypsum ($CaSO_4$), grossular ($Al_2Ca(SiO_4)_3$), sodium calcium silicate ($Na_2Ca_2Si_3O_8•OH$), oligoclase ($(Na,Ca),Al(Al,Si)Si_2O_8$), belite (Ca_2SiO_4), meionite ($Ca_4Al_6SiO_4•6CO_3$) and foshagite ($5CaSiO_3•3H_2O$). However, these phases have smaller counts (about 5-50 counts). Other phase occurred in cement pastes was heavy metals phases that will be presented in the next section.

The formation of C-S-H is very difficult to detect by XRD since it has a poor crystalline non-stoichiometric structure and the composition is variable over a wide range. However, this poor crystalline material is responsible for the strength of cement and it reduces the pore between the cement particles also.

The diffractograms of the major phases in each sample are shown Figures 4.20 through 4.32 together with their abbreviated symbol. This shorten notation is used to describe each crystalline phases: CC = $CaCO_3$, CH = $Ca(OH)_2$, C_2S = Ca_2SiO_4, C_3S = Ca_3SiO_5, C_4A = $Ca_4Al_6(SiO_4)6CO_3$, C_5A = $Ca_5Al_6O_4$, Fe 1 = Fe_2O_3, Fe 2 = Fe_2SiO_4, Fe 3 = $Ca_2Fe_2O_5$, Fe 4 = Fe_2O_4, Fe 5 = $FeCO_3$, Fe 6 = $22MgO•5Al_2O_3•Fe_2O_3•22SiO_4•40H_2O$

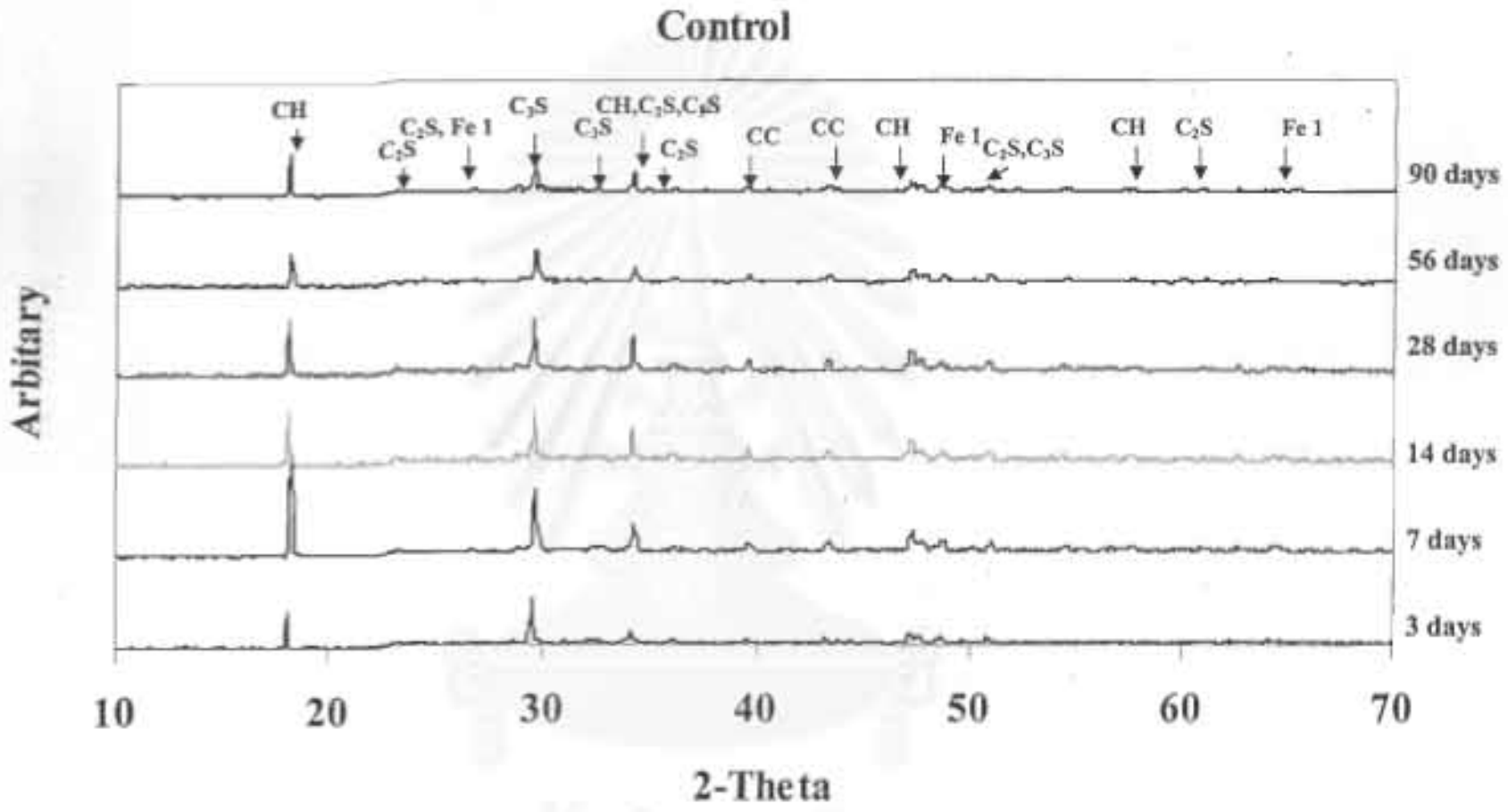

Figure 4.20 X-ray Diffraction Patterns of the Control at Different Ages

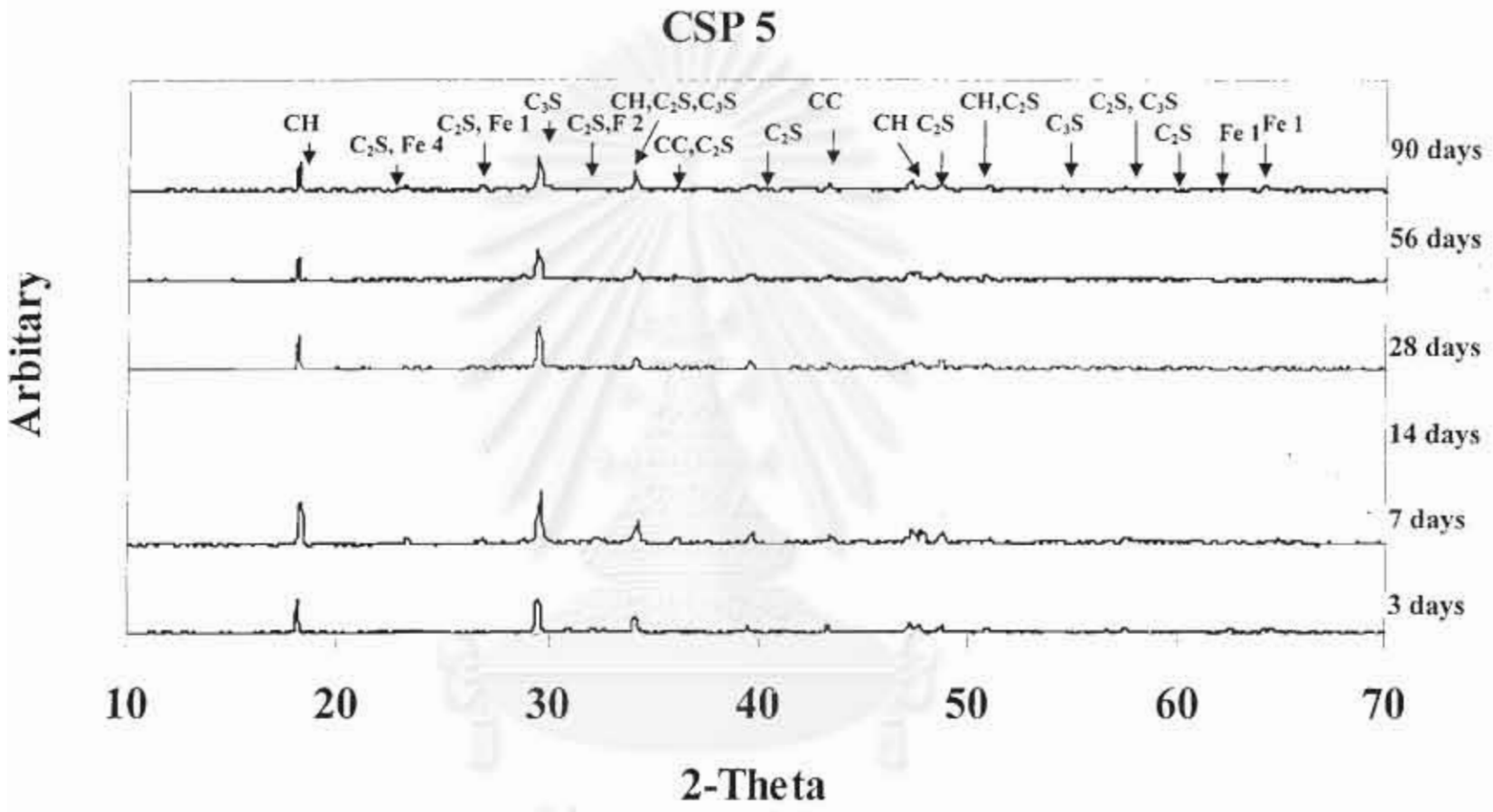

Figure 4.21 X-ray Diffraction Patterns of CSP 5 at Different Ages

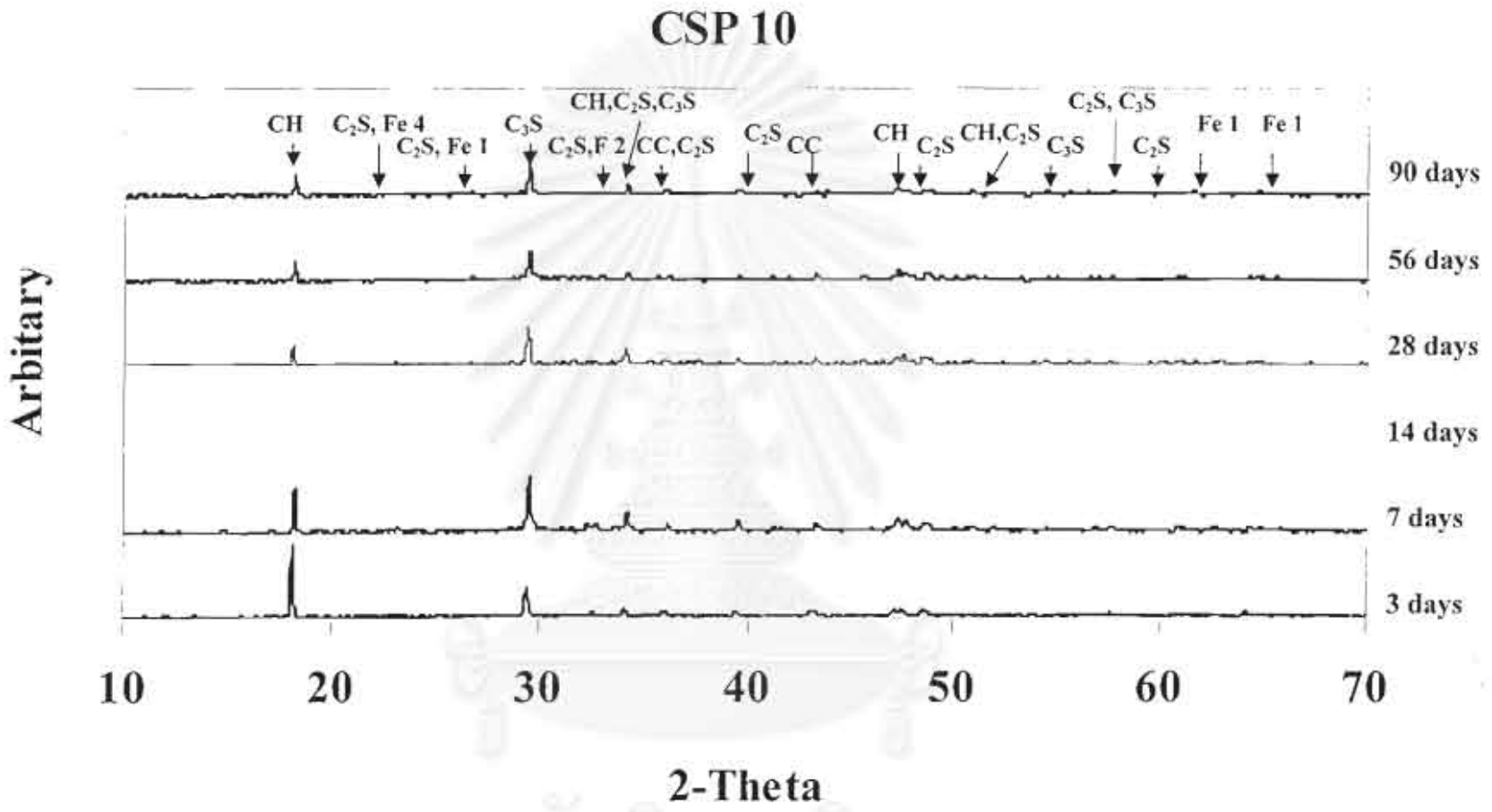

Figure 4.22 X-ray Diffraction Patterns of CSP 10 at Different Ages

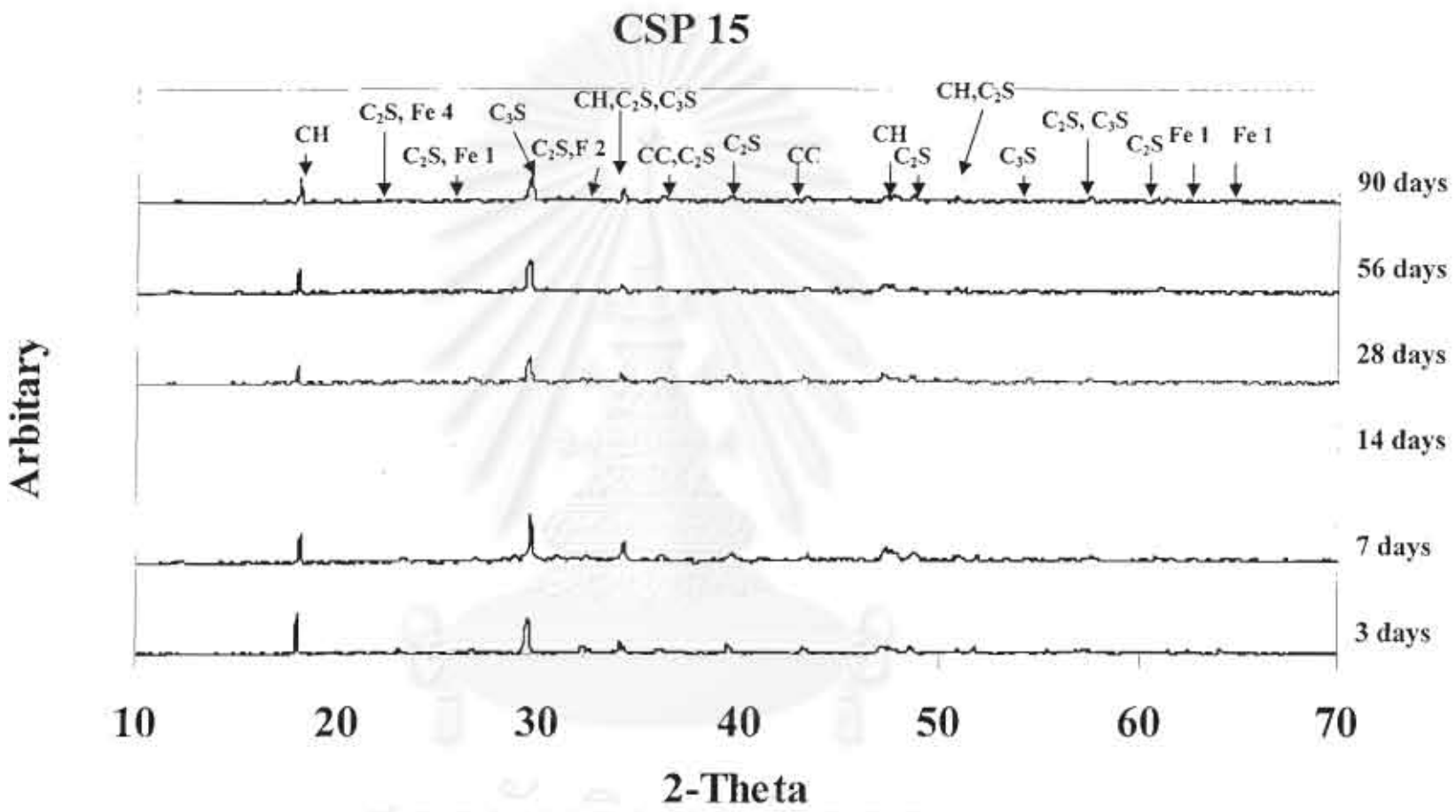

Figure 4.23 X-ray Diffraction Patterns of CSP 15 at Different Ages

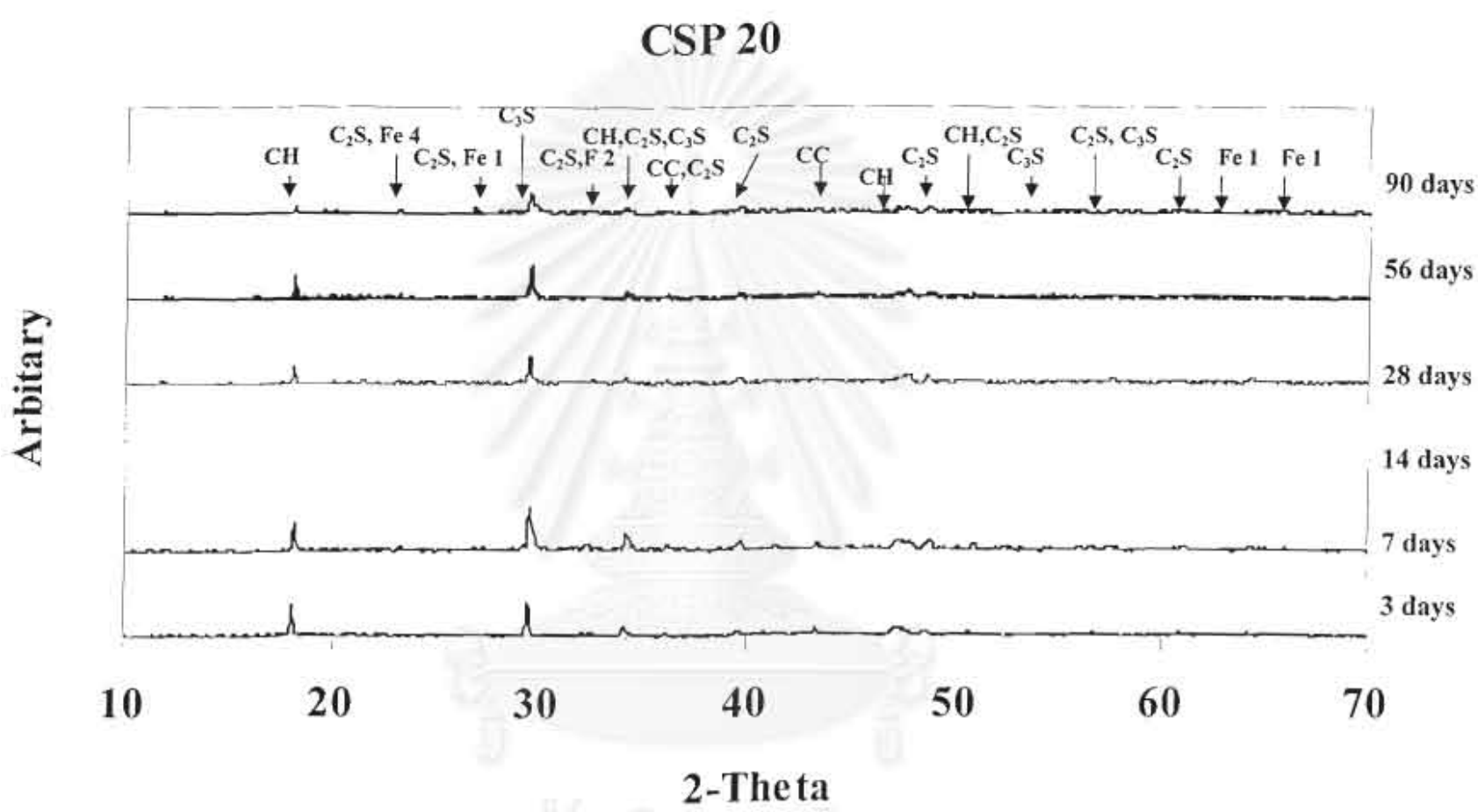

Figure 4.24 X-ray Diffraction Patterns of CSP 20 at Different Ages

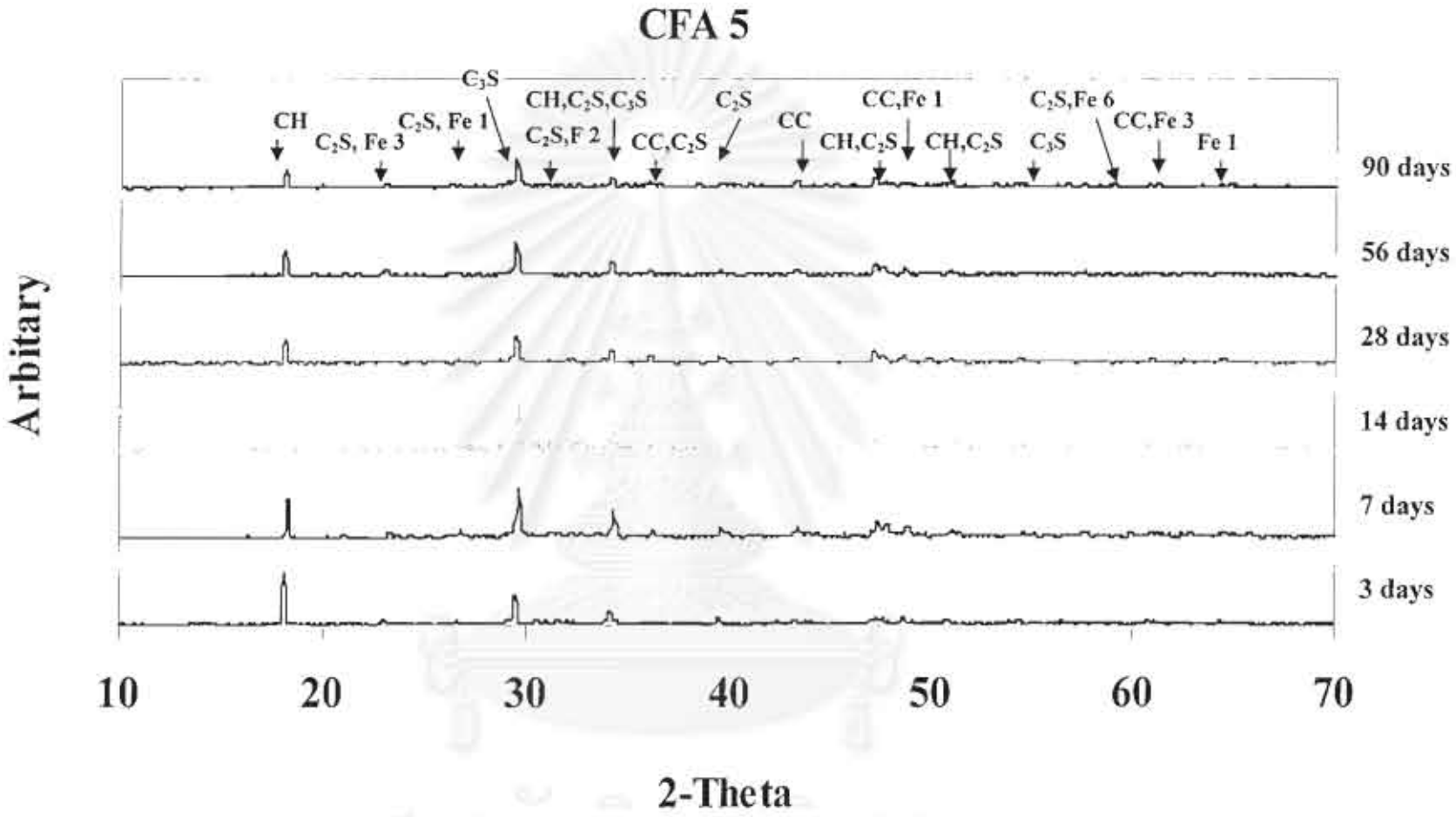

Figure 4.25 X-ray Diffraction Patterns of CFA 5 at Different Ages

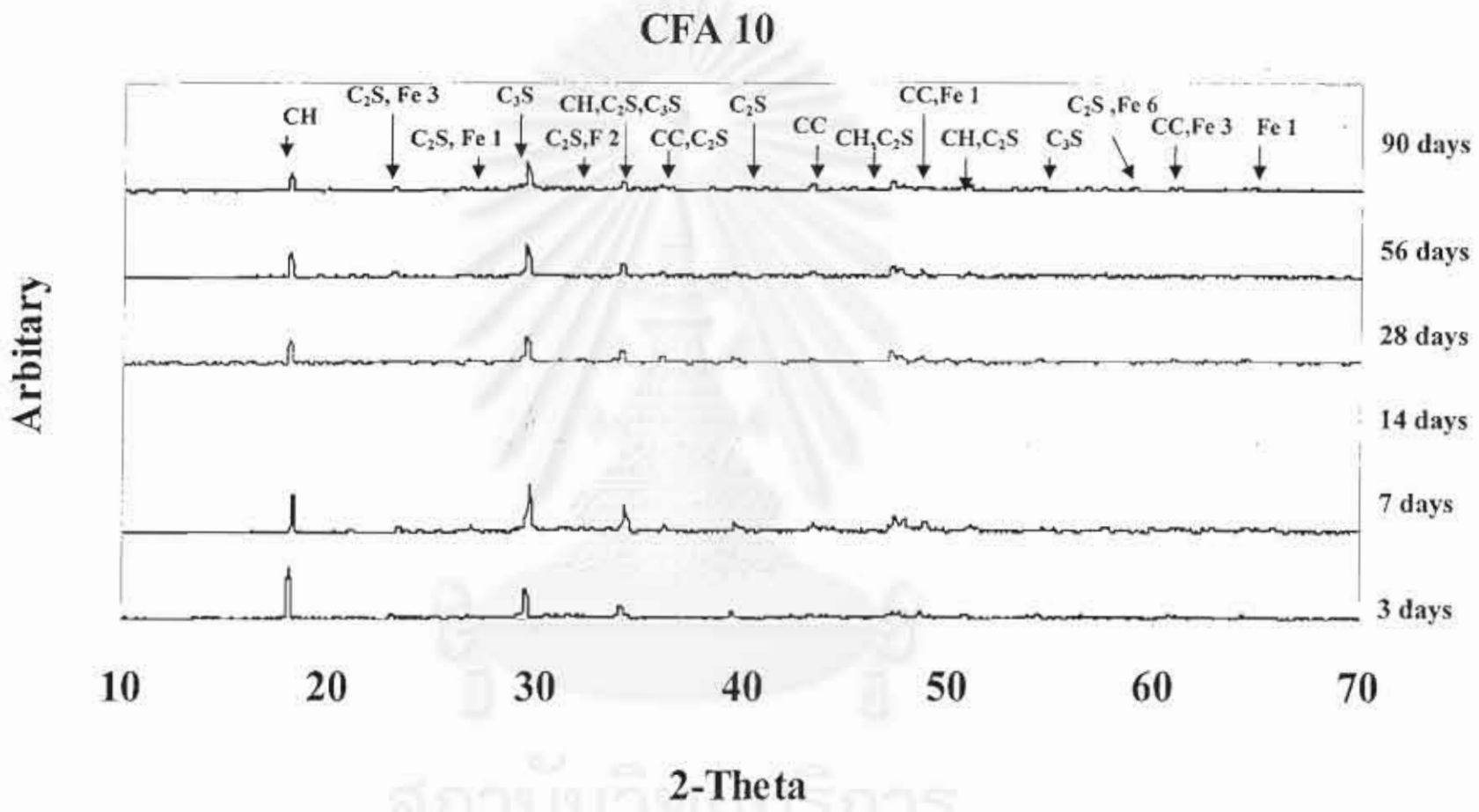

Figure 4.26 X-ray Diffraction Patterns of CFA 10 at Different Ages

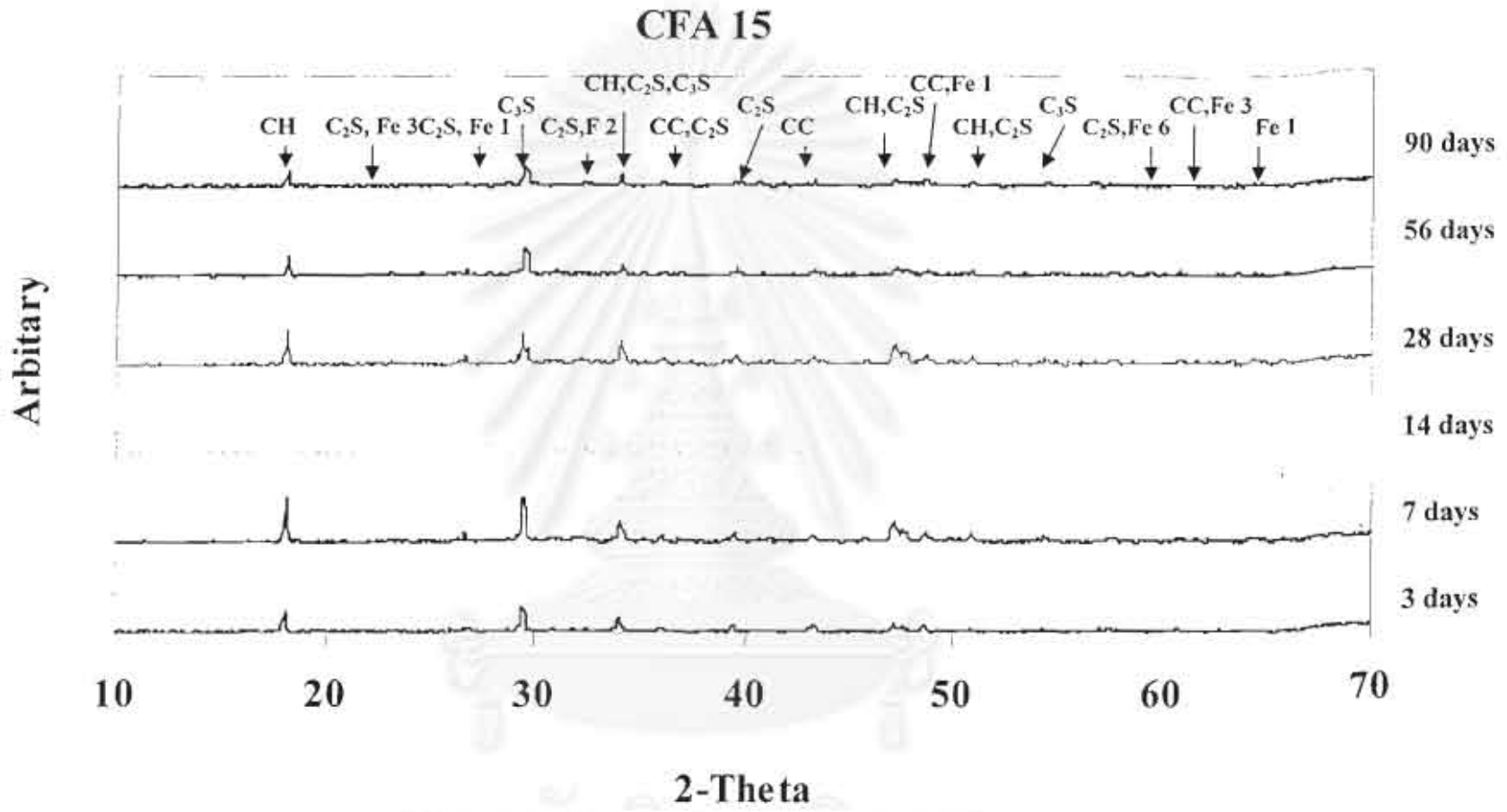

Figure 4.27 X-ray Diffraction Patterns of CFA 15 at Different Ages

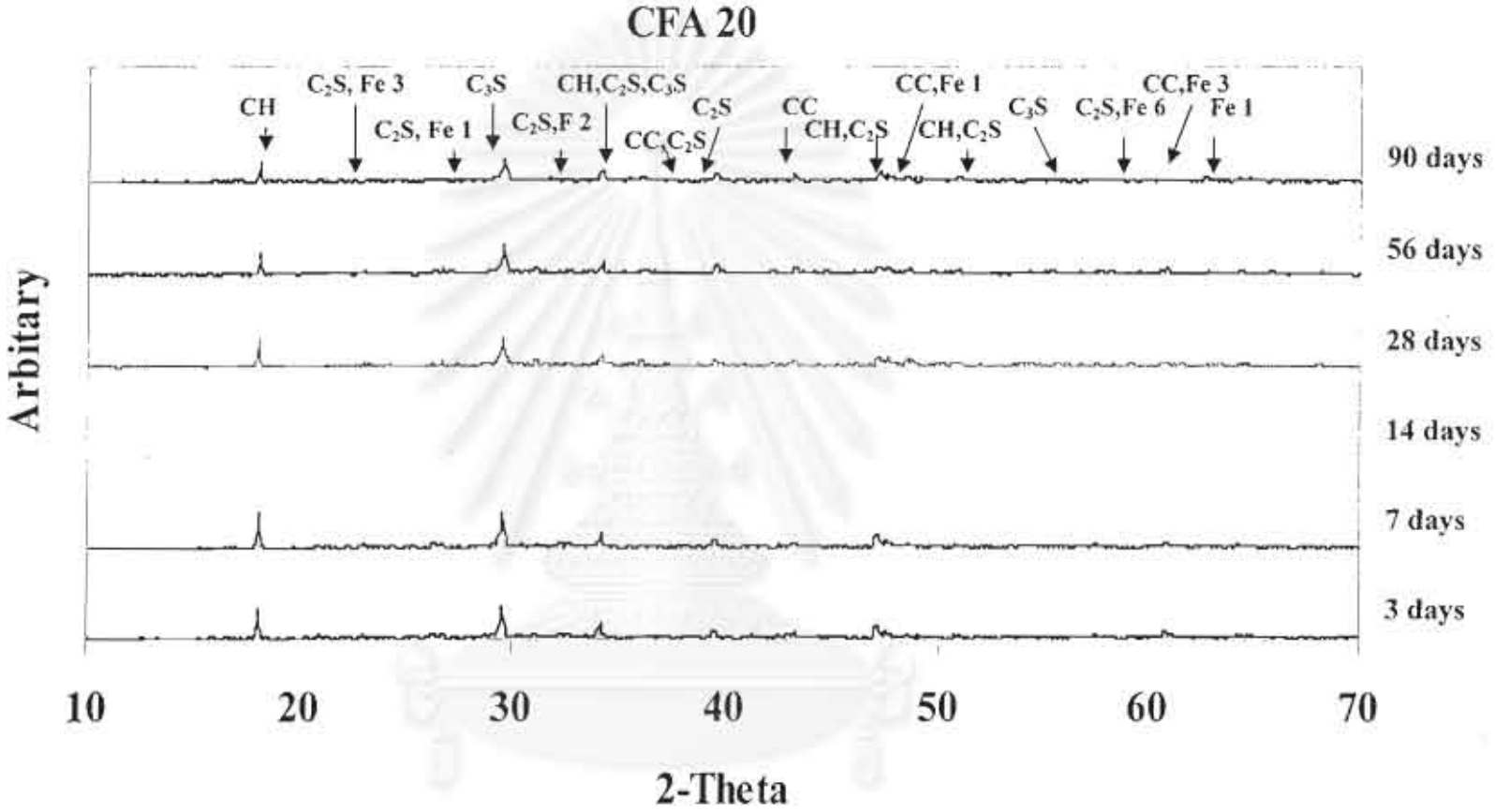

Figure 4.28 X-ray Diffraction Patterns of CFA 20 at Different Ages

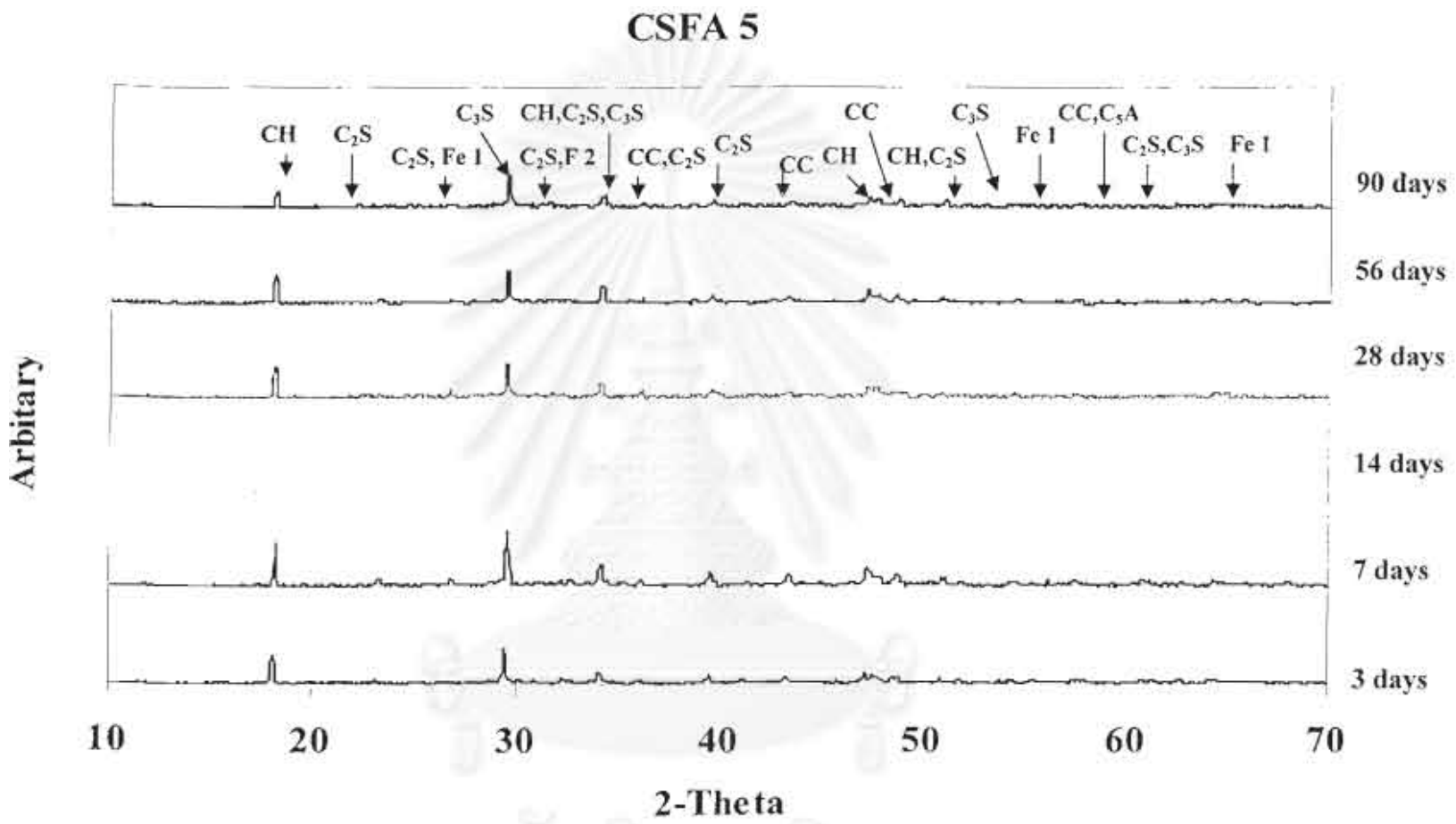

Figure 4.29 X-ray Diffraction Patterns of CSFA 5 at Different Ages

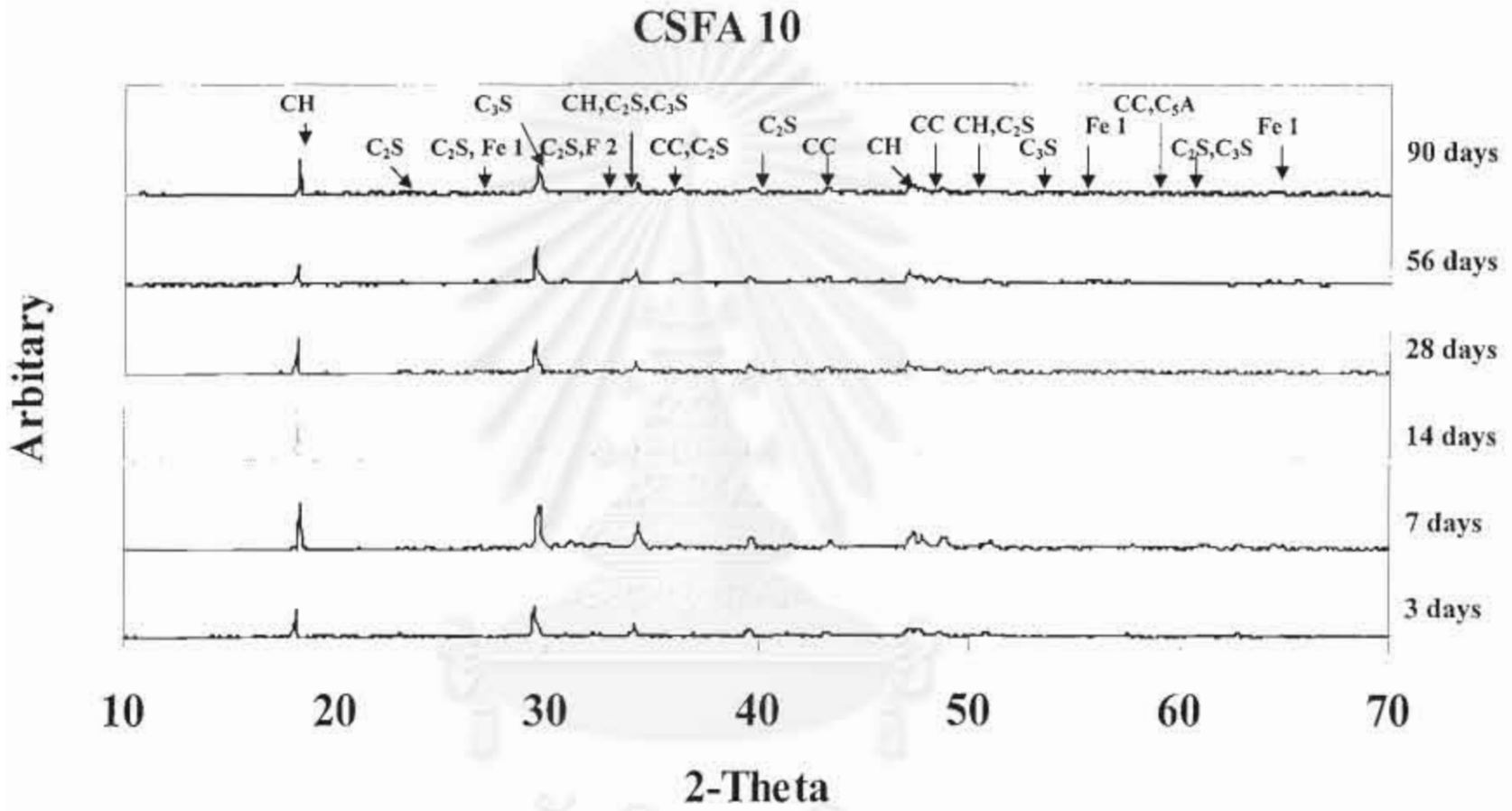

Figure 4.30 X-ray Diffraction Patterns of CSFA 10 at Different Ages

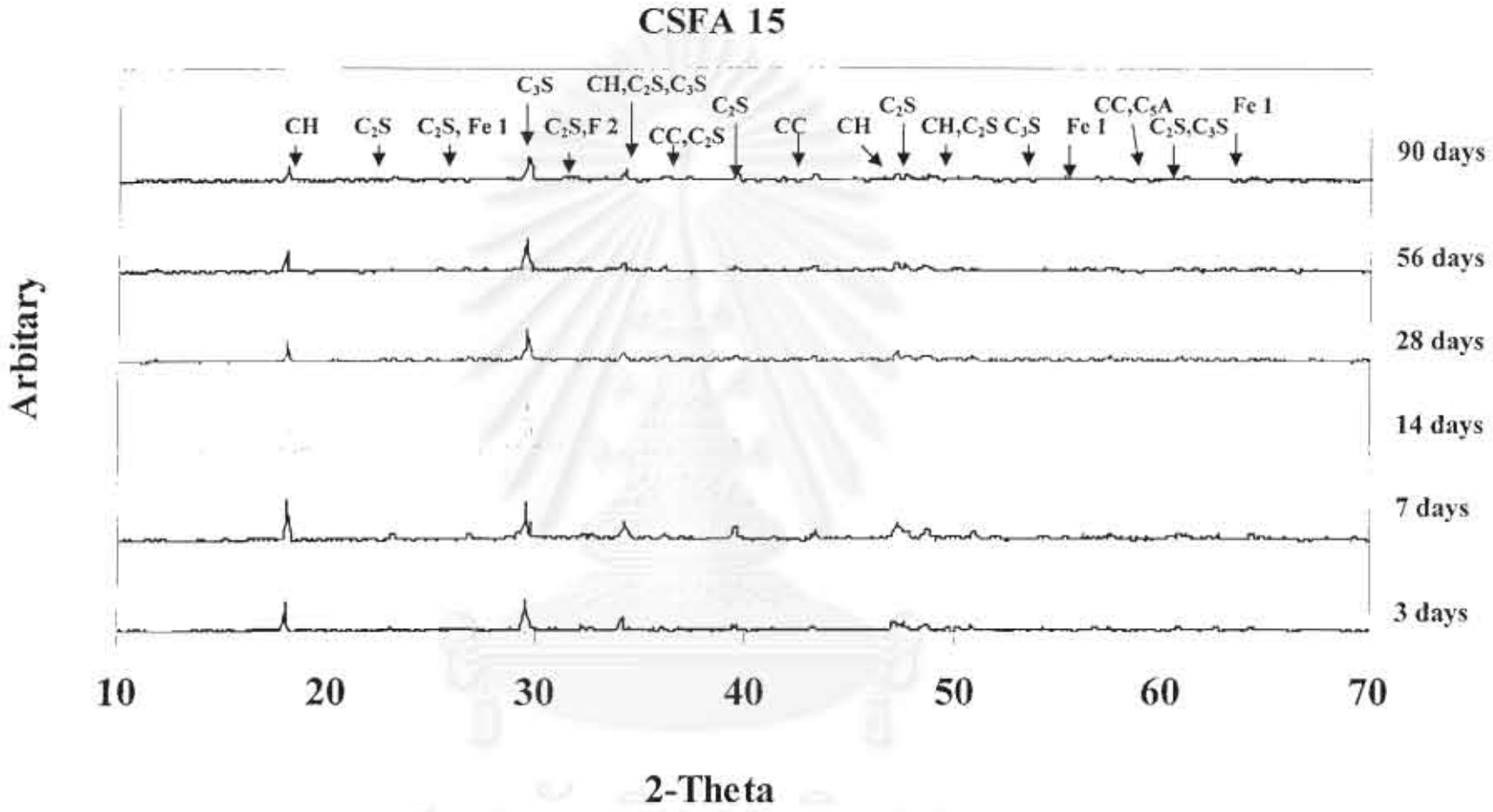

Figure 4.31 X-ray Diffraction Patterns of CSFA 15 at Different Ages

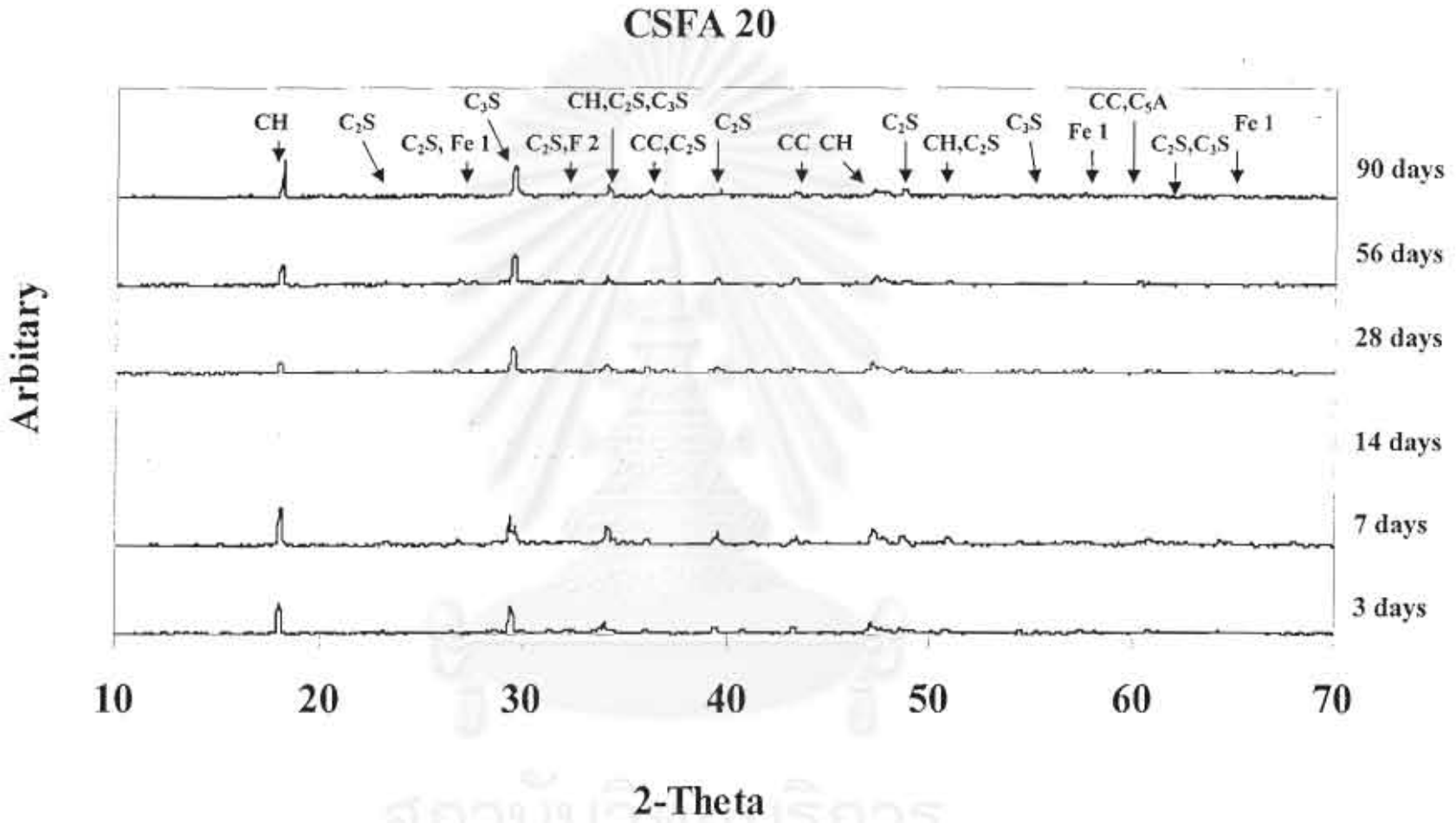

Figure 4.32 X-ray Diffraction Patterns of CSFA 20 at Different Ages

4.2.1.5 Implication of Heavy Metal Phase in Cement Phase

The fixation of metallic waste species in cement paste from the following solubility reduction and precipitation, ionic substitution and incorporation in cement hydrates and sorption onto the surface area of cement hydrates. The composition of Portland cement is dominated by the anhydrous calcium silicate phases (C-S-H), which typically comprise 70-80% by weight. Moreover, C-S-H plays an important role in the retention of metals. The fixation mechanism of metal salts by C-S-H is as showed below (Deja, 2002).

$$\text{C-S-H} + \text{Metal} \longrightarrow \text{Metal- C-S-H}$$

$$\text{C-S-H} + \text{Metal} \longrightarrow \text{Metal- C-S-H} + Ca^{2+}$$

The mechanism may occur that metal reacts with calcium hydroxide to produce insoluble compounds as a form of metal hydroxide. This mechanism inhibited the hydration and decreased of strength, especially at the concentration of metal in solidified waste is more than 0.3 wt % by weight (Qin, Sun, and Tay, 2003). This is because they are formed as metal hydroxide completely cover the cement grains. In general, when metal waste species are present as hydroxide or silicate salt. It means that they are compatible with Portland cements in the hydration reaction. This is because they form low solubility precipitates and the leachability are reduced (Gougar et al., 1996).

This study investigated the effect of heavy metals; copper (Cu), iron (Fe), nickel (Ni), vanadium (V), and zinc (Zn) in CSP pastes, CFA pastes, and CSFA pastes by XRD testing. XRD pattern is used to identify crystalline phase of cement paste with 5%, 10%, 15% and 20% in spent FCC catalyst and fly ash replacements. These major phases identified are $Ca(OH)_2$, C_2S, C_3S, and C_3A. In addition, small peak of Fe phase can detected by XRD. These metal oxide phases are Fe_2O_3, Fe_2SiO_4, $FeCO_3$, $(Mn,Fe)_2O_3$,$FeAl_2O_4$,$Ca_2FeAl2(SiO_4)(Si_2O_7)OH_2$-$H_2O$,$Ca_4Fe_5Al_{16}O_{14}$, and $22MgO•5Al_2O_3•Fe_2O_3•22SiO_4•40H_2O$. Even though, the intensity of these phase is smaller than major phases it affects to the lechability of Fe in solidified waste. This is confirmed by the leachability result of solidified/stabilized waste in Section 4.2.4.

However, there is no crystalline phase that has Ni, V, Cu, and Zn. From this result, it can not conclude that there is no reaction occurred which can be explained by following reasons;

(1) There might be too small amount of crystalline phase formed from metal ion in spent FCC catalyst and fly ash so it is difficult to detect by XRD. This can happen because the bulk concentration of these metals are relative low in all sample.

(2) Some heavy metal may not be fixed by serious hydration product therefore these metal may locate in the pores of cement paste or be adsorbed on the pore walls. This mechanism is called “Physical encapsulation” (Poon et al., 1984). Although no evidence of these metal compounds has been found by the SEM and XRD tests. The absence of $Ca(OH)_2$ crystals in the cement pastes containing spent FCC catalyst and fly ash indicate that $Ca(OH)_2$ plays an important role in the fixation of these metal. The ability of those metal to react readily with calcium hydroxide or silicate to produce insoluble compound with the solidified material this mechanism is called “Chemfix” (Poon et al., 1984).

(3) The heavy metals in spent FCC catalyst and fly ash did not significantly affect the phase composition of the cement paste. Due to low crystallinity phase of the C-S-H phase and limited sensitivity of the XRD make it difficult to determine of differences. Concerning the rate of hydration in the cement paste containing heavy metal.

(4) From the limited sensitive of XRD, Baur et al. (2003) used radioisotopes to investigate the uptake mechanism of contaminants in cement mixes. The results also confirmed that heavy metals exist inside C-S-H structure of cement paste which can not be detected by XRD. Therefore, is not these heavy metals are not detected by XRD.

4.2.2 SEM Application for Examining Macroencapsulation of Solidified/ Stabilized Materials

Scanning Electron Microscopy (SEM) was utilized to observe the microstructure of the different S/S waste during the temporal hydration process. This is to evaluation of degree of hydration reaction of cement and the ratio of cementitious material in sample. These techniques can reveal about the macroinhomogeneities and their distribution, such as size and distribution of entrained and entrapped air, as well as the existence and density of cracks. Moreover, SEM may provide information on the capillary porosity of the paste itself (by using transmitted light on thin polished section). Equally, these techniques may reveal information on the existence and possible distribution of spent FCC catalyst and fly ash in the cement paste.

A summary of properties of hydration products is provide in Table 4.11

Table 4.11 Properties of Hydration Products of Portland Cement (Mindess and Young,1981)

Compound	Morphology in Paste	Crystallinity	Typical Crystal Dimension in Paste
C-S-H	Spine; unresolved Morphology	Very poor	1 x 0.1 μm less than 0.01 μm
CH	Nonporous striated material	Very good	0.01 to 0.1 mm
Ettringite	Long slender prismatic needle	Good	10 x 0.5 μm
Monosulfoaluminate	Thin hexagonal plates; irregular rosettle	Fair - good	1 x 1 x 0.1 μm

The microstructure observation of the cement paste under the SEM were examined after mixing at the age 3, 7, 14, 28, 56, and 90 days.

(a) Control at 3 days, 3500x

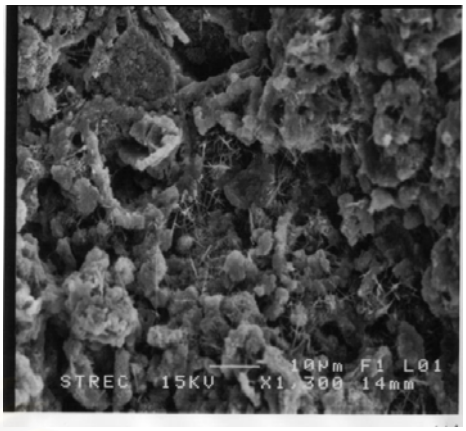

(b) Control at 7 days, 1300x

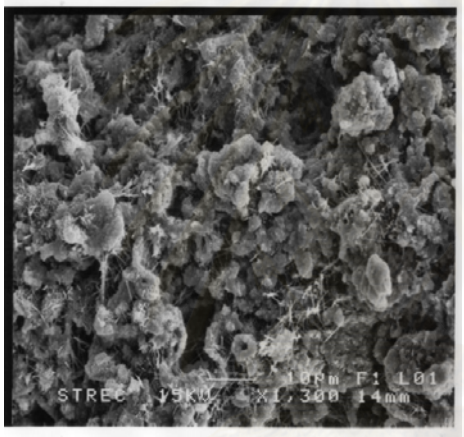

(c) Control at 14 days, 1300x

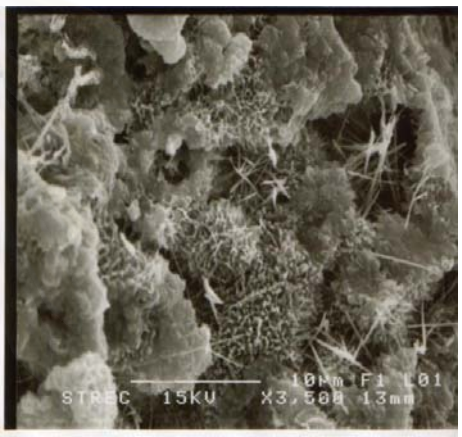

(d) Control at 28 days, 3500x

(e) Control at 56 days, 3500x

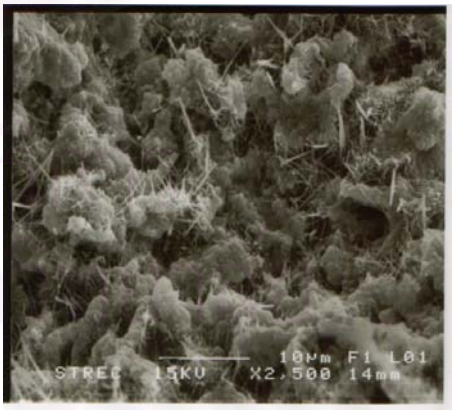

(f) Control at 90 days, 2500x

Figure 4.33 The SEM Photographs of the Control at Different Ages

(a) CSP 5 at 3 days, 5500x

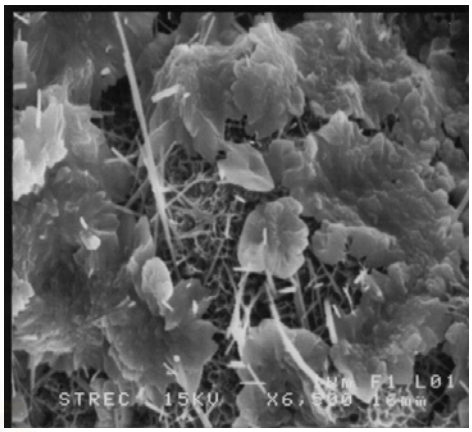

(b) CSP 5 at 7 days, 6500x

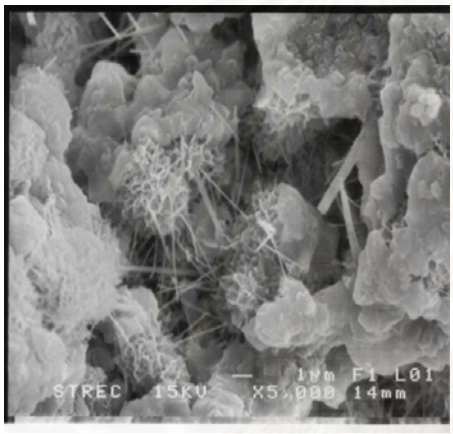

(c) CSP 5 at 14 days, 5000x

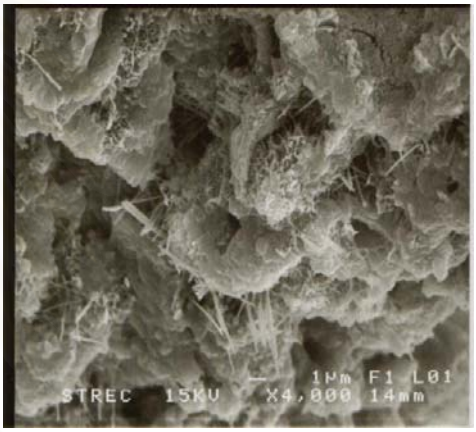

(d) CSP 5 at 28 days, 4000x

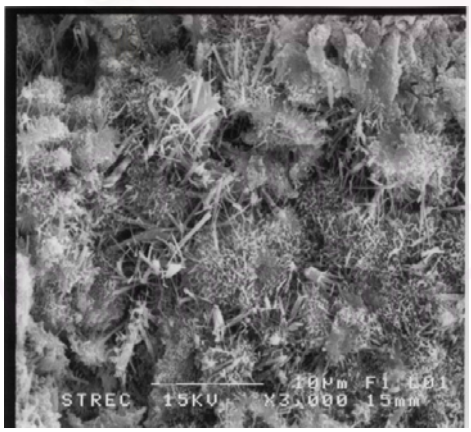

(e) CSP 5 at 56 days, 3000x

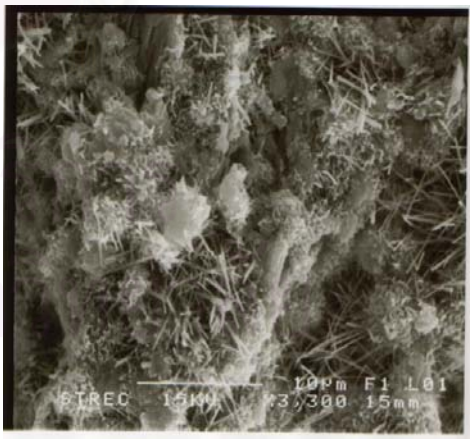

(f) CSP 5 at 90 days, 3300x

Figure 4.34 The SEM Photographs of CSP 5 at Different Ages

(a) CSP 10 at 3 days, 3000x

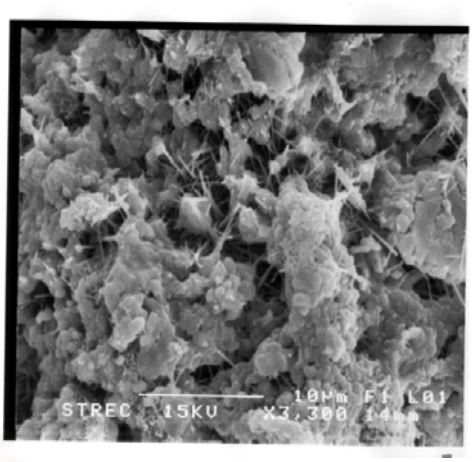

(b) CSP 10 at 7 days, 3300x

(c) CSP 10 at 14 days, 5000x

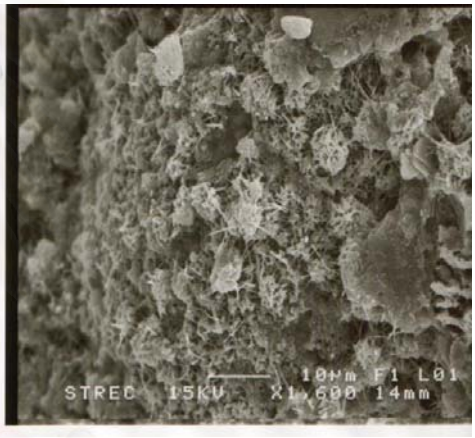

(d) CSP 10 at 28 days, 1600x

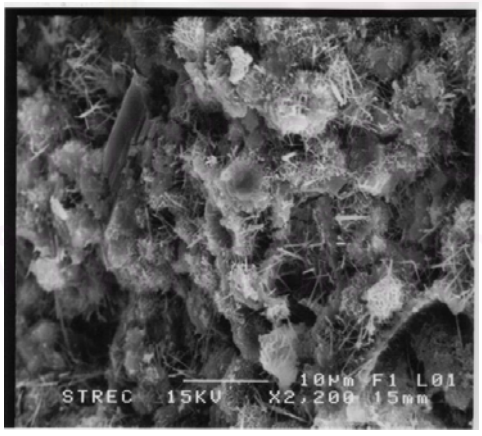

(e) CSP 10 at 56 days, 2200x

(f) CSP 10 at 90 days, 3300x

Figure 4.35 The SEM Photographs of CSP 10 at Different Ages

(a) CSP 15 at 3 days, 2500x

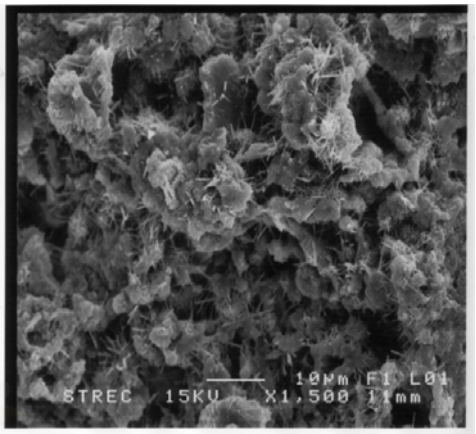

(b) CSP 15 at 7 days, 1500x

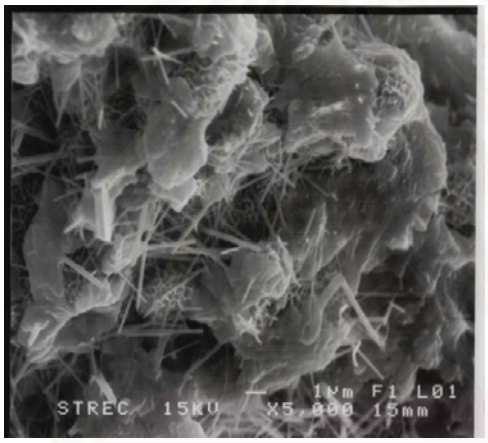

(c) CSP 15 at 14 days, 5000x

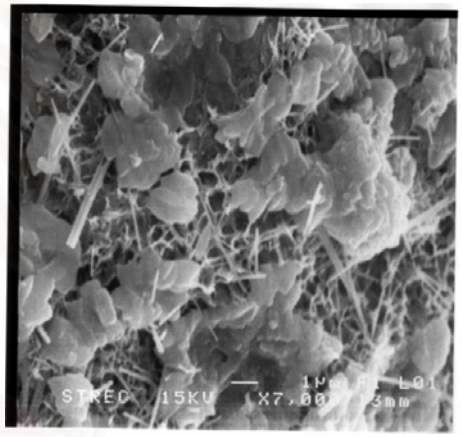

(d) CSP 15 at 28 days, 7000x

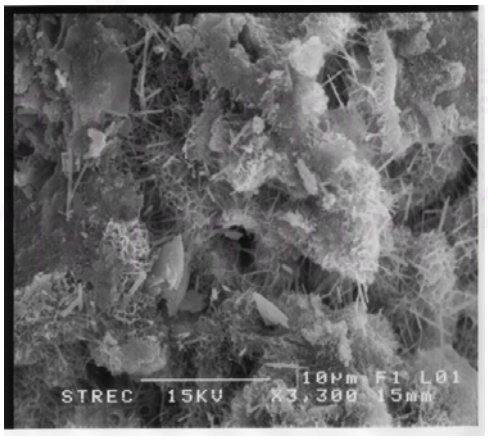

(e) CSP 15 at 56 days, 3300x

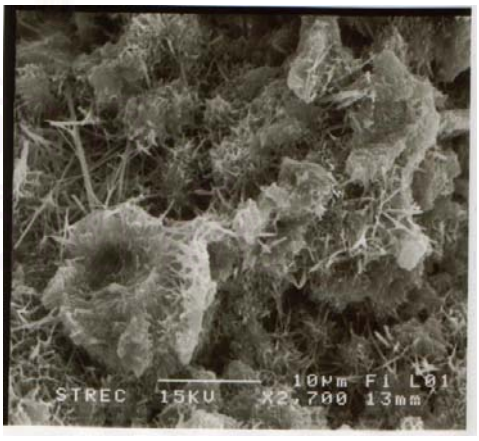

(f) CSP 15 at 90 days, 2700x

Figure 4.36 The SEM Photographs of CSP 15 at Different Ages

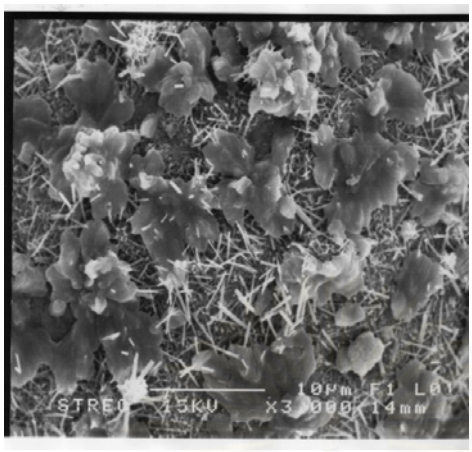

(a) CSP 20 at 3 days, 3000x

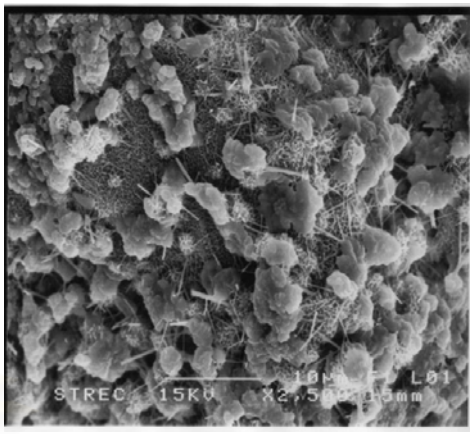

(b) CSP 20 at 7 days, 2500x

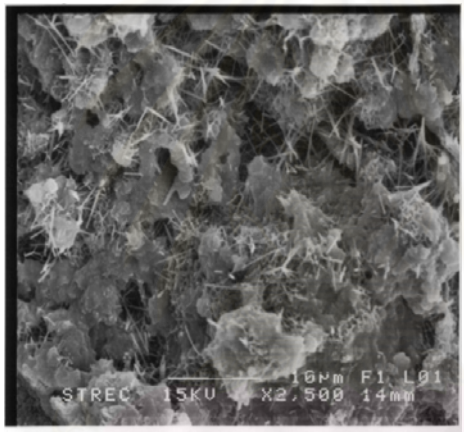

(c) CSP 20 at 14 days, 2500x

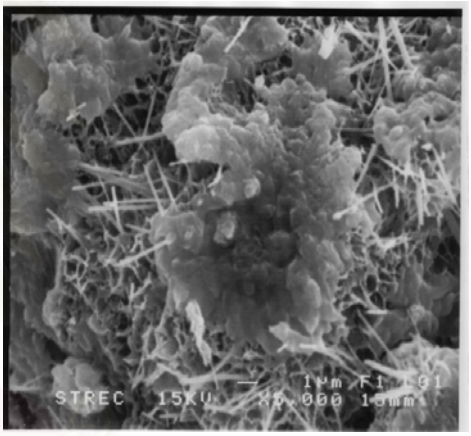

(d) CSP 20 at 28 days, 5000x

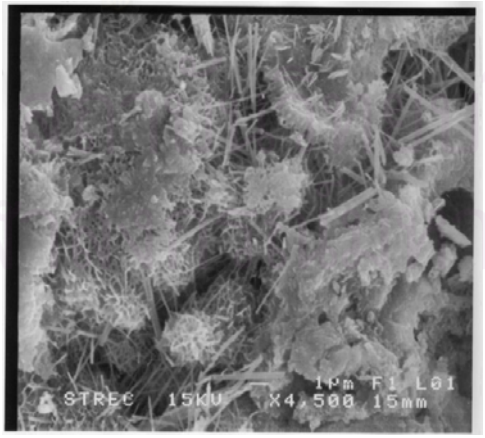

(e) CSP 20 at 56 days, 4500x

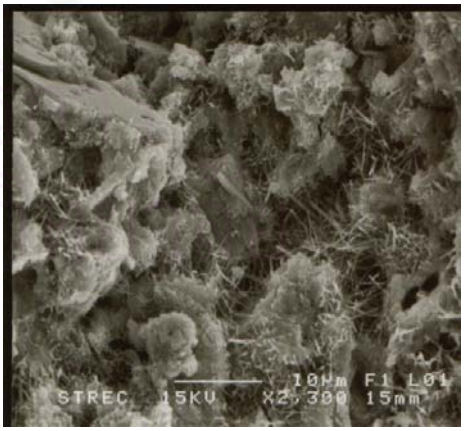

(f) CSP 20 at 90 days, 2300x

Figure 4.37 The SEM Photographs of CSP 20 at Different Ages

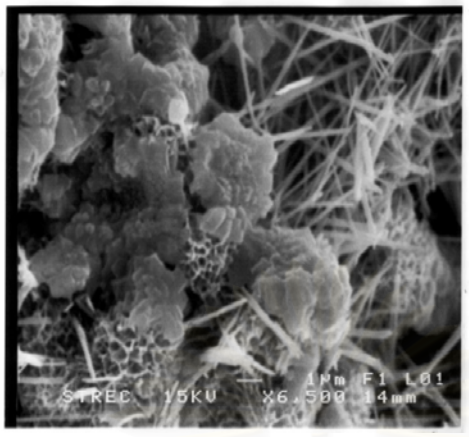

(a) CFA 5 at 3 days, 6500x

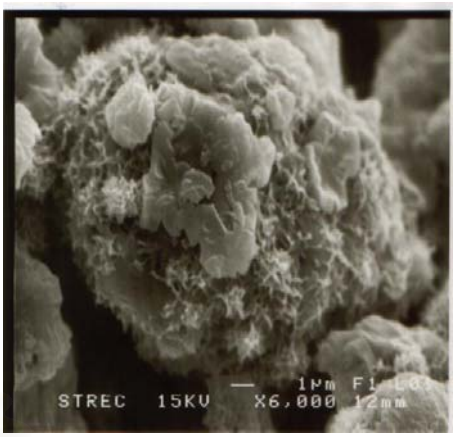

(b) CFA 5 at 7 days, 6000x

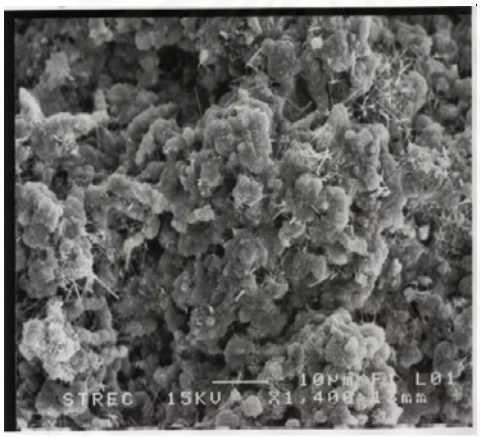

(c) CFA 5 at 14 days, 1400x

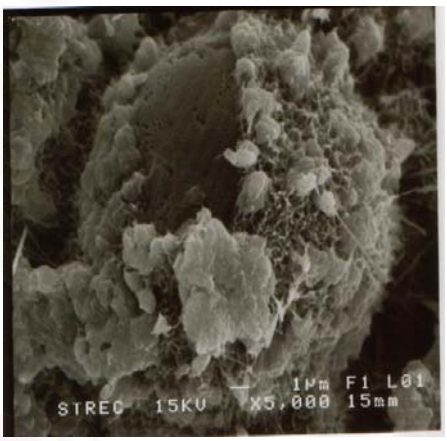

(d) CFA 5 at 28 days, 5000x

(e) CFA 5 at 56days, 4000x

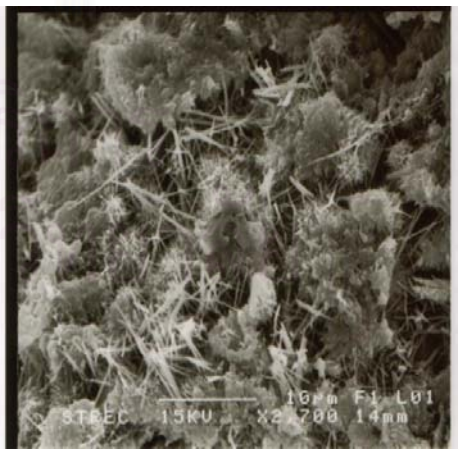

(f) CFA 5 at 90 days, 2700x

Figure 4.38 The SEM Photographs of CFA 5 at Different Ages

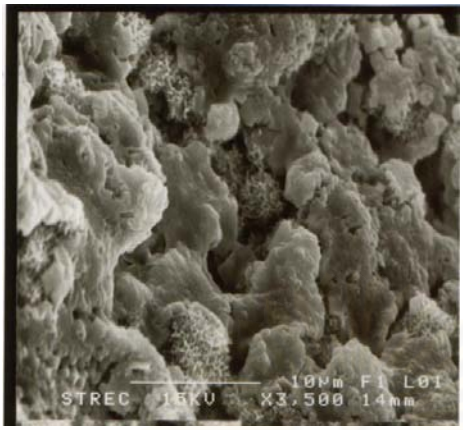

(a) CFA 10 at 3 days, 3500x

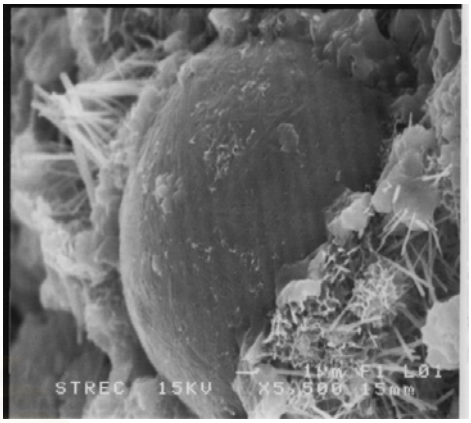

(b) CFA 10 at 7 days, 5500x

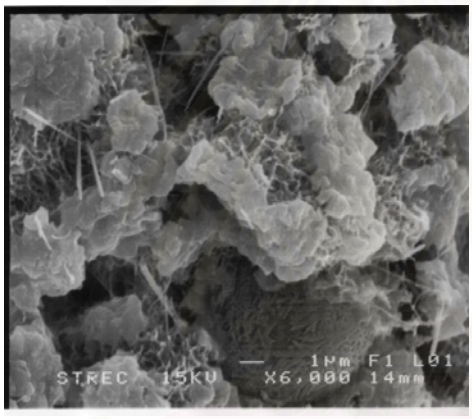

(c) CFA 10 at 14 days, 6000x

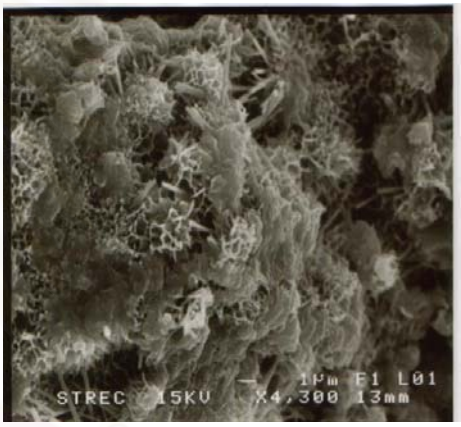

(d) CFA 10 at 28 days, 4300x

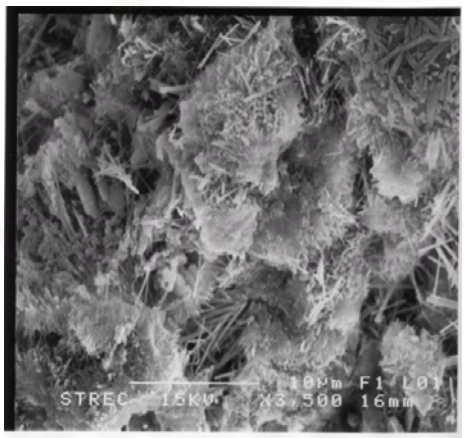

(e) CFA 10 at 56 days, 3500x

(f) CFA 10 at 90 days, 4500x

Figure 4.39 The SEM Photographs of CFA 10 at Different Ages

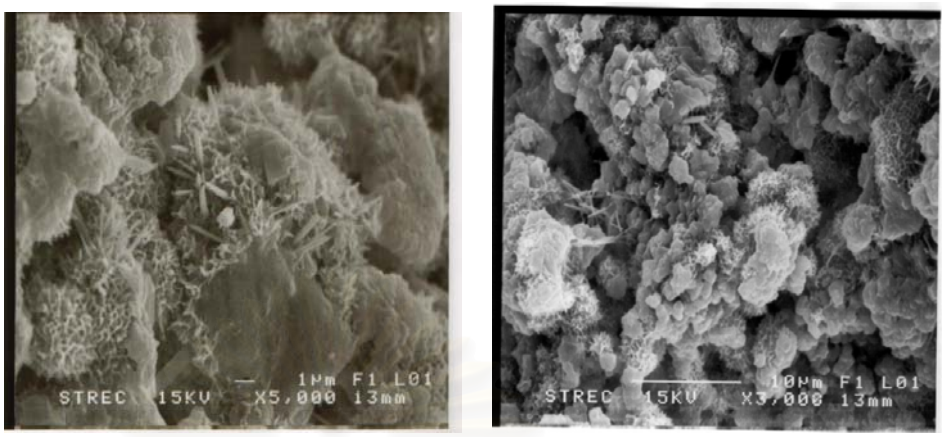

(a) CFA 15 at 3 days, 5000x **(b) CFA 15 at 7 days, 3000x**

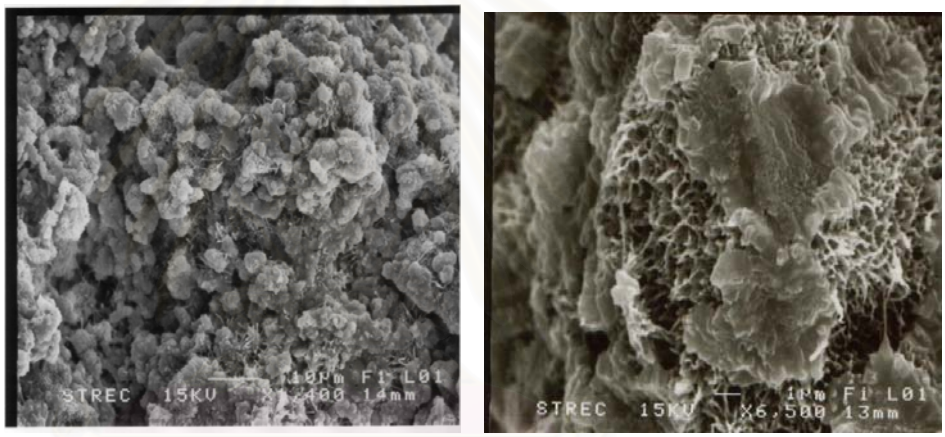

(c) CFA 15 at 14 days, 1400x **(d) CFA 15 at 28 days, 6500x**

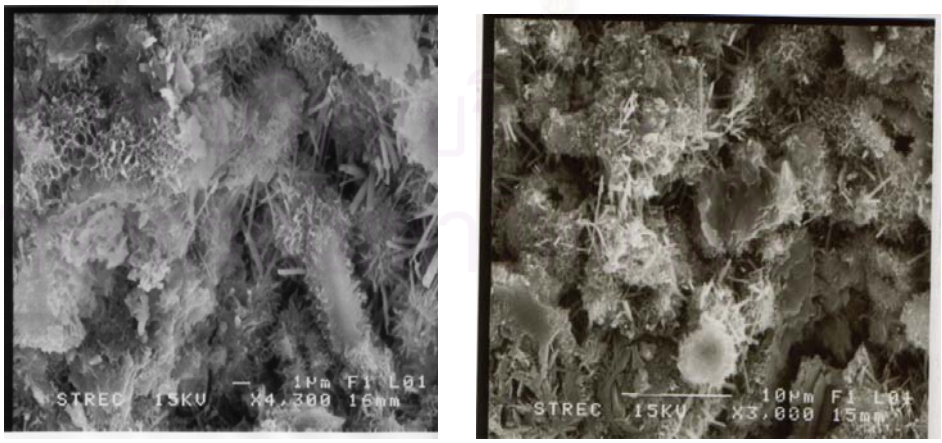

(e) CFA 15 at 56 days, 4300x **(f) CFA 15 at 90 days, 3000x**

Figure 4.40 The SEM photographs of CFA 15 at Different Ages

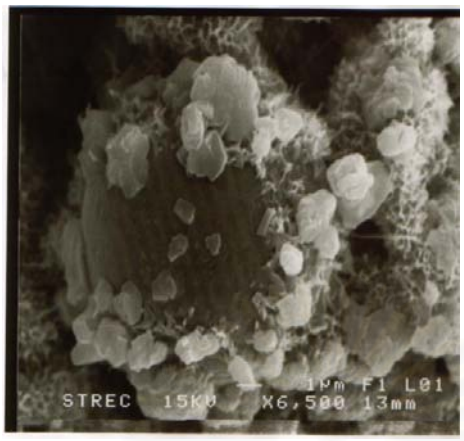

(a) CFA 20 at 3 days, 6500x

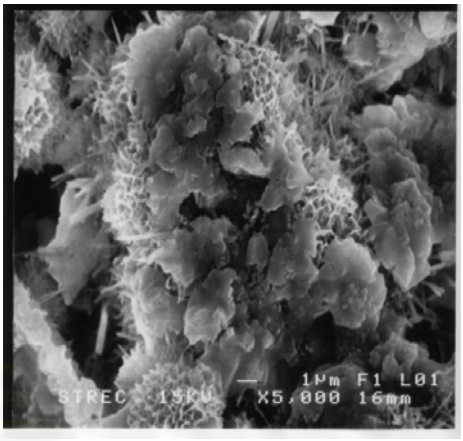

(b) CFA 20 at 7 days, 5000x

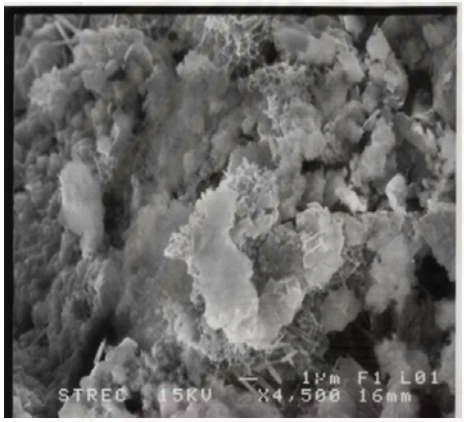

(c) CFA 20 at 14 days, 4500x

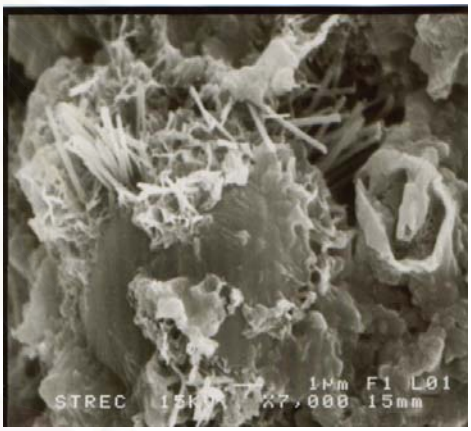

(d) CFA 20 at 28 days, 7000x

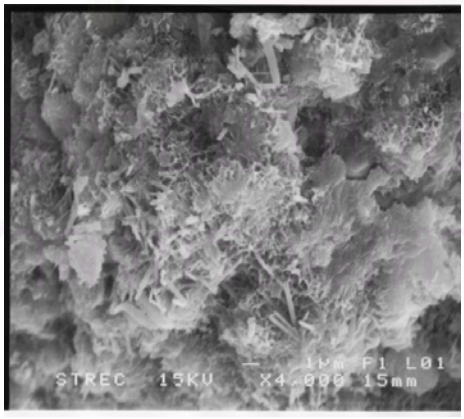

(e) CFA 20 at 56 days, 4000x

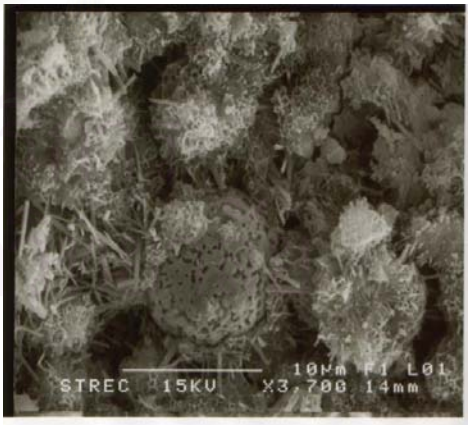

(f) CFA 20 at 90 days, 3700x

Figure 4.41 The SEM Photographs of CFA 20 at Different Ages

(a) CSFA 5 at 3 days, 2200x

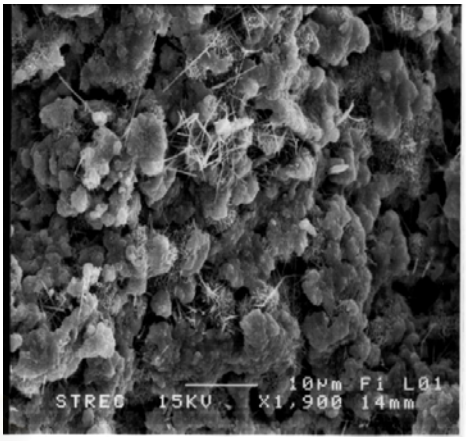

(b) CSFA 5 at 7 days, 1900x

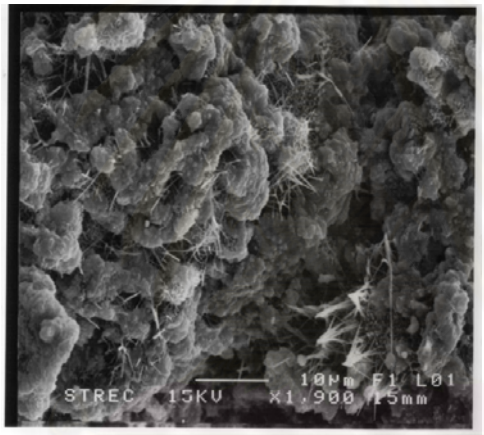

(c)CSFA 5 at 14 days, 1900x

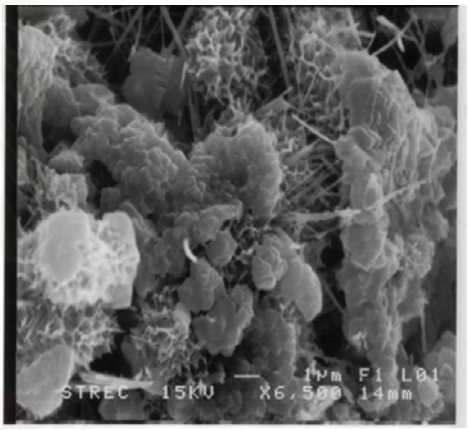

(d) CSFA 5 at 28 days, 6500x

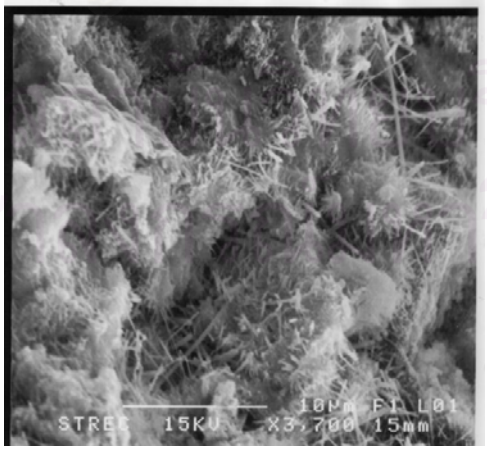

(e) CSFA 5 at 56 days, 3700x

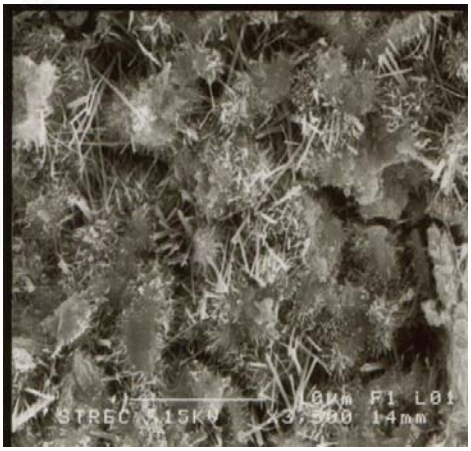

(f) CSFA 5 at 90 days, 3500x

Figure 4.42 The SEM Photographs of CSFA 5 at Different Ages

(a) CSFA 10 at 3 days, 2500x

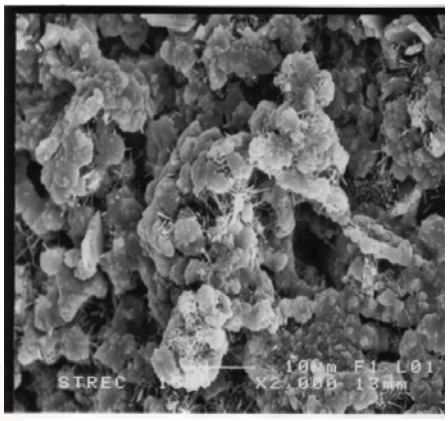

(b) CSFA 10 at 7 days, 2000x

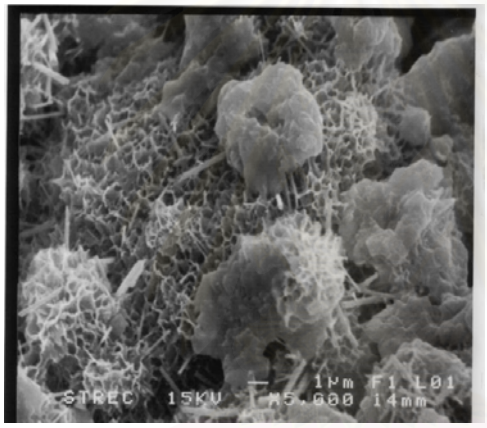

(c) CSFA 10 at 14 days, 5000x

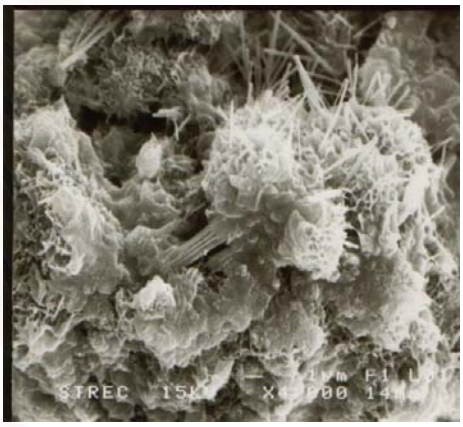

(d) CSFA 10 at 28 days, 4000x

(e) CSFA 10 at 56 days, 4500x

(f) CSFA 10 at 90 days, 3700x

Figure 4.43 The SEM Photographs of CSFA 10 at Different Ages

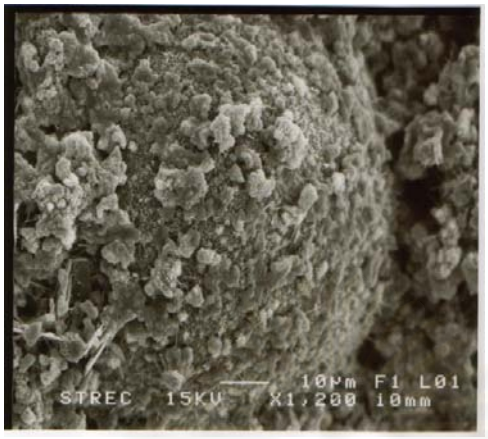

(a) CSFA 15 at 3 days, 1200x

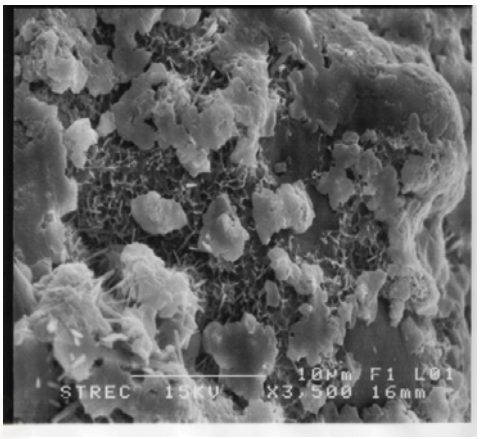

(b) CSFA 15 at 7 days, 3500x

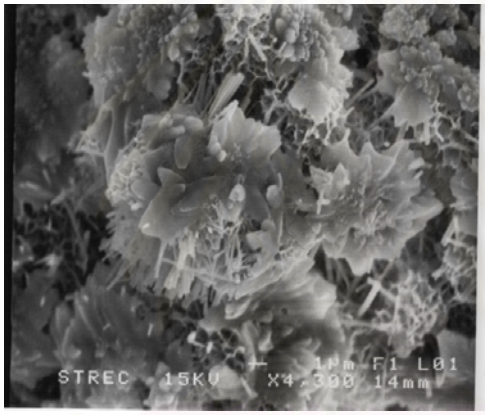

(c)CSFA 15 at 14 days, 4300x

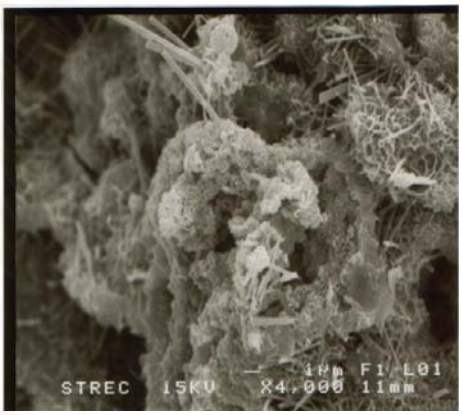

(d) CSFA 15 at 28 days, 4000x

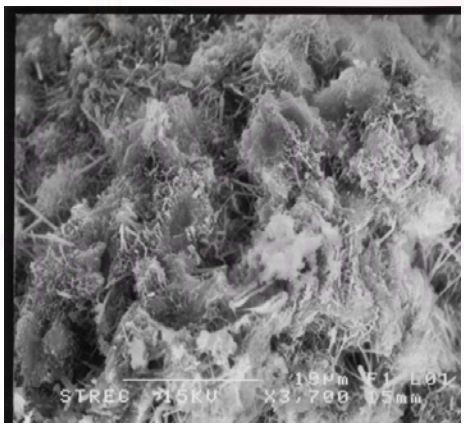

(e) CSFA 15 at 56 days, 3700x

(f) CSFA 15 at 90 days, 3300x

Figure 4.44 The SEM Photographs of CSFA 15 at Different Ages

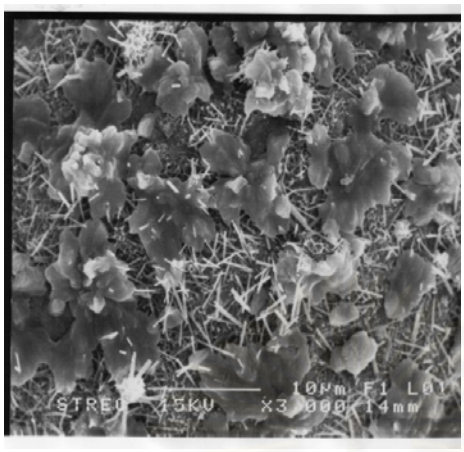

(a) CSFA 20 at 3 days, 3000x

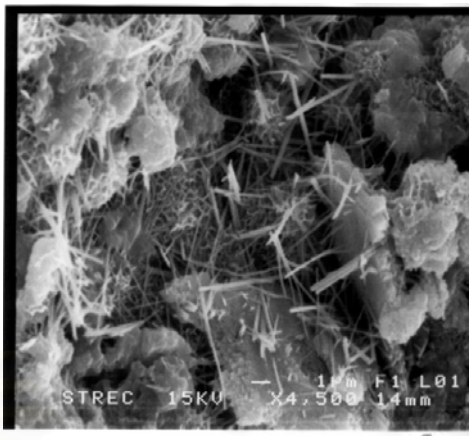

(b) CSFA 20 at 7 days, 4500x

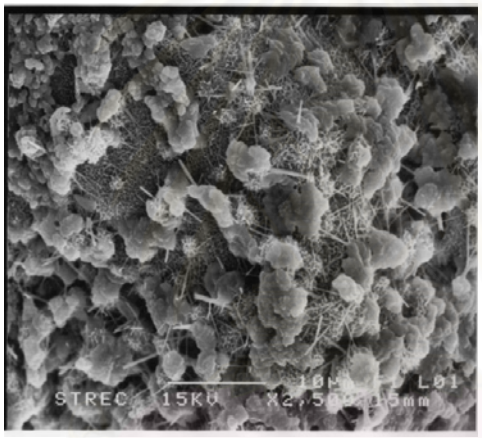

(c) CSFA 20 at 14 days, 2500x

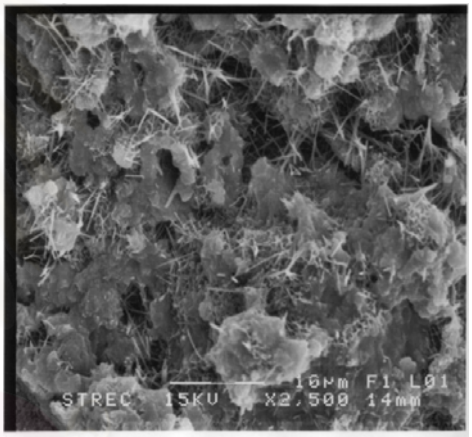

(d) CSFA 20 at 28 days, 2500x

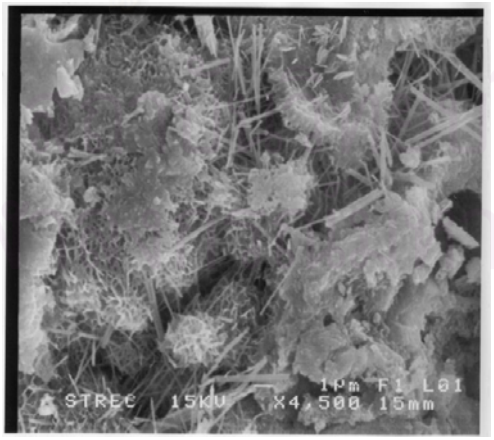

(e) CSFA 20 at 56 days, 4500x

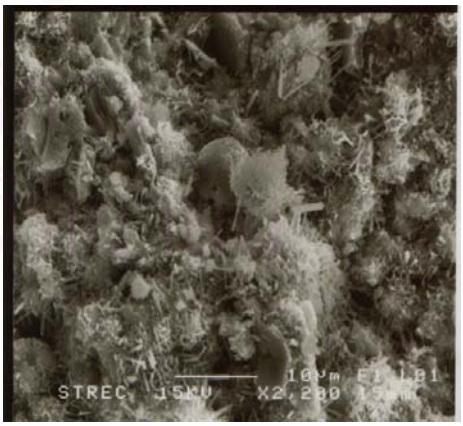

(f) CSFA 20 at 90 days, 2200x

Figure 4.45 The SEM photographs of CSFA 20 at Different Ages

4.2.2.1 3 days

The cement hydration of tricalcium silicate (C_3S) and dicalcium silicate (C_2S), produce are C-S-H, Portlandite (CH), and those of C_3S. However, the reaction rate and the number of moles CH produced by C_3S are much higher than C_2S. Another reaction taking place during the cement hydration is the hydration of tricalcium aluminate (C_3A) in the presence of gypsum. As a result, ettringite ($C_3S•3CaSO_4•32H_2O$) is produced as long as there is a large supply of available. On the other hand, if there is not enough sulfate ions, ettringite is then converted to monosulfoaluminate ($C_3S•CaSO_4•12H_2O$) (Malhotra, 1987). Within one day, the rapid formation of hydration products C-S-H, CH, and ettringite stops. However, the reaction is still going at a much lower rate for as long as one year.

The microstructure of the paste at this age shows a larger gap between the grains and the precipitation of the hydration product. Figure 4.33(a) shows the microstructure of the control cured for 3 days. The paste is composed of irregular particles, which is supposed to be unreacted cement grain. Moreover, it had been etched on the surface although smooth grain still exists. It can also be noticed that the needle-like particles and fibrous or ettringite are found covering at the surface of cement grains. CH initially presents as thin hexagonal plates and then developed into vacant space in the pore. This produce can developed into vacant space and any part in pastes because it is homogenous texture as a result it can be produced anywhere in the pastes.

The CSP pastes microstructure are shown in Figures 4.34(a), 4.35(a), 4.36(a), and 4.37(a). These figures show that the microstructures of each percentage (CSP 5, CSP 10, CSP 15, and CSP 20) does not show a significantly different. The large crystal in CSP is assumed to be CH while C-S-H fibril penetrating in CH crystals and grows on the surface of the cement grains. There are plenty of ettringite needles growing around the cement grain. The irregular shape of the ground spent FCC catalyst cannot be seen since its morphology is very close to other crystals structure. Moreover, most of the ground spent FCC catalyst particles found in vicinity of large CH. Therefore, the reaction between spent FCC catalyst and CH might occur at their

interface. As a result, these particles are embedded in the large CH crystal. At this time, the precipitation rate of CSP paste is quite low; hence, large void spaces still existed. The large number of void space has an adverse effect on its strength because the density of paste is lower (Bumrongjaroen, 1999).

The microstructure of CFA pastes are shown in Figures 4.38(a), 4.39(a), 4.40(a), and 4.41(a). The overall of microstructure, distribution of fly ash, crystals grains, and pores of the CFA can be observed. CFA 5 had higher vacant space compare with other CFA replacement. Number of pores around the clusters of particle in CFA 5 is evident which related to high porosity at this age. CFA surfaces have small amounts of ettringite and small size CH crystals that embedded among the cluster, but C-S-H fibrous was lying on the fly ash particle.

Figures 4.42(a), 4.43(a), 4.44(a), and 4.45(a) show the microstructure at age of 3 days of CSFA paste. The morphology of the CSFA pastes is similar to that CSP and CFA pastes. It can also be noticed that the surface of the CSFA particle was covered with angular porlandite crystals (CH) and the smaller particles of CH crystals became integrated together like clusters. In addition, C-S-H spines and the needle-like crystals grew around the paste. At this stage, the pore size larger than the older age, leading to low strength but high permeability in the CSFA pastes at the age of 3 days.

4.2.2.2 7 -14 Days

At this time, the pozzolanic action occurs together with hydration reaction and goes through a major reaction in cement pastes. There are several methods to determine the pozzolanic action of the materials such as a determination of the formation of its products or the reduction of its source. However, the morphology of its product, C-S-H can not be identified by XRD because it has amorphouse phase. Therefore, the pozzolanic action at this age could not confirmed by their microstructure.

The microstructure of the control (Figures 4.33 (b-c)) pastes at the curing time 7-14 days do not change from the 3 days paste much.

The morphology of CSP pastes are dominated by large amount CH. Ettringite needles is developed to longer needle-like hexagonal plate or monosulfoaluminate and interlock to form void spaces and filling in the pore as shown in Figures 4.34(b-c), 4.35(b-c), 4.36(b-c), and 4.37(b-c). While C-S-H fibril penetrated in CH crystals and grow on the surface of cement grains. As seen that, the rate of hydration product growing in this day was higher than 3 days. At high magnification, it can be seen the connection between hydrated particles.

As seen from a micrograph, Figures 4.38(b-c), 4.39(b-c), 4.40(b-c), and 4.41 (b-c), a number particles of fly ash was continuously etched. The CFA paste became denser than in the young paste because of the formation of the hydration products, CH, C-S-H spines, and ettringite on the surface of the paste. The amount of CH crystals in all CFA pastes were increased significantly, which was also obvious in the XRD pattern of cement paste in Section 4.2.1. Intermeshed between the C-S-H spines, are noticeable in Figure 4.41 (b). However, at the same time, there are some fly ash spheres that have not reacted very much.

The morphology of the CSFA pastes are shown in Figures 4.42(b-c), 4.43(b-c), 4.44(b-c), and 4.45 (b-c). As the reaction progresses, the microstructure of the fracture surface CSFA paste shows advanced degree of hydration. It can be noticed that the number of C-S-H spines increases significantly with a higher percent replacement (Figures 4.44(b-c), and 4.45 (b-c) and they interlocked around the paste. In addition, the clusters of C-S-H spines became cluster and denser to honeycombed C-S-H form as shown in Figures 4.43(b-c), 4.44(b-c), and 4.45 (b-c).

In summary, at the age of 7-14 days, all of samples reacted as the degree of hydration advanced and more hydration product was observed.

4.2.2.3 28-56 Days

For the pozzolanic action of spent FCC catalyst and fly ash in this stage, it can be said that the reaction was in progress but the reaction rate could not be obtained from the observations of the microstructure. This is because the surface of some

particles could not be examined. However, the pozzanic is continuing to fill in pore and vacant space of the pastes, as a result reducing in the pore volume and high strength.

At this age, in the microstructure of the control shown in Figures 4.33(d-e). The number of CH crystals increased significantly. This figures show that CH crystals grow from thin hexagonal plates to massive plates. The short ettringite grew longer needles and started to interlock in the void spaces. In addition, the C-S-H spines continued growing in anywhere of cement grains and forming the honeycombed C-S-H structure (Figures 4.36(d-e) and 4.37(d-e)).

At the same time, the CSP structure became complex since the hydration product continuously precipitates. Even at this age, the morphologies of early stage hydration product are still present as shown in Figures 4.34(d-e), 4.35(d-e), 4.36(d-e), and 4.37(d-e). Ettingite was found to grow into the capillary pore between the CSP pastes while the honeycombed C-S-H structure also present.

As was seen from a micrograph, in Figures 4.38(d-e), 4.39(d-e), 4.40(d-e), and 4.41(d-e), that the microstructure of CFA is denser with the hydration products that were well developed in the paste. These hydration products also continued to fill the void space. However, less hydrate fly ash grains were still visible and the boundary between fly ash particles and other hydration products could not be easily distinguished at the same time.

For CSFA paste, there are less hydrate grains. The characteristic of cement hydration products are shown in Figures 4.42(d-e), 4.43(d-e), 4.44(d-e), and 4.45(d-e). At this age, the increasing rate of angular portlandite crystal (CH) is lower than the beginning. This confirmed with XRD result in Section 4.2.1. At high magnification, the honeycombed of C-S-H structure can be seen clearly. C-S-H spines which short spikes is also present in the void space. These silicate phases are present as either masses of plates or splines (Lea, 1971).

4.2.2.4 90 Days

After curing for a long period of time, all of the entire paste structure became denser, which was due to an increase in the bonding of particles and the surrounding paste at this age. In addition, the individual phases were very difficult to be identified. At this age, it has lower pore sizes than the earlier that confirmed with the permeability of the solidified/ stabilized materials, as discussed in Section 4.2.3.

As reaction progresses, the microstructure of the control paste was almost completed (Figure 4.33 (f)), it can be said that there is no segregate particle. As a result, the pore volume in the control paste reduces leading to lower permeability.

Figure 4.34(f), 4.35(f), 4.36(f), and 4.37(f) show the microstructure of CSP paste at the same age. The system was very dense by the hydration and pozzolanic products. These products were bond together and interlocked the void space.

Some of the fly ash particles show an evidence that they involved in pozzolanic action significantly (Figures 4.38(f), 4.39(f), 4.40(f), and 4.41(f)). The higher density of the CFA paste leaded to the future growth of hydration and pozzolanic products. Moreover, some of fly ash particles have been dissolved, while some surface spheres still have smooth surface. This may be because they still had not reacted.

The CSFA structure is more denser with hydration and pozzolanic products. As a result, they have refined porosity, Figures 4.42(f), 4.43(f), 4.44(f), and 4.45 (f). This leads to lower permeability, which corresponds with the permeability results in the Section 4.2.3.

Even though, the amount of hydration products and pozzolanic products in each replacement of CSP paste are different, the mechanism occurred in each sample do not significant different. The formation of $Ca(OH)_2$, C-S-H gel, and ettringite, which are the major phase characteristics of hydrated cement pastes, accelerates from

the start of the curing time. At 28 days of curing time, it shows a slightly higher proportion of C-S-H crystals. Therefore, it seems that the cement paste has a lot of C-S-H crystal but small $Ca(OH)_2$ content at the age of 28–90 days. Most of investigators reported that the hydration reaction almost completes at 28 days where pozzolanic reaction is the major reaction in cement pastes (Malhotra, 1987). Moreover, the $Ca(OH)_2$ is absent because spent FCC catalyst also retards the hydration product.

In the CFA pastes, it shows that the morphology of the hydration products is not easy to distinguished. The reaction of fly ash in cement pastes is also similar CSP pastes. It appears that the reaction usually occurs more or less particle-by-particle basis with some particles never reacts while others reacts at different rates. After a few weeks, the pitting and eroding of individual spheres is seen and the results of various chemical studies suggest that the $Ca(OH)_2$ content of the cement pastes begins to decline. The amount of fly ash reacted depends on the glassy content and on the amount of $Ca(OH)_2$ present in the system. It appears that the glass is dissolved by the alkaline pore solution that builds up with time and they react with $Ca(OH)_2$ to produce a gel of calcium alkali silicate hydrate (with Al, Fe, SO_4^{2-}, and possible other species) which is not distinguishable from the ordinary C-S-H gel (Stephan, Maleki, Knofel, Eber, and Hardtl, 1999).

CSFA pastes show very little change in each sample. Up to 3 months, some of spent FCC catalyst spheres and fly ash spheres reacted significantly and some spheres have been eroded. While at the same time, some spheres do not show sign of reaction.

By comparing the microstructure of CSP pastes, CFA pastes, and CSFA pastes, one should be note that, unlike the control, there are small amount of the hydration products. These results are also similar to the XRD patterns where intensity of $Ca(OH)_2$ in CSP pastes, CFA pastes, and CSFA pastes were lower than the control. The absence of $Ca(OH)_2$ in cement paste that contained spent FCC catalyst and fly ash is because these materials retarded the hydration process of the cement compounds. Moreover, the microstructure development indicates that CSP pastes, CFA pastes and CSFA had only a minor effect on the morphology at all time.

The microstructure observations confirm that heavy metal in CSP pastes, CFA pastes, and CSFA pastes have little effect on the morphology and it is difficult to distinguished single metal with a particle hydration product from the SEM. However, the structure of the particles as the heavy metal spiked cementitious waste is also dominated by hydration and pozzolanic products.

4.2.2.5 Element Mapping of Solidified/ Stabilized Materials

Due to the fact that it is not possible to conduct any reliable quantitative analysis from the SEM. Their element mapping revealed only information regarding distribution of their components such as Al, Ca, Cu, Fe, Ni, Si, V, and Zn from the outer surface to 10 μm deep down into the solidified/ stabilized materials. Therefore, the purpose of the element mapping in this part is only to illustrate some physical characteristics and area that the element is located in the cement pastes by selecting CSP 15, CFA 15, and CSFA 15 at age 90 days of curing time.

The quadrilateral and the circle in Figures 4.46-4.48 are represented spent FCC catalyst and fly ash in cement pastes, respectively. It can be noticed that spent FCC catalyst particle is located at high concentration of Al and Si while fly ash particle is located at high concentration of Fe, Ca, Al and Si. This is confirmed by bulk chemical compositions result in Section 4.1.6 because these metals are the major composition in spent FCC catalyst and fly ash particles.

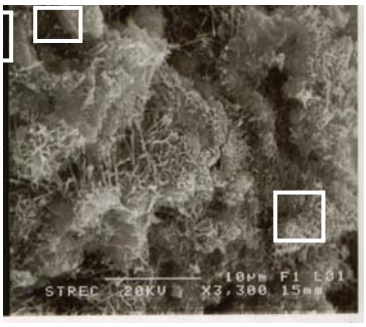

(a) Image, 3300x

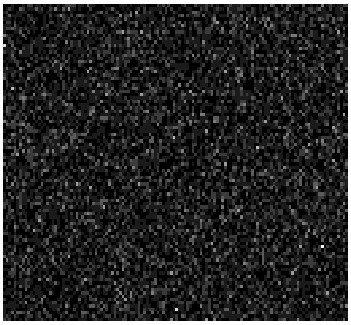

(b) Cu Mapping

(c) Fe Mapping

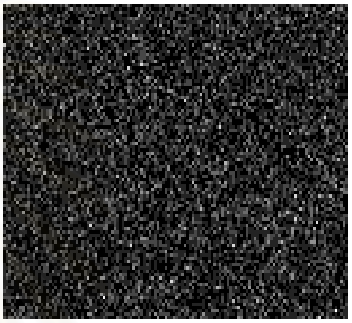

(d) Ni Mapping

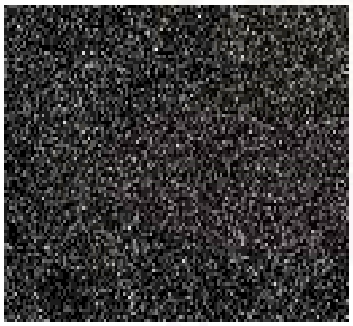

(e) V Mapping

(f) Zn Mapping

Figure 4.46 Element Mapping of CSP 15 at 90 days

Note: ☐ = Spent FCC Catalyst

(g) Al Mapping

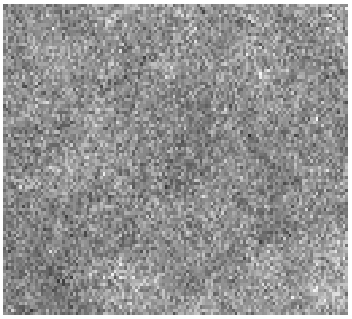

(h) Ca Mapping

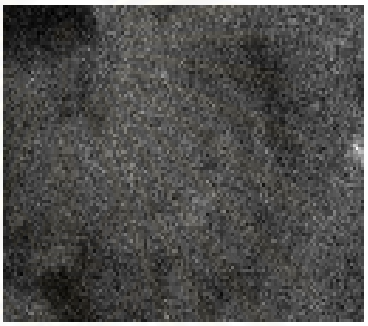

(i) Si Mapping

Figure 4.46 Element Mapping of CSP 15 at 90 days (Continued)

Figure 4.46 shows the element mapping of CSP 15 at age 90 days. It is apparent that there are more Al and Si on the surface of particles because spent FCC catalyst is composed mainly of silica-alumina (Sadeghbheigi, 2000). In addition, it can be seen that the Ca is found in high concentration everywhere. Most of Ca in the mapping came from Portland cement (63.82%) since spent FCC catalyst had lower percentage of Ca (0.01%). This evidence can be related to the microstructure of cement pastes because Al and Si on the surface of spent FCC particle react with Ca to produce C-S-H gel. Another metal has only low concentration and is found scatting around the pastes. This may be because the solidified and stabilized process can fix heavy metal inside the structure as a result it will stay inside the C-S-H structure that cannot be detected by SEM.

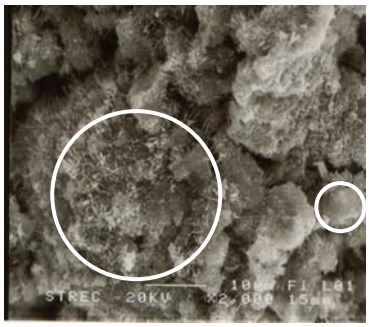

(a) Image, 2000x

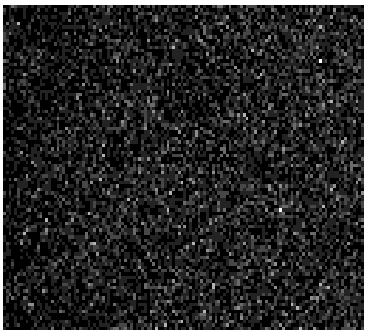

(b) Cu Mapping

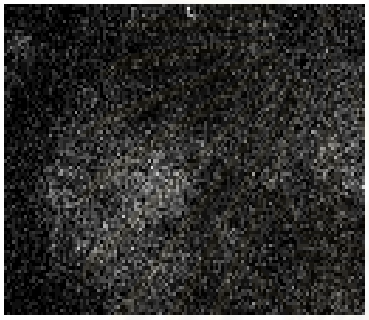

(c) Fe Mapping

(d) Ni Mapping

(e) V Mapping

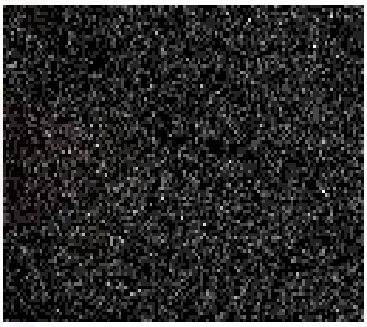

(f) Zn Mapping

Figure 4.47 Element Mapping of CFA 15 at 90 days.

Note: ○ = Fly Ash

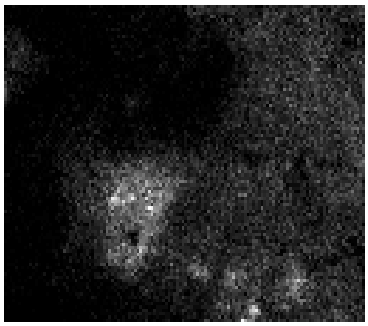

(g) Al Mapping

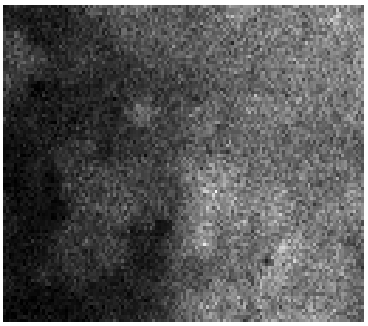

(h) Ca Mapping

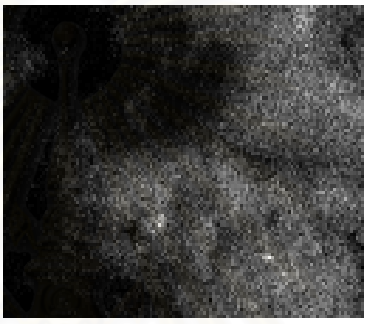

(i) Si Mapping

Figure 4.47 Element Mapping of CFA 15 at 90 days (Continued)

The element mapping of CFA 15 at 90 days is shown in Figure 4.47. The selected image was an area around the fly ash particle, which had already loosened out. The image is selected in order to show the mobility or diffusing of element from the fly ash particles. The elements are appearing in white on this mapping. From the picture it can seen that the Ca was found in high concentration in the fly ash particle and in the area close to fly ash particles but reduce with distance from the fly ash particle. Ca ion was absorbed on to the surface of fly ash and reacted with the Al, Si and Fe element in the fly ash particles. Most of Ca in the mapping came from Portland cement (63.82%) since the fly ash had low percentage of Ca (14.02%). From the elemental mapping of the heavy metal leached found that Al and Si still exist inside particle even though it was stimulated from the leaching test. Therefore, it can be indicated that the right bottom of picture is fly ash particle.

On the other hand, the mapping shows that Cu, Ni, V, and Zn are scattering everywhere but in low concentration. This may be because the concentration of these metals in CFA 15 quite low.

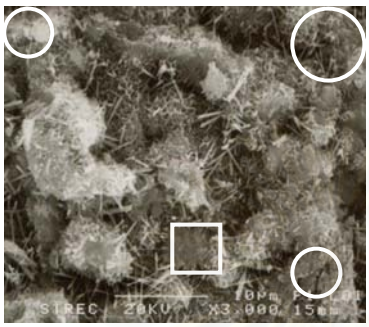

(a) Image, 3000x

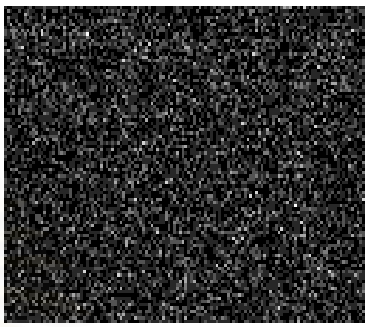

(b) Cu Mapping

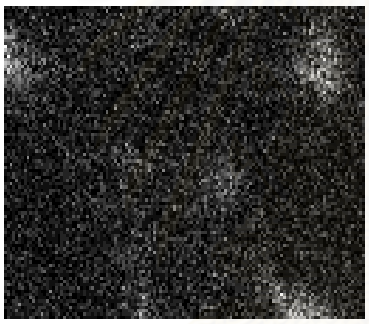

(c) Fe Mapping

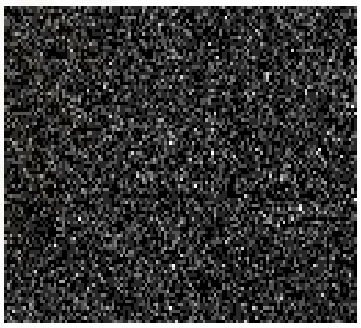

(d) Ni Mapping

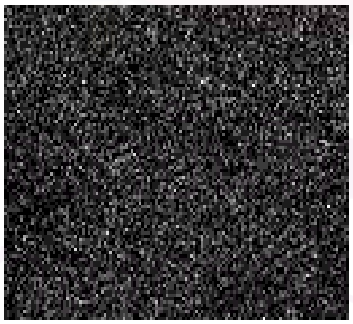

(e) V Mapping

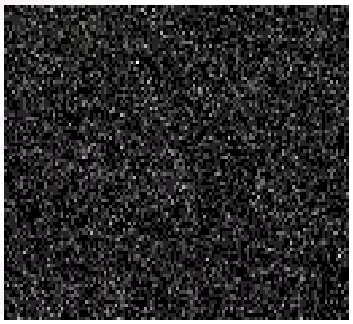

(f) Zn Mapping

Figure 4.48 Element Mapping of CSFA 15 at 90 days

Note: □ = Spent FCC Catalyst
○ = Fly Ash

(g) Al Mapping

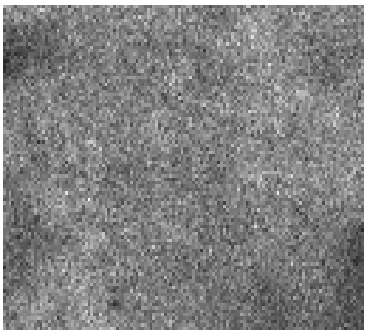

(h) Ca Mapping

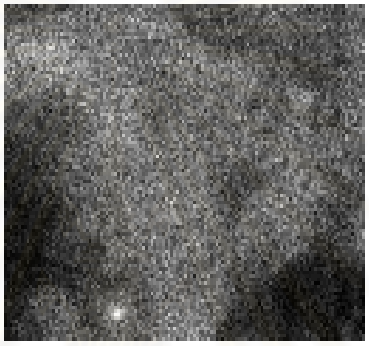

(i) Si Mapping

Figure 4.48 Element Mapping of CSFA 15 at 90 days (Continued)

As seen from the element mapping of CSFA 15 at 90 days in Figure 4.48, the Cu, Ni, V, and Zn in the mapping have low concentration and their density is about the same in every part of pastes. As a result, it cannot be used to interpret the concentration of these components. However, the result from Fe, Al, and Si mapping indicate that high concentration of these elements in the CSFA paste, especially where the spent FCC catalyst and fly ash were. Most of Fe in CSFA 15 came from fly ash but Al and Si came from spent FCC catalyst more than fly ash and Portland cement. In addition, these is high concentration of Ca all over the image except the spent FCC catalyst and fly ash were. This is because most of Ca came from Portland cement (63.82%). From Figures 4.46-4.48, it can be seen that the mapping of some element cannot be used because it were found scatting everywhere and same density. This is because the detection limit of SEM equipment is lower (1000 ppm) so it might be detected as noise in result.

4.2.3 Permeability of the Solidified/ Stabilized Materials

The movement of aggressive solutions into cement mass or the removal from cement of dissolved reaction products plays an important factor to determine the rate of progress of cement paste deterioration caused by chemical attack. Permeability of the cement is; therefore, fundamental in determining the rate of mass transport relevant to destructive chemical action. It should be recognized that all of the cementitious material and some of aggregates are inherently subject to attack, not only sulphates, chlorides, acids, organic and inorganic agents, but by water also (Bach, 1991). Given any combination of cement and aggregate, it is generally observed that the less permeable cement.

Mercury intrusion porosimetry (MIP) is very informative to determining pore sized distribution, density, and specific surface area of porous materials. The pore size distribution is approximated by estimating the intruded volume of mercury under pressure. MIP, used to study the micro porosity of the cement paste after 28 and 90 days of curing time by means of the average pore diameter. In addition, it used to characterizing the influences of spent FCC catalyst and fly ash on the micro porosity of cement pastes bond.

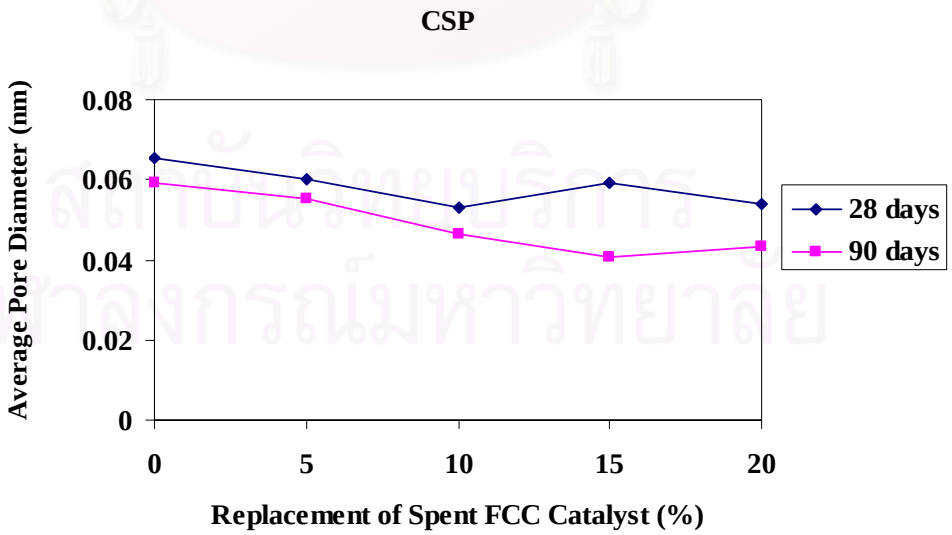

Figure 4.49 Comparison Average Pore Diameter of CSP pastes at the age 28 and 90 Days

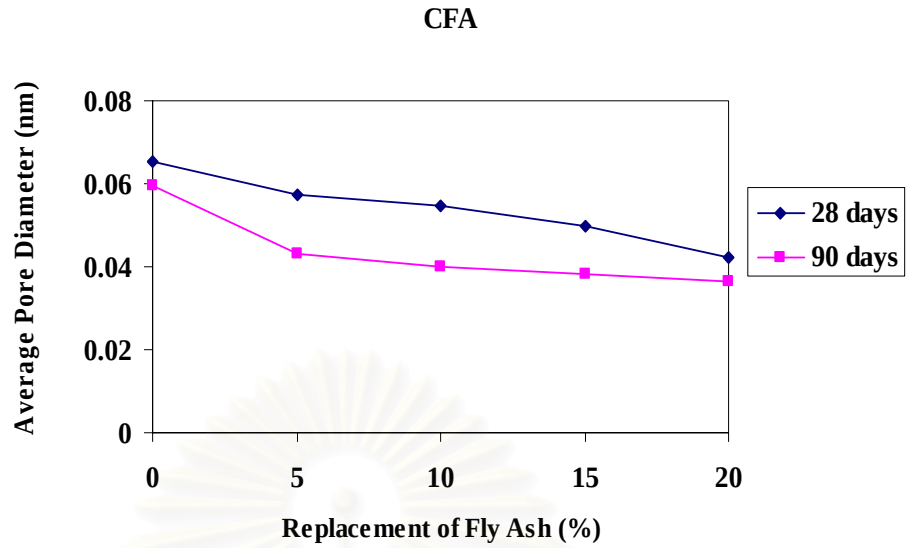

Figure 4.50 Comparison Average Pore Diameter of CFA pastes at the age 28 and 90 Days

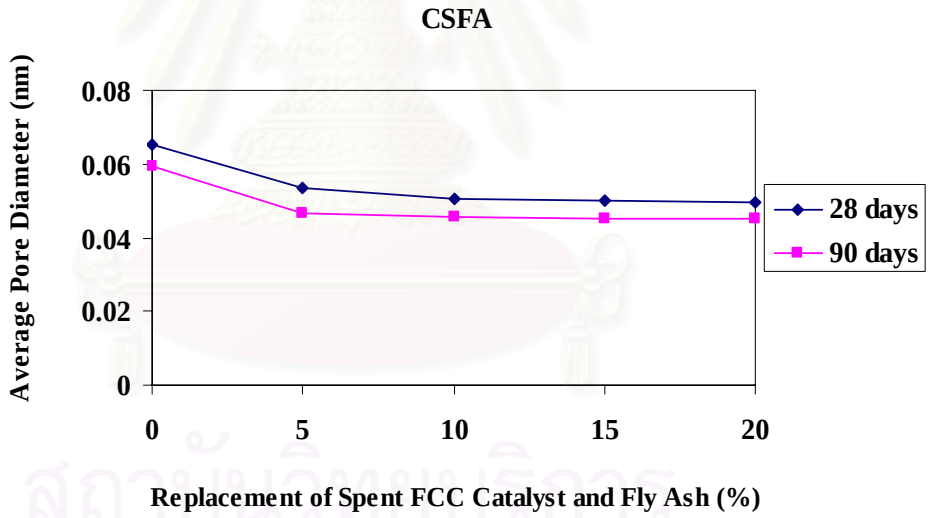

Figure 4.51 Comparison Average Pore Diameter of CSFA pastes at the age 28 and 90 Days

Figures 4.49-4.51 show the effect of percent replacement of spent FCC catalyst and fly ash on the average pore size in cement pastes at age 28 days and 90 days. It can be observed that the average pore size of additives sample (CSP pastes, CFA pastes, and CSFA pastes) is decreased at the respective period of hydration. Due to the gradual filling of large pores by the hydration products of cementitious

materials but the extent of decrease is variable. It is a greater decrease for CSP paste and CFA pastes and comparatively less for CSFA pastes. In the case of CSP pates and CFA pastes, the average pore size tends to decrease as percent replacement increases. The possible reason to explain this situation is the addition of spent FCC catalyst and fly ash in the cement paste will increase the hydration and pozzolanic reaction in cement pastes by decreasing the total porosity of cement pastes. The pore sizes become finer and finer as hydration process, pozzolan action and the progress of time. The cement hydration products continues to gradually fill in pores such as ettringite, C-S-H crystalline, Portlandite, and other products. From the initial to the ultimate of curing time, the pore sizes of CSP pastes, CFA pastes and CSFA pastes are finer than the control.

Evidently, the difference of pore size value between control and additive samples are quite smaller. This is because the pozzolanic activity will occur after 28 days of curing time. As a result, its product gradually fill in pores structure like hydration product. When the pozzolan material is replaced in cement pastes, two mechanisms should be considered; (1) it is gradual filling in pores structure and (2) it is products C-S-H crystal. Therefore, the empty spaces or the total porosity structure in cement paste is reduced from the mechanisms. However, presumably as the pozzolanic reaction and the hydration products of spent FCC catalyst and fly ash had developed to fill the empty spaces of cement pore at more curing time. Therefore, all of CSP pastes, CFA pastes and CSFA pastes exhibited a significant lower porosity than the control. In addition, since the particle size of ground spent FCC catalyst and sifted fly ash are smaller than Portland cement so it is easy to fill in the pore. This observation is in good agreement with Bach, (1987).

Upon comparing the pore size with difference percentage of CSP pastes, CFA pastes, and CSFA paste. It can be seen that the pore size decreased as percent replacement is higher. This is because it has high quantity of SiO_2 and Al_2O_3 to react with $Ca(OH)_2$ in the pozzolanic reaction, hence producing C-S-H gel more. However, it cannot be concluded that the lower porosity have been occurred at high percent replacement. Because it has another factors controlling the permeability. One of the most important factors is particle size of waste replacement. Especially, larger particle

size of waste replacement in cement will lead to higher permeability than smaller particle replacement (Bishop, 1988). Therefore, waste replacement should be grounded several times before mixing with Portland cement until it has the particle size smaller than Portland cement.

The influence of mixing spent FCC catalyst and fly ash in cement (CSFA) is shown in Table 4.12 by used CSP pastes and CFA pastes as reference. It is evident that the average pore diameter between CSFA pastes is insignificantly different. However, the average pore diameter of higher percent replacement is larger than smaller replacement. In fact, the pore size of CSFA pastes should be lower as high percent replacement because spent FCC catalyst and fly ash exhibited the pozzolan properties, but it is not. This may be because they are different in chemical and physical properties such as particle size, source of collection, pH, and etc. that have effect on the porosity of CSFA pastes.

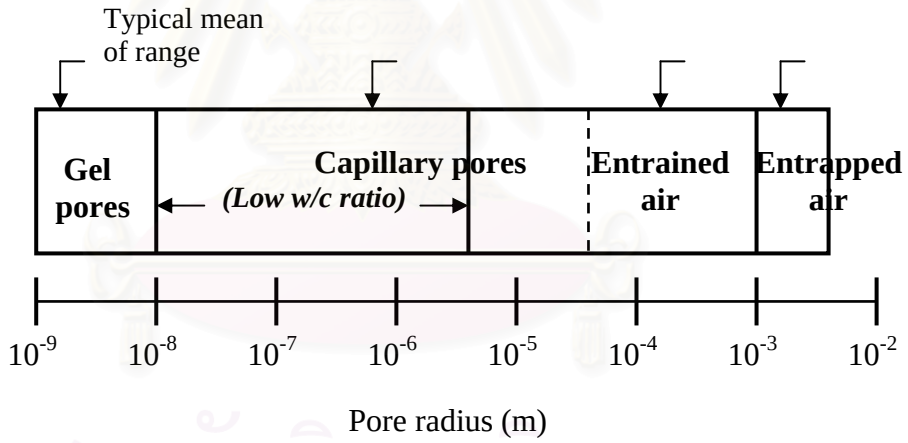

Figure 4.52 Pore Structure in Cement Pastes (Sinsiri, 2003)

The major range of pore structure in cement pastes (Figure 4.52) can be divided into three major types; air voids, capillary pores, and gel pore.

1. Air voids; it occurs during mix cement with water and has the circle shape. It can be divided into two types; if the porosity of pores diameter ≥ 3 mm, it is considered as entrapped air voids while entrained air voids has the pore size between 50-100 μm. Most of entrained air result from add air-entraining admixture during

mixing with cement. However, both types of air void affect strength and permeability of cement paste.

2. The capillary porosity; is the porosity of pores diameter ≥ 0.01 μm. Capillary pore is the water pores that remain from hydration reaction and has irregular shape. The volume and size of these pores depend on the w/c ratio and the reaction in the pastes (Pandey and Sharma, 2000). If the w/c < 0.35, it has the capillary pore in the range of 10-50 nm. while it have the pore size between 3-5 μm for w/c > 0.50.

3. Gel pores; the pores with diameter < 0.01 μm are considered as gel pores whose effects on permeability should be counted differently. This assumption is made based on the findings of Cui and Cahyadi (2001) that the pores with diameter < 0.029 μm do not affect on the permeability much. The physical meaning of gel pores is the pore that cannot be found the connected path throughout the sample.

The pore size distribution of cement pastes cured at 28 and 90 days is shown in Figure 4.53- 4.55. It is clearly seen that the permeability of cement paste is directly correlated with percent replacement and type of waste material. Due to the average pore diameters reveals remarkable difference. From this figure, peaks between the incremental intrusion volumes and pore diameter are shown two major of peaks. The first peak is larger than 10 μm and the second is always smaller than 10 μm.

For the control, at 28 days, the volume of pore size between entrained air voids and capillary pore is insignificant different. With more curing time, the pore size became finer than beginning. However, at these days, big pore diameter that is defined as entrained air still existed in the control. It can be seen that it has the volume of pore diameter between 70-100 μm.

For CSP pastes, at the age 28 days, the major peak of CSP pastes is appear at the pore diameter between 1-100 μm so it can be defined as entrained air voids; however, the capillary pore also appears but it still has small intrusion volume. At this

day, the incremental intrusions of CSP 15 and CSP 20 have higher at pore diameter 36.29 nm and 24.32nm, respectively which means that they have more air void. In 90 days, most of pore diameter of CSP pastes can be found in the pore range 0.01-0.1 μm, which are in capillary porosity and gel pore range. However, entrained air voids still appear in the pastes that this pore can be affected to permeability of cement pastes.

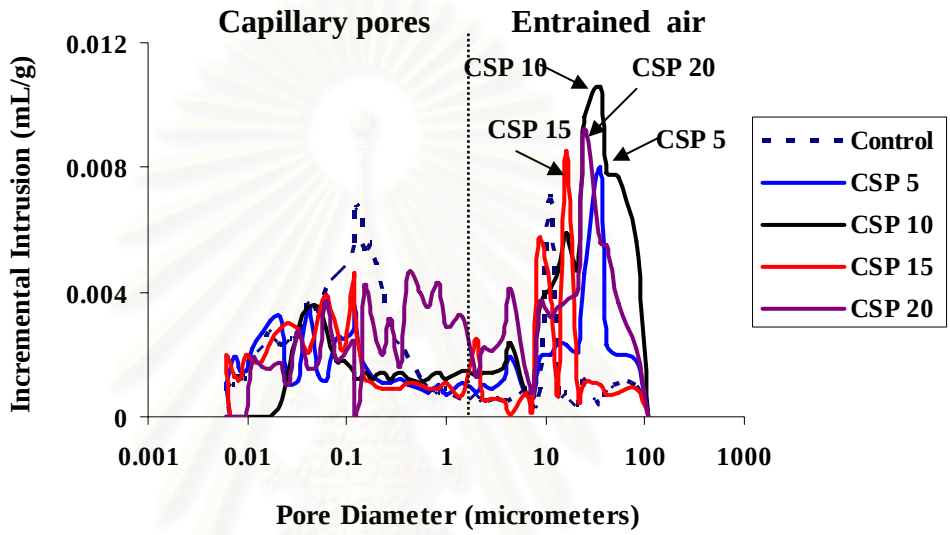

(a) 28 days

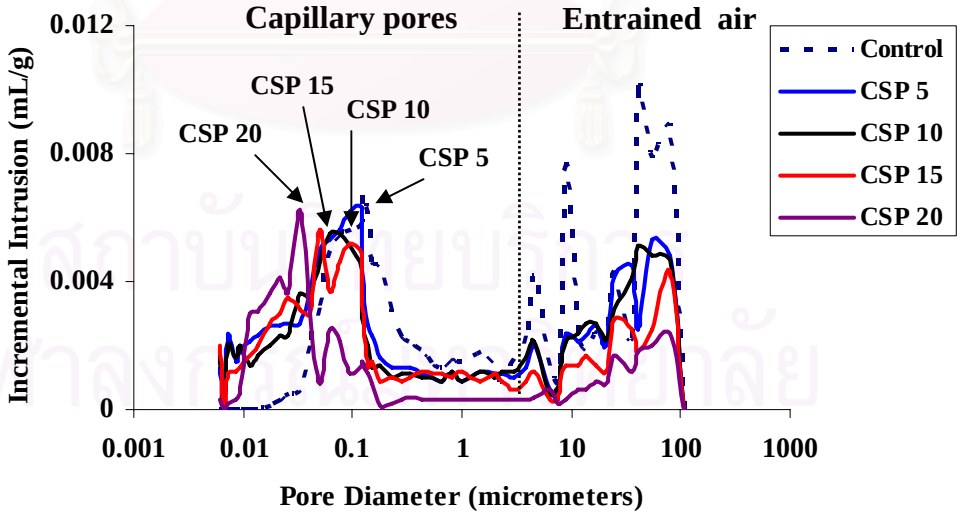

(b) 90 days

Figure 4.53 Incremental Intrusion and Pore Size Distribution of CSP pastes, (a) at 28 days and (b) at 90 days

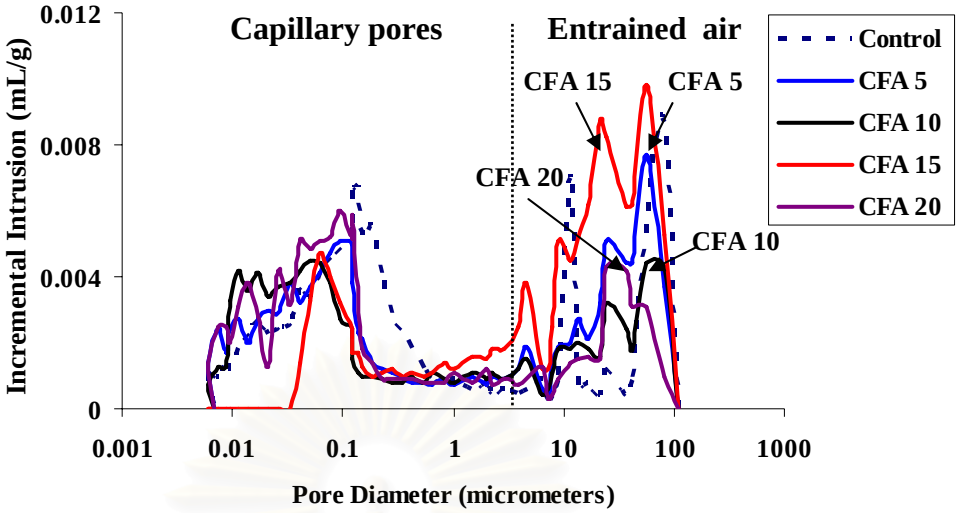

(a) 28 days

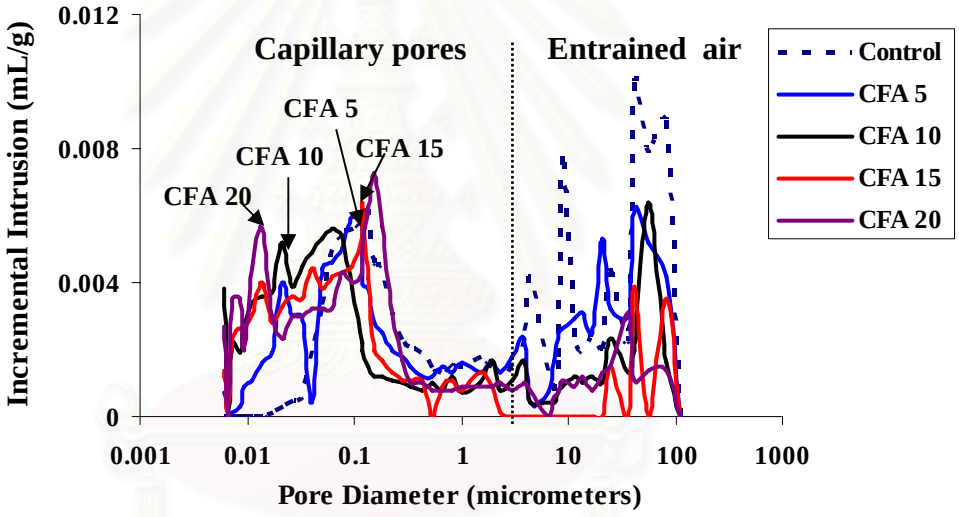

(b) 90 days

Figure 4.54 Incremental Intrusion and Pore Size Distribution of CFA pastes, (a) at 28 days and (b) at 90 days

For CFA pastes, it can be separated into two major peaks, the pores diameter between 0.01-0.1 μm and the pores diameter between 10-100 μm. With more curing time, peak of CFA pastes have changed because the intrusion volume is higher at the range between 0.01-0.1 μm. From this evidence, it can be concluded that the pore size became smaller with the increase of curing time. After 28 days of curing, the reaction of fly ash in cement paste almost complete. In addition, more intrusion volume for smaller pore in CFA pastes than control at later age. The amount of the capillary pore

in CFA 20 higher than another CFA pastes both 28 and 90 days of curing. Nevertheless, the pore size between diameter 0.01-0.1 μm and 10-100 μm of CFA 5 is insignificantly different.

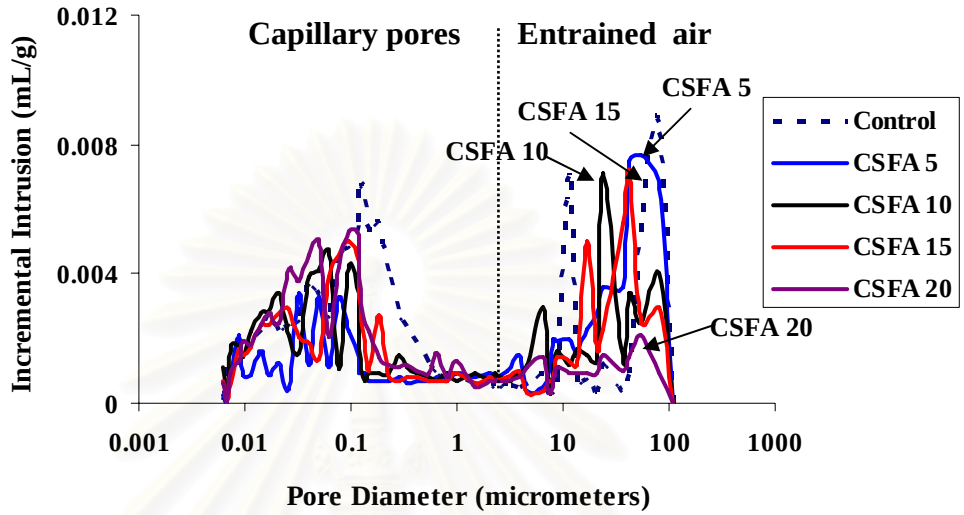

(a) 28 days

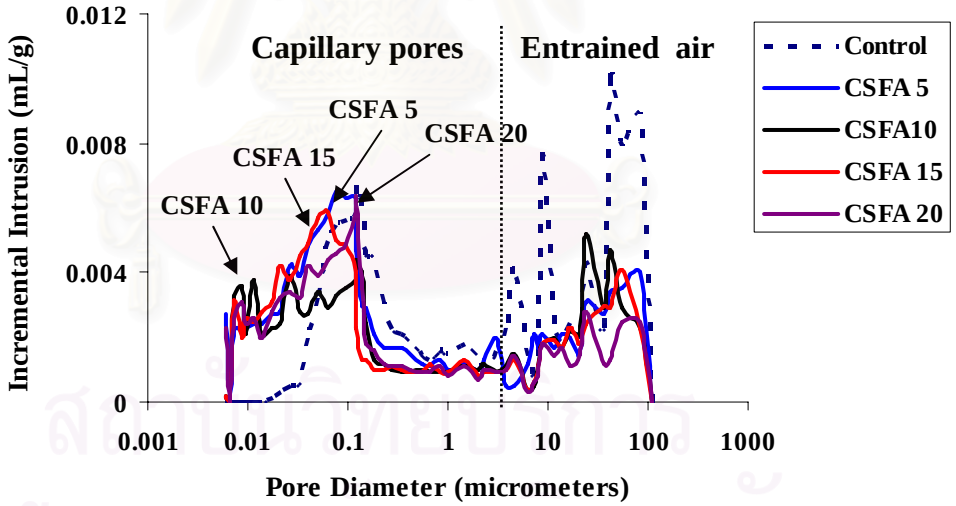

(b) 90 days

Figure 4.55 Incremental Intrusion and Pore Size Distribution of CSFA pastes, (a) at 28 days and (b) at 90 days

The major peak of pore diameter of CSFA pastes can be divided into two major types, which similar to CSP pastes and CFA pastes but it is differenced in term of incremental intrusion volume. Both of 28 and 90 days, the amount of pore size

between the range of 0.01-0.1 μm and 10-100 μm is not different which means that it is not homogenous. In addition, the volume of capillary pore in each CSFA paste almost similar.

The effect of heavy metal in CSP pastes, CFA pastes and CSFA pastes on the pore size is not significantly different. This is because the pozzolan material of spent FCC catalyst and fly ash capture heavy metal inside the pastes. As a result heavy metal intruded volume lower than the control. Another investigators (Halim et al. 2004) show that the effect of heavy metal in the paste. The cement hydration is reduced by greater than 50% and at the same time significantly increase observable porosity. However, in this experiment, heavy metals in spent FCC catalyst and fly ash does not pose serious problem on permeability of cement paste. This is because the amount of metals in sample is lower. From this result, it is interested to increase the quantity of heavy metal in cement paste until it shows the negative effect to environmental.

Upon comparing the effect of percentage variation in term of incremental intrusion and pore size of control, CSP pastes, CFA pastes, and CSFA paste. From Figures 4.53-4.55, it can be to noticed that there are no significantly different in each sample (except, control). Since the amount of the two major peaks are similar. Therefore, used the average pore diameter that is explained in the last topic instead.

The permeability testing can be related to the leachablity of metals in solidified/stabilized material in Section 4.2.4. It reveals that the decreasing of pore diameter as a result the metal concentrations in leachate are significantly reduced.

4.2.4 Leaching Characteristics of the Solidified/Stabilized Materials

The extraction results from two types of leaching procedures on the 13 different solidified/stabilized (S/S) materials are shown in Figures 4.56 - 4.57 in which the concentration (ppm) of Cu, Fe, Ni, V, and Zn are given along with pH of the leachate. According to the results, there are interesting issue that should be taken into consideration.

The comparison of the extraction test between the TCLP test and LP-No.6 extraction test is made. From Figures 4.56 and Figure 4.57, it can be clearly seen that, all of S/S materials, pH and the concentration of Cu, Fe, Ni, V, and Zn in the leachate subject to the TCLP are not significantly different from that submitted to LP-No.6 extraction test.

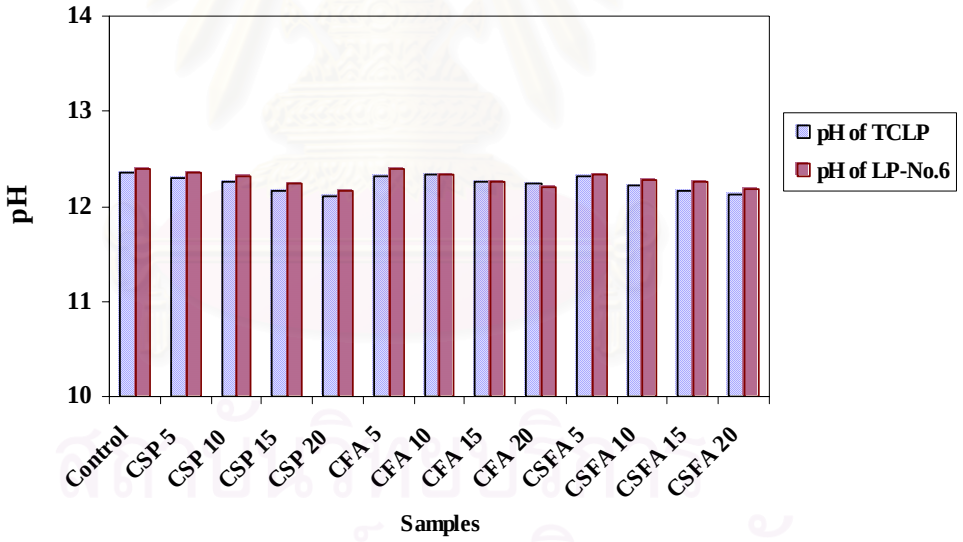

Figure 4.56 pH Extraction by the TCLP and LP-No.6 of all S/S materials

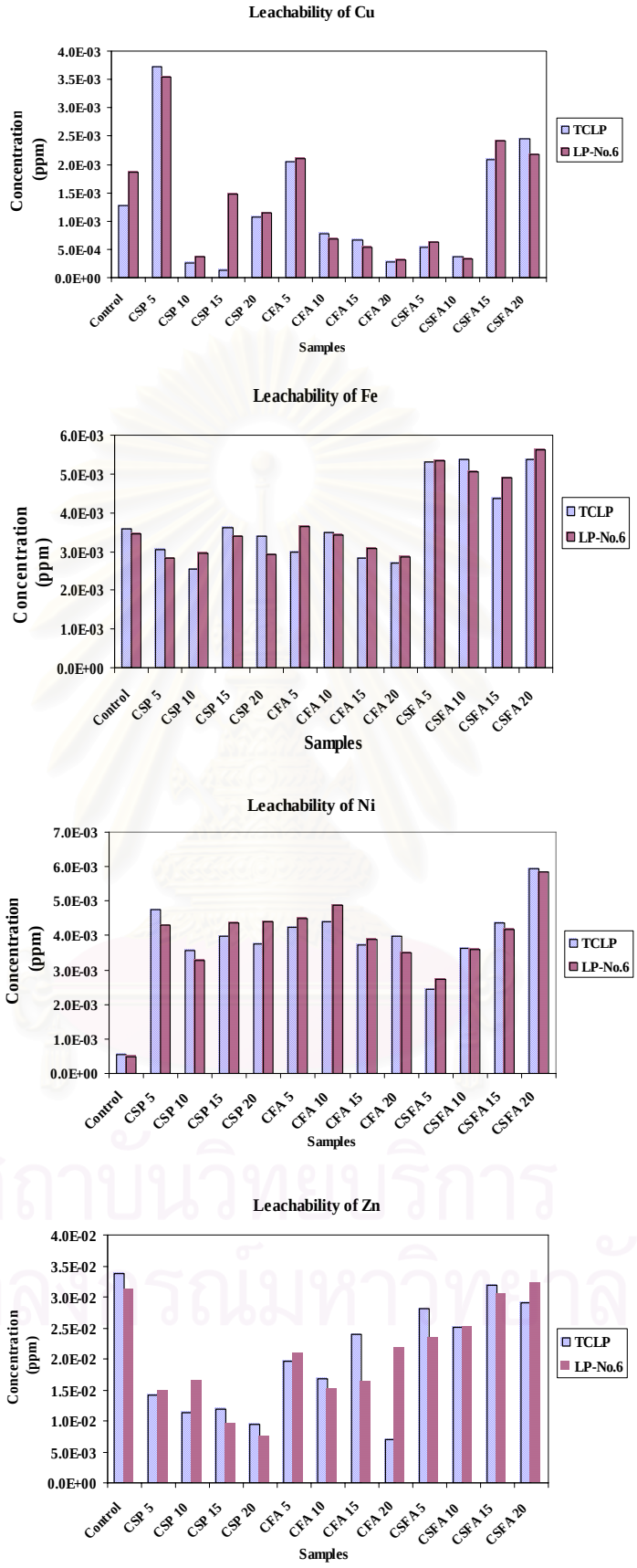

Figure 4.57 Concentration of Copper (Cu), Iron (Fe), Nickel (Ni), and Zinc (Zn) in Leachate of all S/S Materials Extracted by the TCLP and LP-No.6

4.2.4.1 Factor Affecting to the Leachability of S/S Materials

To clarify this issue, the factors that controlling leachability are investigated in detail into two broad categories; the properties of waste itself and a function of the leaching test or disposal environment (Corner, 1993). Under the assumption of the properties of spent FCC catalyst and fly ash such as chemical, physical, and biological properties of waste are different. In another way, except pH of extraction fluid, almost all of external factors of the TCLP and LP-No.6 extraction procedures including surface area of waste, particle size, nature of the extraction vessel, the agitation technique, the ratio of extraction fluid to waste, the contact time, temperature, and the method used to separate extract from solid were the same (Tanapon, 2003).

4.2.4.1.1 pH

Another important factor affect to the leachability of S/S materials is pH control. Even though, the initial pH of spent FCC catalyst and fly ash are significantly different, the initial pH value of the extraction fluid of the two leaching procedure are the same. As a result, the leachability of heavy metal by these two procedures is similar. It is not affect to the leachability. As can seen in Figures 4.56 that pH of leachate from all of S/S samples by the TCLP and LP-No.6 are almost similar within pH 12, suggesting that the immobilization mechanism of heavy metal in leachate of solidified products should be similar.

Figure 4.58 and Figure 4.59 shows that the pH value of leachate with long contact time is higher than the one in the initial period of hydration. Most of S/S systems are quite alkaline, usually above pH 12 (at least initial). At the age 28 days, all samples have pH value between 12.10-12.36 for the TCLP test, and 12.16-12.39 for the LP-No.6 extraction tests.

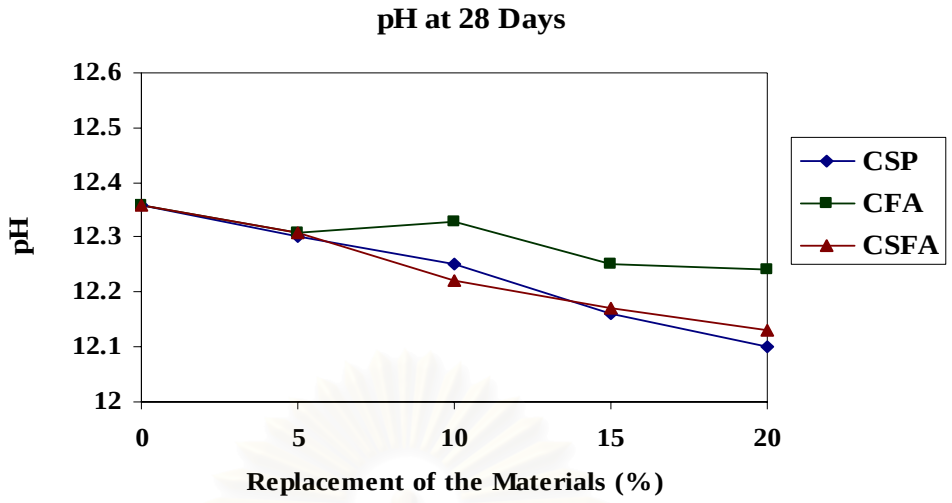

Figure 4.58 pH After Filtrate at Day 28 Determined by the TCLP Test

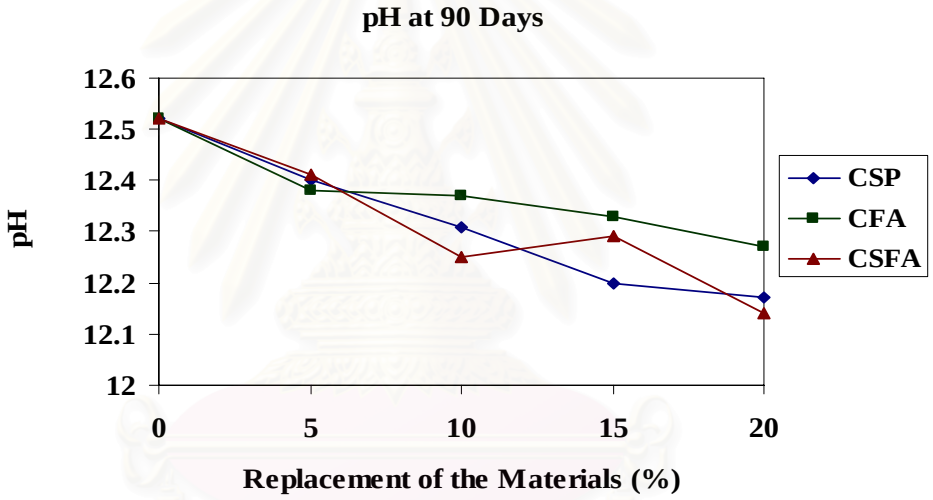

Figure 4.59 pH After Filtrate at Day 90 Determined by the TCLP Test

4.2.4.1.2 Solubility

It is widely accepted that solidified/stabilized-base waste forms rely heavily on pH control for metal containment. However, it should be noticed that each metal has the maximum solubility not the same pH. When the system becomes acid condition, as it does in the TCLP test and LP-No.6 extraction test, metal hydroxide becomes very soluble. The concentration of dissolved solid in the leachate should depend on total metal content where metal content exceeds its soluble as metal hydroxide. This is illustrated by the solubility curve of various metal hydroxides in water as shown in Figure 4.60

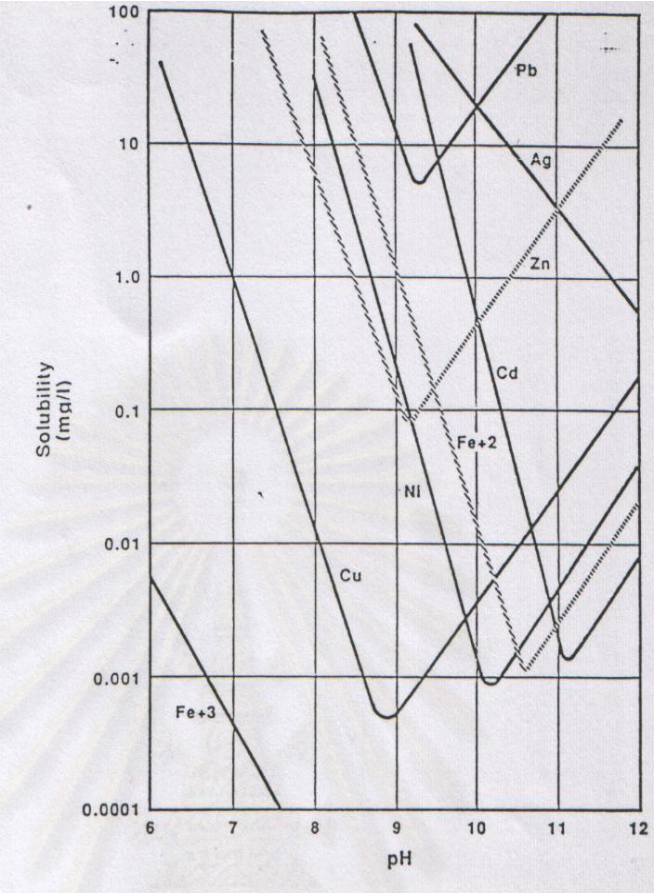

Figure 4.60 Solubility of Metal Hydroxide as a Function of pH (Corner, 1990)

Since pH in the cement pore solution is above 12, thus, Zn and Cu remain in soluble form and they are available to participate in the cement reaction. On the other hand, Fe and Ni are present as a semi-solid form so they might be not participate in cement reaction. However, the solubility data in Figure 4.60 is obtained from the calculation in the stability constants of individual species alone and in a specific solvent. Therefore, different results were obtained when different experimental conditions were used.

4.2.4.2 The Cumulative of Metals in the Leaching Tests

The cumulative of metals in the leaching tests are reported in Figures 4.61-4.64. Here, it can be seen that the absolute quantity released is much smaller in all of test. In addition, all of pastes show that the leaching concentration tend to reduce with more curing time.

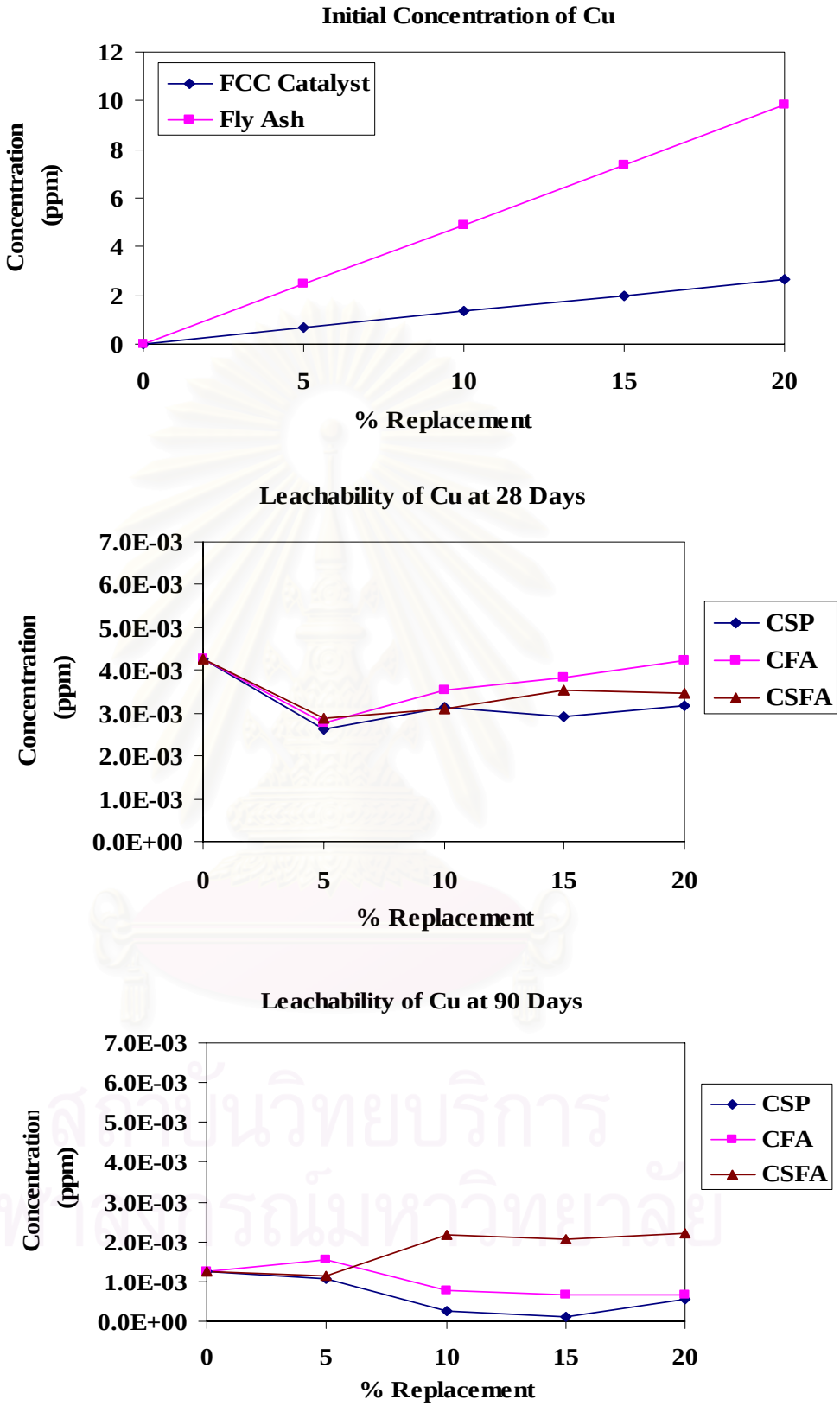

Figure 4.61 The Relationship between Initial Concentration and Leaching Concentrations of Copper (Cu) at the age 28 and 90 days of Curing Period Determined by the TCLP Test

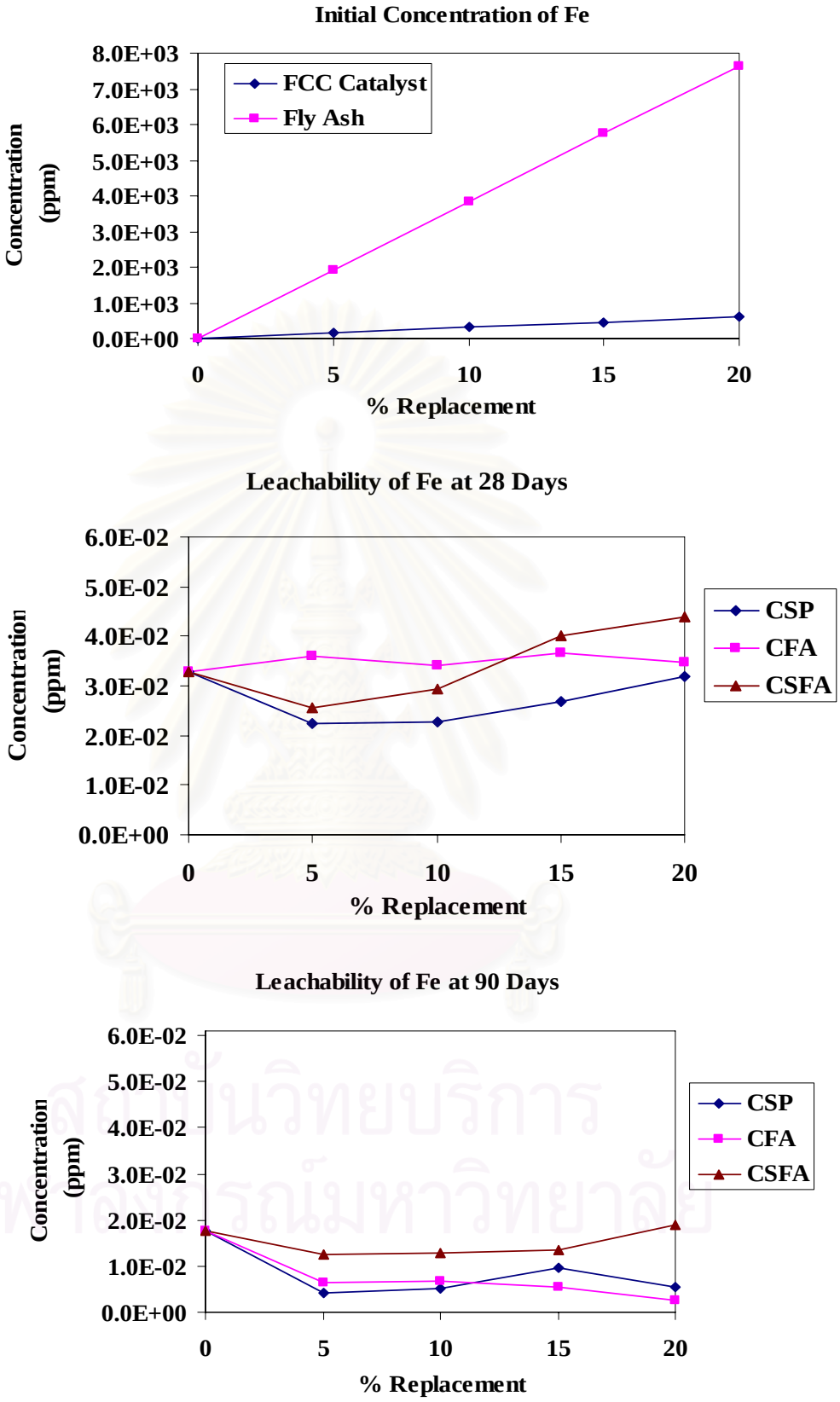

Figure 4.62 The Relationship between Initial Concentration and Leaching Concentrations of Iron (Fe) at the age 28 and 90 days of Curing Period Determined by the TCLP Test

4.2.4.2.1 Copper (Cu)

In the case of Cu, the leaching concentration of Cu from fly ash is much higher than spent FCC catalyst. The results of each sample (CSP, CFA, and CSFA pastes) at age 28 days are quite similar, in spite of the amount of Cu are different in each sample. This may be because the reaction in cement pastes might be not completed at these days. However, after that the leaching value began to change. It can be seen that the concentration of Cu in CSFA, especially in CSFA 10, CSFA 15 and CSFA 20 have higher leaching value than CSP and CFA pastes. This is because Cu in pastes may exist as copper hydroxide phases or copper hydroxide precipitated on the surface of $Ca(OH)_2$ and C-S-H particles that leading to lower permeability of cement paste (Li et al., 2001).

4.2.4.2.2 Iron (Fe)

At 28 days, CSP 20, CFA 20, and CSFA 20 have higher leaching concentration than smaller percent replacement. However, it is interested to note that the leachability of Fe between CFA pastes are not different. Even through, the initial concentration of Fe in CFA 20 is much higher than another CFA pastes. So it should be released more. This may be because they form a new phase that can be detected in XRD. As a result the leaching concentration is reduced. The new phase of Fe that can be found in CSP, CFA, and CSFA pastes are Fe_2O_3, Fe_2SiO_4, $FeCO_3$, Fe_2O_3, $FeAl_2O_4$, $Ca_2FeAl_2(SiO_4)(Si_2O_7)OH_2$-$H_2O$, and $Ca_4Fe_5Al_{16}O_{14}$. The reduction of Fe in the leaching result correlates well with the finding from XRD result. This is confirmed by Stephan et al. (1999) who found in their work that Fe could be reacted with $Ca(OH)_2$ to produce $Fe(OH)_3$ and precipitate on the surface of cement pastes or entrapped in C-S-H crystals. All of these lead to the reduction of leachability of Fe compounds. The leachate of CSP paste, CFA pastes, and CSFA paste also have lower Fe concentration than control. This is because they have smaller amount of C-S-H crystals to entrap metals.

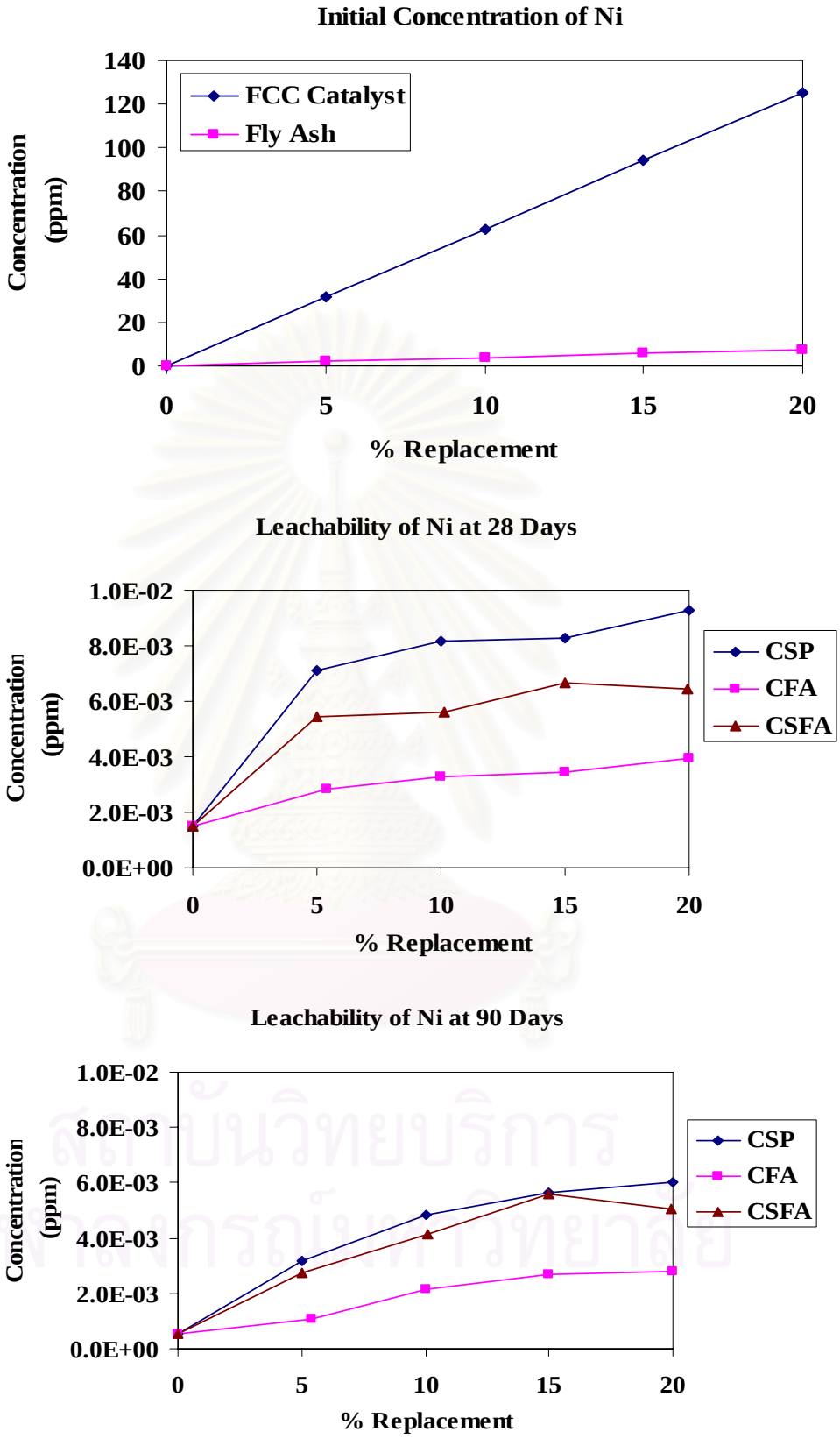

Figure 4.63 The Relationship between Initial Concentration and Leaching Concentrations of Nickel (Ni) at the age 28 and 90 days of Curing Period Determined by the TCLP Test

4.2.4.2.3 Nickel (Ni)

The leaching concentration of Ni is much lower than the other metals. Figure 4.63 shows that the initial concentration of Ni in spent FCC catalyst is much higher than fly ash and Portland cement. This is because Ni is a major contaminant in spent FCC catalyst that decomposes and deposits on the FCC catalyst surface during the operation process (Furimsky, 1996). As a result, CSP pastes, especially CSP 20 has the highest concentration of Ni in the leaching (0.00928 ppm). However, at age 90 days, the leaching concentration of Ni is quite lower than the initial. In can be seen that the concentration between CSP and CSFA pastes are not different. For CFA paste, especially CFA 5, it has lower concentration, which is only 0.00105 ppm. In addition, the leachate of Ni in CFA pastes are lower than CSP and CSFA pastes. This may be because small amount of Ni is found in fly ash and Portland cement. In addition, it can be predicted that most of Ni in the CSFA pastes came from spent FCC catalyst. Moreover, when the pozzolanic action progress, it produces more C-S-H crystal to entrap Ni resulting lower leaching of Ni from cement pastes (Roy et al., 1991).

4.2.4.2.4 Vanadium (V)

In the case of V, the leaching results is much lower than detection limit of ICP (0.007 ppm) as a result it can be shown only the estimate value was < 0.007 ppm. In addition, SEM and XRD were never detected the hydration product of V. This may be because it had only small amount in waste.

4.2.4.2.5 Zinc (Zn)

Figure 4.64 reveals the presence of Zn in the leachate of all pastes. The initial concentration of Zn in spent FCC catalyst is much lower than fly ash. As a result, the amount of Zn in the leachate from CSP pastes is lower than CFA and CSFA paste. For CFA pastes, at age 28 days, CFA 10 and CFA 15 have leaching concentration of Zn lower than another CFA pastes are 0.0345 ppm and 0.0367 ppm, respectively. It can be seen that the leaching concentration of CFA pastes at 90 days is less than that

of 28 days, especially in CFA 15 which is reduced to 0.0128 ppm. For CSFA pastes, the leaching concentration of CSFA 20 at age 28 days is 0.0341 ppm, which is higher than other pastes. In addition, the leaching concentration of CSFA pastes at 90 days is still higher than CSP and CFA pastes. The leaching concentration of Zn between age 28 days and age 90 days of the control sample are very similar. It means that after 28 days the reaction in cement pastes almost complete and it cannot increase stabilization of Zn. Moreover, in an alkaline condition, the soluble zinc salts exist as zinc hydroxyl, $Zn(OH)^{-}$ and $Zn(OH)^{-}_{3}$ (Coke et al., 1992).

The main mechanism of Zn in the cement pastes that retardation the hydration may be summarized as follows:

1. Sorption onto surface area of C-S-H. Zn from solution is adsorbed onto the surface of cement particles and inhibited the hydration of cement,

2. Precipitation of Zinc hydroxide due to high pH, and

3. Incorporation into C-S-H. However, in the case of low concentrations, Zn could incorporate into the C-S-H without other products. The site of incorporation may be either replacement of Ca^{2+} or link directly at the end of silicate chains through Zn-O-Si bounds (Rose, Moulin, Mason, Bertsch, Wiesner, Bottero, Mosnier, and Haehnel, 2000).

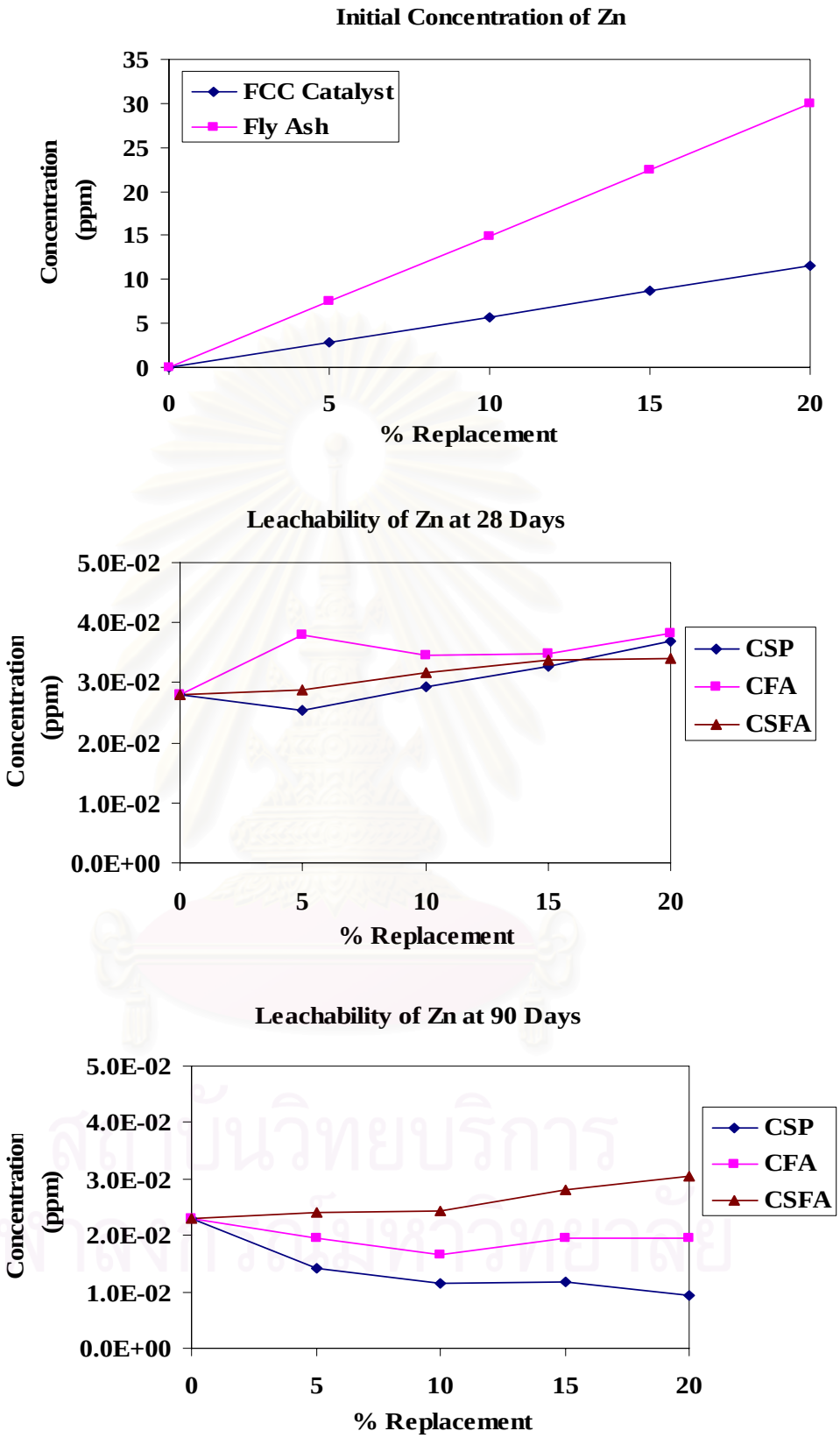

Figure 4.64 The Relationship between Initial Concentration and Leaching Concentrations of Zinc (Zn) at the age 28 and 90 days of Curing Period Determined by the TCLP Test

4.2.4.3 The Relationship between the Leachate Concentration and Average Pore Diameter

The concentrations of Cu, Fe, Ni, V, and Zn in leachate were found to decrease relatively to pore size distribution as well as hydration and pozzolanic action of cement paste. Figure 4.65-4.68 showed the relationship between concentration of these metals in leachate and average pore diameter of CSP pastes, CFA pastes and CSFA pastes. It can be seen that the leachates of metal depends on the pore size of cement pastes.

4.2.4.3.1 Copper (Cu)

Cu concentration in leachate of CSP pastes is shown in Figure 4.65. At the age of 28 days, CSP 10 and CSP 20 had lower concentration at the average pore diameter of 0.0532 nm and 0.0541 nm, respectively. At later time, the Cu concentration of CSP pastes is lower than earlier. Especially in CSP 15, its average pore diameter decreased to the average pore diameter of 0.0408 nm, its Cu concentration in leachate decreased to 0.0012 ppm. From this result, it can be seen that the decreasing of the average pore diameter leading to low Cu concentration in leachates. For CFA pastes, the Cu concentrations in leachate of CFA 5 reduced from 0.00277 ppm to 0.00180 ppm at average pore diameter of 0.0576 nm and 0.0432 nm, respectively. For CFA 10, CFA 15 and CFA 20, the Cu concentration in leachates decreased when the average pore diameter reduced. From these results, CFA 20 had lower copper concentration in leachate (0.00062 ppm) and had lower average pore diameter (0.0364 nm) than other CFA pastes. Therefore, it can be concluded that the higher amount of fly ash replacement in cement paste, the lower leaching concentration behavior and smaller pore size. For CSFA pastes, CSFA 5 had lower Cu concentration in leachate and low average pore diameter. The Cu concentration in leachate of CSFA 5 at the average pore diameter of 0.0465 nm was 0.00288 ppm and when the average pore diameter decreased to 0.0432 nm, the copper concentration decreased to 0.00115 ppm. Both Cu concentration in leachate and pore diameter tend to decrease in all CSFA pastes with longer curing time.

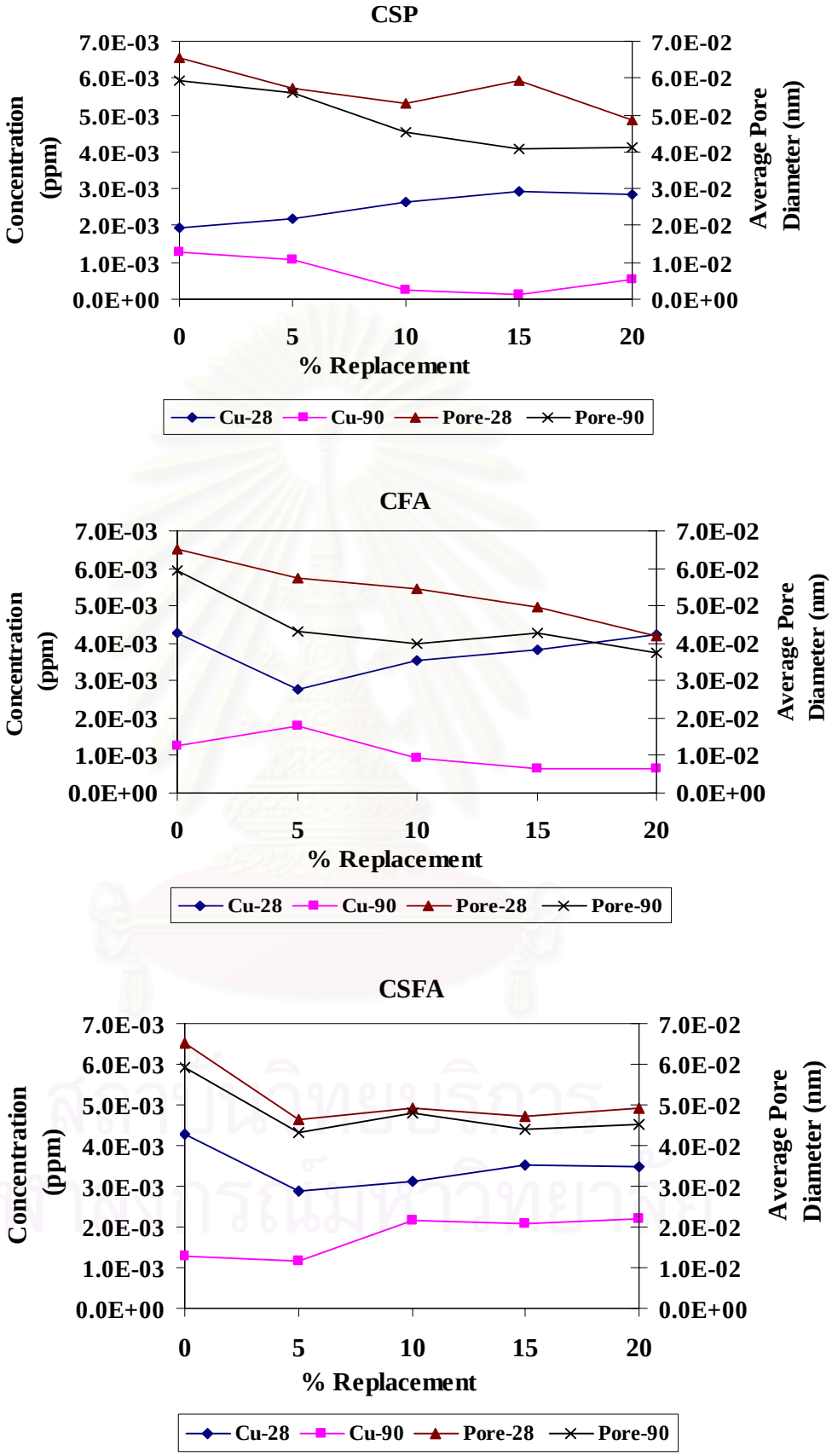

Figure 4.65 The Relationship between Leaching Concentrations of Copper (Cu) and Average Pore Diameter at the age 28 and 90 days of Curing Period Determined

4.2.4.3.2 Iron (Fe)

In the case of Fe, at age of 90 days, the Fe concentrations in leachate were lower than 28 days. For CSP pastes, CSP 5 had the lowest Fe concentration in leachate. The Fe content were 0.0224 ppm and 0.0042 ppm at the average pore size of 0.0572 nm and 0.0561 nm, respectively. For CFA 5 paste, the Fe concentrations in leachate were 0.0360 ppm and 0.0064 ppm at the average pore diameter of 0.0573 nm and 0.0432 nm. CFA 20 had the Fe concentration in leachate lower than other CFA pastes. This behavior is similar to that of CSFA pastes that the average pore diameter relates to its low iron concentration in leachates. These results confirm that Fe could be fixed in cement. The leaching results of Fe correlate well with the finding from XRD results that explained in Section 4.2.1.

4.2.4.3.3 Nickel (Ni)

The relation of Ni content and pore size diameter in leachate was investigated. The CSP paste at early age had larger average pore diameter than the paste at later age. For example, CSP 5 had the concentration of Ni about 0.00711 ppm at the pore diameter of 0.0572 nm but it rapidly lowers to 0.00317 ppm when the average pore diameter decreased to 0.0561 nm. For CFA pastes, the leachates of Ni reduced as the average pore diameter of cement pastes decreased. In the case of CSFA pastes, the Ni concentrations in leachate tends to reduce as the average pore size reduces. For example, CSFA 5, the leachates of Ni concentrations was 0.0054 ppm and 0.0037 ppm at the average pore diameter of 0.0465 nm and 0.0432 nm, respectively.

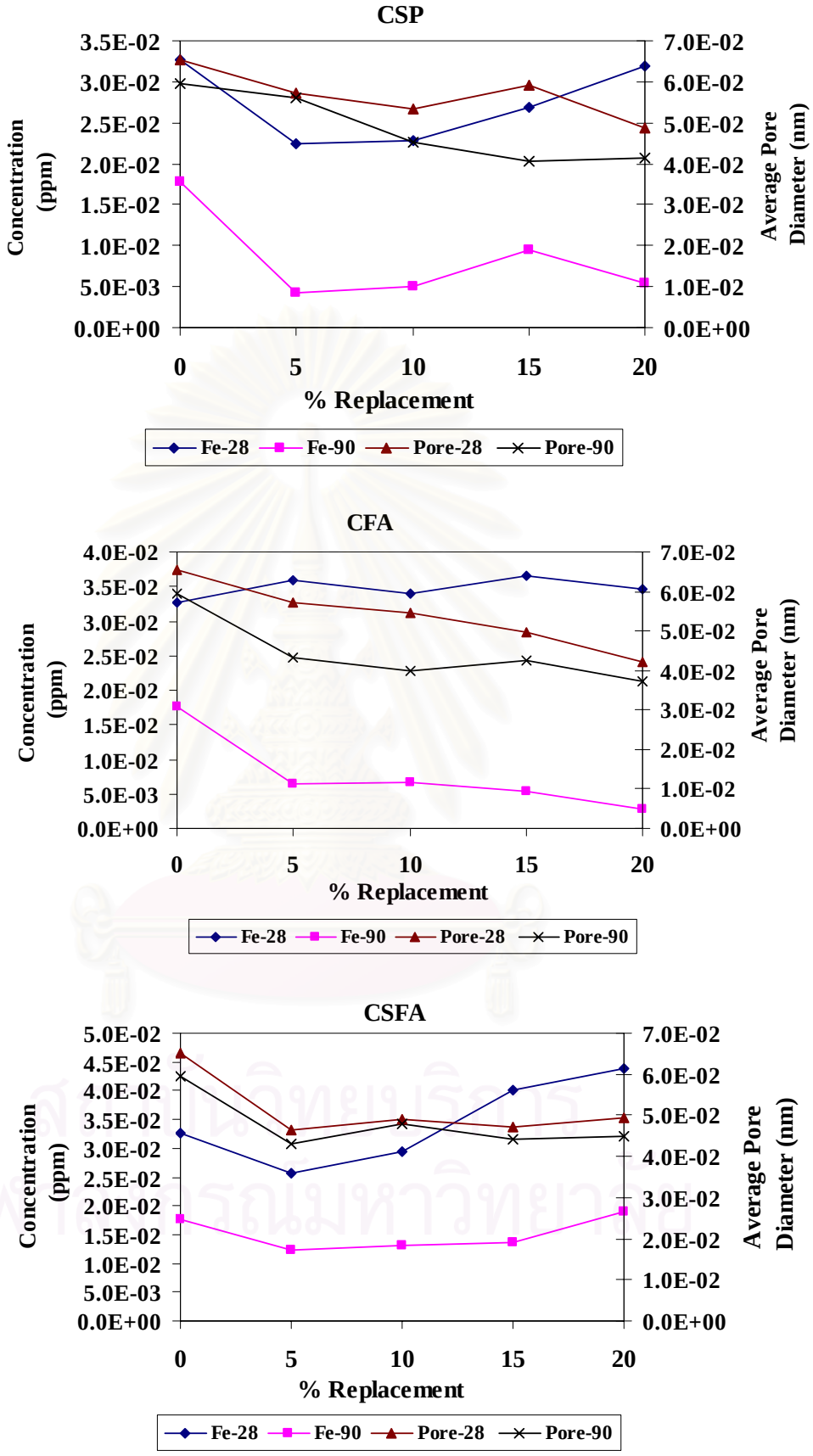

Figure 4.66 The Relationship between Leaching Concentrations of Iron (Fe) and Average Pore Diameter at the age 28 and 90 days of Curing Period Determined

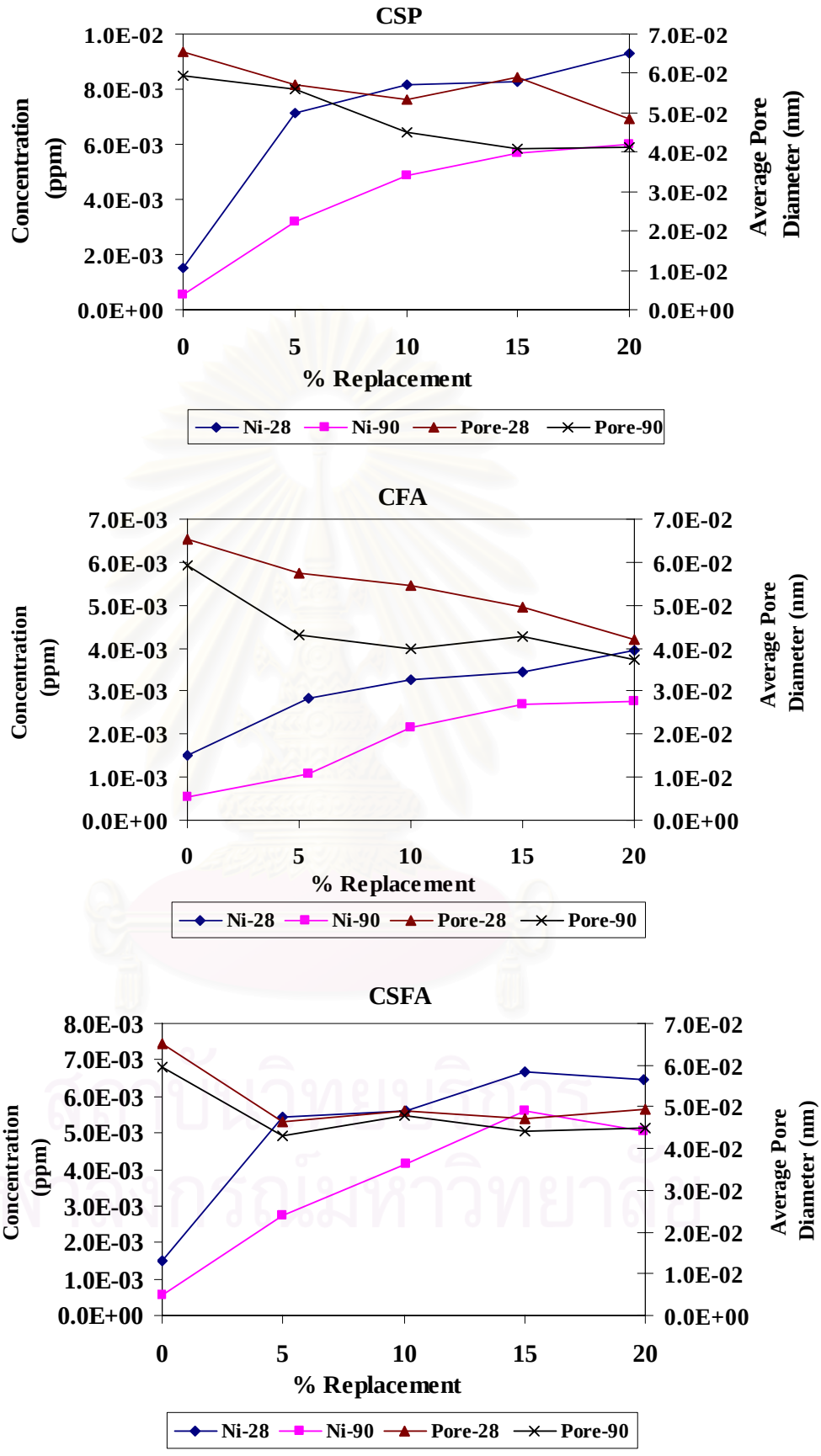

Figure 4.67 The Relationship between Leaching Concentrations of Nickel (Ni) and Average Pore Diameter at the age 28 and 90 days of Curing Period Determined

4.2.4.3.4 Zinc (Zn)

The same result is shown in Zn concentration in leachate. For CSP pastes, at the later age, CSP 20 had lower concentration than other CSP pastes. The concentrations of Zn were 0.0370 ppm and 0.0094 ppm when the average pore diameters were 0.0486 nm and 0.0413 nm, respectively. Similar to CSP 5, CSP 10, and CSP15, the concentration of Zn reduced when the average pore diameter decreased. The leachate of CFA pastes and CSFA pastes are similar to that of CSP pastes, the Zn concentration tend to reduce as the average pore diameter decreases. In the case of CFA pastes, the Ni concentration in leachate of CFA 10 was lower than other CFA pastes. Therefore, high percent replacement of fly ash in cement pastes can reduce the leaching of Zn more. Roy et al. (1991) expressed that percentage of fly ash has influence on leaching rates by reducing the permeability of cement paste. Most investigators (Qin et al., 2003) postulated that the Zn was fixed by hydration reaction, forming a metallic calcium silicate hydrate (almost certainly not a stoichiometric form). Others regarded that Zn reacts readily with $Ca(OH)_2$ to produce possible insoluble compounds which was encapsulated in the silicate (Poon et al., 1985).

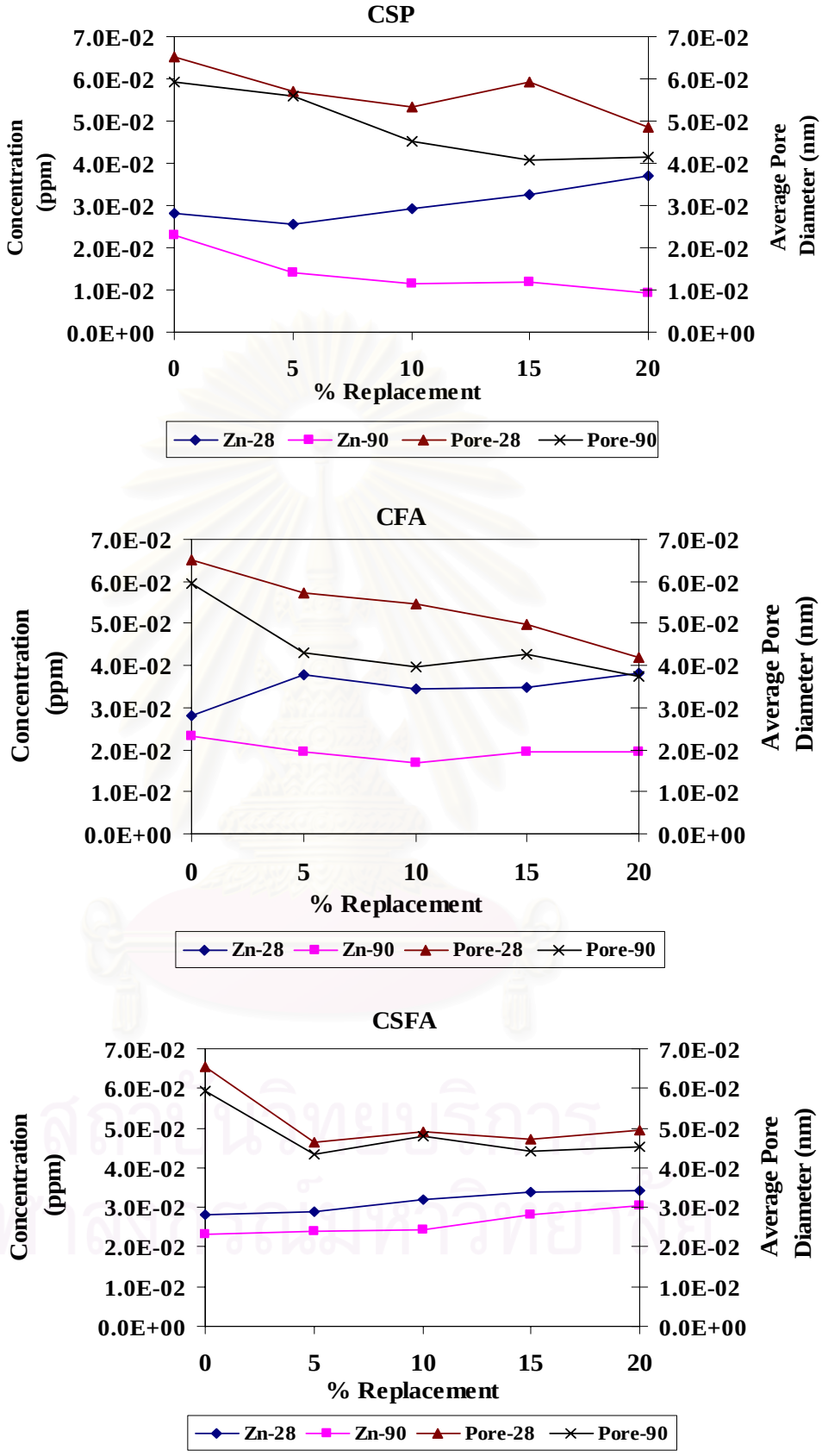

Figure 4.68 The Relationship between Leaching Concentrations of Zinc (Zn) and Average Pore Diameter at the age 28 and 90 days of Curing Period Determined

4.2.4.4 Degree of Immobilization

All results confirmed the “high immobilization” potential of heavy metal from leaching (Figure 4.69). The degree of heavy metals concentration from leaching is quite low because the leachability of heavy metals in waste material is controlled by the solubility of metal compounds in the leachate. It is evident that mechanisms for limit solubility of S/S waste are complex (Constantino et al., 2001). The “leaching rate” of heavy metal in the 90 days of curing time is significantly lower than in the initial period of hydration. This is because the heavy metal in leaching rate was greatly affected by the composition of cement, especially the amount of $Ca(OH)_2$, Al, and Si in cement pastes (Deja, 2002). An optimum of $Ca(OH)_2$ content would show the maximum inhibition of heavy metal leaching (Su et al., 2000). In some case, the degree of heavy metal immobilization from CSP pastes, CFA pastes, and CSFA pastes were higher than in the control because spent FCC catalyst and fly ash have a great potential for binding within the cementitious matrix. However, degree of heavy metal immobilization in different waste types and percent replacement are not significantly different. This is because these waste are pozzolanic materials.

The Thai regulations for consideration of Surface Water Standard and Ground Water Quality Standards for Drinking Water. It is interesting to note that all metals leaching from cement mixture pastes (Control, CSP, CFA, and CSFA pastes) met the regulatory limits. Therefore, spent FCC catalyst and fly ash have a great potential to be utilized as a cement replacement since the leachates from the spent FCC catalyst and fly ash products were legally acceptable. Moreover, it is expected since spent FCC catalyst is classified as non-hazardous waste according to the Resource Conservation and Recovery Act (RCRA).

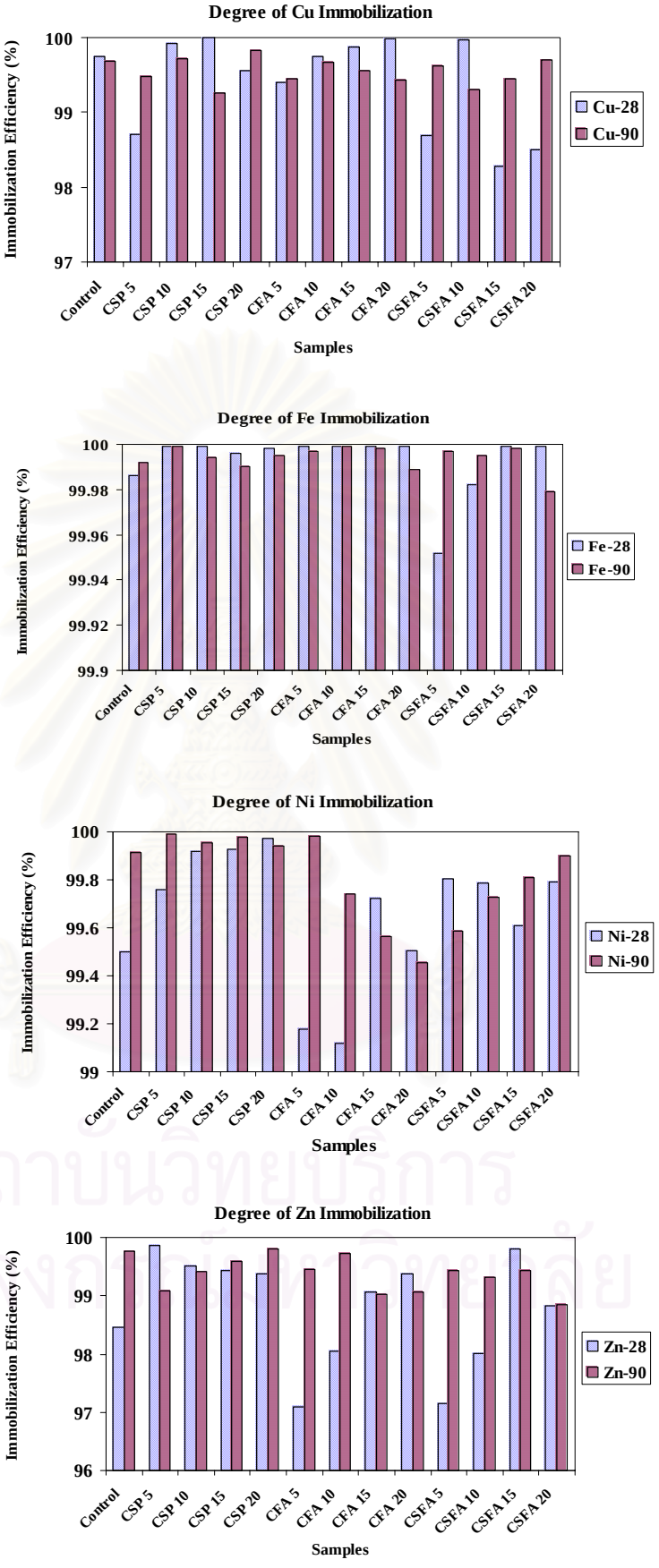

Figure 4.69 Degree of Copper (Cu), Iron (Fe), Nickel (Ni), and Zinc (Zn) Immobilization Determined by the TCLP Test

CHAPTER IV

CONCLUSIONS AND SUGESSIONS FOR FUTURE WORKS

This research was conducted to investigate the mechanism that stabilizes and solidifies heavy metals containment in spent FCC catalyst and fly ash. This was done by relating the effect of physical properties, chemical properties, and mineralogical compositions on leaching behavior of heavy metals from spent FCC catalyst-cement pastes (CSP), fly ash-cement pastes (CFA), and spent FCC catalyst and fly ash-cement pastes (CSFA). The conclusions this study are shown in the following:

5.1 Characterization of Raw Materials

The unground spent FCC catalyst was present mainly in spherical particle. The spent FCC catalyst was grounded and passed through a sieve No. 325 (45 micrometer openings). It has the median particle size ($d_{50\%}$) of 15.7 microns while that of unground spent catalyst is 70.6 microns. Fly ash was sifted through a standard sieve No.200 (75 micrometer opening) but an appearance and particle size between raw fly ash and sifted fly ash particle are not significantly different. Moreover, ground spent FCC catalyst and sifted fly ash have particle size smaller than Portland cement. The advantage of finer particle size is that it is not only suitable to be used in cement pastes but also suitable for cement reaction by increasing surface area and reducing heavy metal leachate. Another advantage of having finer particle size of ground spent FCC catalyst and sifted fly ash is that it may improve the properties of spent FCC catalyst pastes and fly ash paste by enhancing the hydration process. It increases the rate of hydration because there will be small amount of unreacted cement developed inside the grain.

5.2 Chemical and Physical Properties of the Solidification/Stabilization (S/S) Materials

Based on the results obtained after solidified/stabilize material, the following conclusion can be made:

1. The $Ca(OH)_2$ intensity of each pastes increases within the 14 days of curing time and then the $Ca(OH)_2$ intensity starts to decrease. This could be the starting point of pozzolanic reaction occurring in the paste.
2. The higher percent replacement of spent FCC catalyst and fly ash (CSP 20, CFA 20, and CSFA 20), the lower hydration product in the paste.
3. The intensity of heavy metal phase cannot be observed by XRD (except, Fe). Only the small amount of Fe phase can be detected by XRD are Fe_2O_3, Fe_2SiO_4, $FeCO_3$, $(Mn,Fe)_2O_3$, $FeAl_2O_4$, $Ca_2FeAl2(SiO_4)(Si_2O_7)OH_2$-$H_2O$, $22MgO•5Al_2O_3•Fe_2O_3•22SiO_4•40H_2O$, and $Ca_4Fe_5Al_{16}O_{14}$. Even though, the intensity of these phase is smaller but it affect to the lechability of Fe in solidified waste. Because it shows higher immobilization degree (about 99.94% - 99.99%).
4. The decreasing rate of $Ca(OH)_2$ crystal in the CSP pastes, CFA pastes, and CSFA pastes relates to the lower in heavy metal content in leachate. The result shows that the pozzolanic action plays an important role in the fixation of these heavy metals.
5. The results of heavy metals in spent FCC catalyst and fly ash did not have significant affect on the phase composition of the pastes. Low crystallinity of the C-S-H phase and the limited sensitivity of the XRD method make it impossible to get precise determination of difference concerning the rate of hydration in the paste containing heavy metals.
6. $Ca(OH)_2$, C-S-H, and ettringite identified as the major cementitious compounds are responsible for reducing pore size of cement paste.
7. Heavy metal in CSP pastes, CFA pastes, and CSFA pastes does not have significant effect on the microstructure. It may be because their content is very low and the surface of some particles could not be examined.

8. Both types of CSP pastes, CFA pastes, and CSFA pastes exhibited a significant lower porosity than the control. In addition, the lower concentrations of Cu, Fe, Ni, V, and Zn in leachate are lower corresponding to the decreasing in average pore size diameter and the curing time.

9. In some case, the degree of heavy metals immobilization in CSP pastes, CFA pastes, and CSFA pastes were higher than in the control because the heavy metal can be fixed more in cemetitious matrix of spent FCC catalyst and fly ash cement paste.

10. The leaching of heavy metals at 90 days of curing time was significantly lower than that of 28 days because the reaction in the cement paste was mostly complete.

11. The result from extraction method (TCLP test and LP-No.6 extraction test) are almost similar which confirms that all heavy metals leached from CSP pastes, CFA pastes, and CSFA pastes met the regular limits.

5.3 Suggestions for Future Works

1. Investigate the effect of particle size of spent FCC catalyst and fly ash on S/S process.

2. Determine suitable water-to-binder ratio that can enhance the reaction of spent FCC catalyst and fly ash in cement pastes.

3. Use spent FCC catalyst and fly ash as the fundamental raw material or main binders in the solidification and stabilization (S/S) of other waste as the result shows that the heavy metal content in spent FCC catalyst and fly ash are not significant.

4. Investigate the role of pH on leaching by increasing the pH value of solution in the paste.

5. Conduct long-term leaching test on the solidified/stabilized material to ensure that heavy metals will not leach to environment.

REFERENCES

Bach, Th. 1991. Effect of various proportions on pore size distribution of cement pastes. Fly ash in concrete properties and performance, pp 56-59. London: E&FNSPON.

Baur, I., Keller, P., Mavrocordatos, D., Wehrli, B., and Johnson, C. A. 2004. Dissolution-precipitation behaviour of ettringite, monosulfate, and calcium silicate hydrate. Cement and Concrete Research 34: 341-348.

Bishop, P. L. 1988. Leaching of inorganic hazardous constituents from stabilized / solidified hazardous waste. Hazardous Waste and Material 5: 129-143.

Bumrongjaroen, W. 1999. Utilization of processed fly ash in mortar. Doctoral Dissertation, Department of Civil and Environmental Engineering, New Jersey Institute of Technology, New Jersey.

Chen, H. L., Tseng Y. S., and Hsu, K. C. 2003. Spent FCC catalyst as a pozzolanic material for high-performance mortars. Cement & Concrete Composites.

Cho, S. I., Kwang S. J., and Woo S. I. 2001. Regeneration of spent RFCC catalytic irreversible deactivated by Ni, Fe, and V contained in heavy oil. Applied Catalysis 33: 245-261.

Choon-Keun, P. 2000. Hydration and solidification of hazardous wastes containing heavy metals using modified cementitious materials 30: 429-435.

Cocke, D. L., and Mollah, M. Y. A. 1993. The chemistry and leaching mechanisms of hazardous substances in cementitious solidification/stabilization system. In R. D. Spence (ed.), Chemical and microstructure of solidified waste forms, pp. 187-242. Ann Arbor: Lewis Publishers.

Constantino, F. P., Miguel R. P., and Jose, V. 2001. Solidification/stabilization of electric arc furnace dust using coal fly ash analysis of the stabilzation process. J. of Hazardous Material B82: 183-195.

Corner, J. R., 1993. Chemistry of cementitious solidified/stabilizate waste forms. In R. D. Spence (ed.), Chemical and microstructure of solidified waste forms, pp. 41-82. Ann Arbor: Lewis Publishers.

Cui, L., and Cahyadi, J. H. 2001. Permeability and pore structure of OPC paste. Cement and Concrete Research 31: 277-282.

Deja, J. 2002. Immobilization of Cr^{6+}, Cd^{2+}, Zn^{2+} and Pb^{2+} in alkali-activated slag binder. Cement and Concrete Research 32: 1971-1979.

Furimsky, E. 1996. Review of spent refinery catalysts: environment, safety and utilization. Catalysis Today. 30: 233-286.

Gougar, M. L.D., Scheetz, B. E., and Roy, D. M. 1996. Ettringite and C-S-H 5% additions. Cement and Concrete Research 20: 219-225.

Halim, C. E., Amal, R., Beydoun, D., Scott, J. A., and Low, G. 2004. Implications of structure of cementitious wastes containing Pb(II), Cd(II), As(V), and Cr(VI) on the leaching of metals. Cement and Concrete Research 34: 1093-1102.

Hopkin, C. H. 1938. Cracking catalysts and cat cracking. Australia: Catoleum Pty.

Hsu, W., Chang, H., Hwange, C., and Liao, C. 1996. Utilization of ceramics products made from waste. Ceramics. 15:20-35.

Inthasaro, P. 2002. Utilization of municipal solid waste incineration fly ash as a partial cement replacement. Master's Thesis, Inter-department of Environmental Management, Graduate School, Chulalongkorn University.

Jin, S.Y. 1998. Metal recovery and rejuvenation of metal-loaded spent catalysts. Catalysis Today 44: 27-46.

Jung-Hsiu, W., Wan-Lung, W., and Kung-Chung, H. 2003. The effect of waste oil-cracking catalyst on the compressive strength of cement paste and mortars. Cement and Concrete Research 33: 245-253.

Lagrega, D., Buckingham, L., and Evans, C. 2001. Chapter 11 stabilization and solidification. Hazardous Waste Management. 2nd ed. Environmental Resources Management.

Lappas, A. A., Nalbandian, L., Iatridis, D. K., Voutetakis, S. S., and Vasalos, I. A. 2001. Effect of metals poisoning on FCC products yields: studies in an FCC short contact time pilot plant unit. Catalysis Today 65: 233-240.

Lea, F. M. 1971. The chemistry of cement and concrete. 3rd ed. New York: Chemical Publish Company.

Li, X.D., Poon, C.S., Sun, H., Lo, I. M. C., Kirk, D. W. 2001. Heavy metal speciation and leaching behaviors in cement based solidified/stabilized waste materials. J. of Hazardous Materials A82: 215-230.

Malhotra, V. M. 1987. 2° in concrete. 2nd edition. Canada: Canmet.

Marafi, M., and Stanislaus, A. 2003. Option and process for spent catalyst handling and utilization. J. of Hazardous Materials B101: 123-132.

Mattle, V., and Moranville, M. 1999. Durability of reactive powder composites: influence of silica fume on the leaching properties of very low water/binder pastes. Cement & Concrete Composites 21: 1-9.

Mindess, S., and Young, J. F. 1981. Concrete. New York: Prentice-HallIrc.

Ministry of Industry. 2002. Notification of Ministry of Industry No.6 B.E.2540 (1997) [Online] Available from: http://www.diw.go.th/law/nmoi6y40.html [2004, June 23].

Minocha, A. K., Jsin, N., and Verma, C.L. 2003. Effect of inorganic materials on the solidification of heavy metal sludge. Cement and Concrete Research 33: 1695-1701.

Nukunkan, T. 2003.Qaulity and control of Mae Moh coal power plan. The Second Conference on Fly ash in Construction and Usage. pp. 36-44.

Ouki, S. K., and Hills, C. D. 2002. Microstructure of Portland cement pastes containing metal nitrate salts. Waste Management 22: 147-151.

Pacewska**,** B., Wilinska, I., and Kubissa, J. 1998. Use of spent catalyst from catalytic cracking in fluidized bed as a new concrete additive. Thermochimica Acta 322: 175-181.

Pandey, S. P., and Sharma, R. L. 2000. The influence of mineral additives on the strength and porosity of OPC mortar. Cement and Concrete Research 30: 19-23.

Paul, B. V., and Thomas, E. H. 1979. Fluid catalytic cracking with zeolite catalysts. Chemical Industrial/1. Mobile Research and Development Corporation Field Research Laboratory Dallas.

Paya, J., Monzo, J., and Borrachero, M. V. 1999. Fluid catalytic cracking catalyst residue (FC3R). An excellent mineral by-product for improving early-strength development of cement mixtures. Cement and Concrete Research 29: 1773-1779.

Paya, J., Monzo, J., and Borrachero, M. V. 2001. Physical, chemical and mechanical properties of fluid catalytic cracking catalyst residue (FC3R) blended cements. Cement and Concrete Research 31: 57-61.

Paya, J., Monzo, J., Borrachero, M. V., and Velazquez, S. 2003. Evaluation of the pozzolanic activity of fluid catalytic cracking catalyst residue (FC3R). Thermogravimetric analysis studies on the FC3R-Portland cement pastes. Cement and Concrete Research 33: 603-609.

Phenrat, T. 2003. Examination of solidified and stabilized matrices as a result of solidification and stabilization process of arsenic containing sludge with Portland cement. Master's Thesis. Inter-department of Environmental Management, Graduate School, Chulalongkorn University.

Plowman, C., and Cabrera, J.G. 1991. The use of fly ash to improve the sulfide resistance of concrete. Cement and Concrete Research 21: 145-149.

Poon, C. S., Qiao, X. C., and Lin, Z. S. 2003. Pozzolan properties of reject fly ash in blended cement pastes. Cement and Concrete Research 33: 1857-1865.

Poon, C. S., Peters, C.J., and Perry, R. 1985. Mechanisms of metal stabilization by cement based fixation processes. The Science of the Total Environment 41: 55-71.

Qin, G., Sun, D. D., and Tay, J. H. 2003. Characterization of mercury- and zinc-doped alkali-activated slag matrix Part II. Zinc. Cement & Concrete Research 33: 1257-1262.

Rachakornkij, M. 2000. Utilization of municipal solid waste incinerator fly ash in cement mortars. Doctoral Dissertation, Department of Civil and EnvironmentalEngineering, New Jersey Institute of Technology, New Jersey.

Rattanasak, U., Jaturapitakkul, C., and Sudaprasert, T. 2001. Compressive strength and heavy metal leaching behaviour of mortars containing spent catalyst. Waste Management and Research 19: 4-9.

Rose, J., Moulin, I., Mason, A., Bertsch, P. N., Wiesner, M. R., Bottero, J. Y., Mosnier,F., and Haehnel, C. 2000. X-ray spectroscopy study of immobilization process for heavy metals in calcium silicate hydrate:2. Zinc Langmuir 17: 3658-3665.

Roy, A., Eaton, H. C., Cartedge, F.K., and Tittlebeam, M.E. 1998. Solidification/ stabilization of heavy metal sludge by Portland cement/fly ash binding mixture. Hazardous Waste & Hazardous Materials 5: 125-141.

Sadeghbeigi, R. 2000. Fluid catalytic cracking handbook. 2nd ed. Houston. Texas: Gulf Publishing Company.

Sinsiri, T., Jaturapitakkul, C., and Jindaprasert, P. 2003. Effect of fly ash to the microstructure of cement pastes. The Second Conference on Fly ash in Construction and Usage. pp. 64-82.

Stephan, D., Maleki, H., Knofel, D., Eber, B., and Hardtl, R. 1999. Influence of Cr, Ni, and Zn on the properties of pure clinker phases. Part II. C_3A and C_4AF. Cement and Concrete Research 29: 651-657.

Stuff works. 1998. Chemical process of oil refining. [Online] Available from: http://www.science.howstuffworkers.com/oil-refining-cracking-unit.html [2004, October 5].

Su, N., Fang, H. Y., Chen, H. C., and Liu, F. S. 2000. Reuse of waste catalyst from petrochemical industries for cement substitution in cement mortar. Cement & Concrete Research 30: 1773-1783.

Su, N., Chen, Z. H., and Fang, H. Y., 2001. Reuse of spent catalyst as fine aggregate in cement mortar. Cement & Concrete Composite 23: 111-118.

Tsivilis, S., Tsantilas, J., Kakali, G., Chaniotakis, E., and Sakellariou, A. 2003. The permeability of Portland limestone cement concrete. Cement & Concrete Research 33: 1465-1471.

Wang, S., and Vipulanandan, C. 2000. Solidification/stabilization of Cr(VI) with cement leachability and XRD analyses. Cement & Concrete Research 30: 385-389.

Wesche, K., ed. 1991. Fly ash in concrete properties and performance. London: E&FNSPON.

Xu, A., and Sarker, S. L. 1994. Microstructure development in high-volume fly ash cement system. J. of Material in Civil Engineering 6: 117-136.

Yun-Sheng, T. Chen-Lin, H., and Kung-Chung, H. 2004. The pozzolanic activity of a calcined waste FCC catalyst and its effect on the compressive strength of cement materials. Cement and Concrete Research.

APPENDICES

APPENDIX A.
EQUIPMENTS

Figure A-1 Mercury Intrusion Porosimetry (MIP)

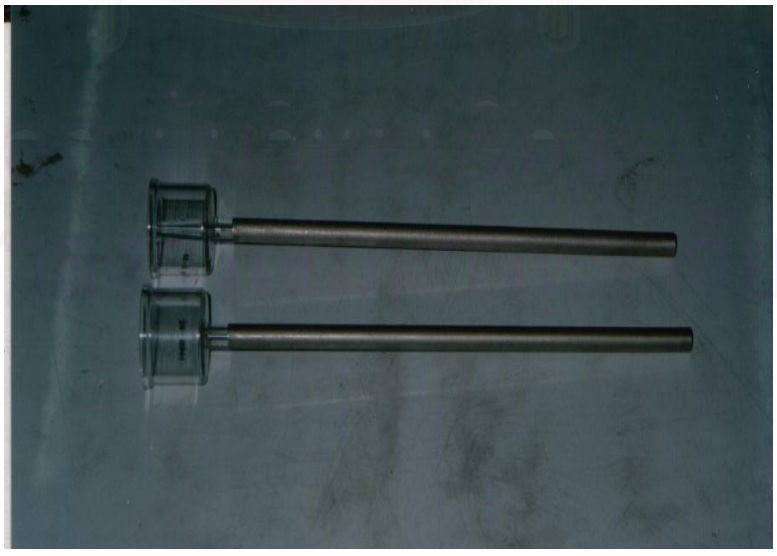

Figure A-2 Penetrometer

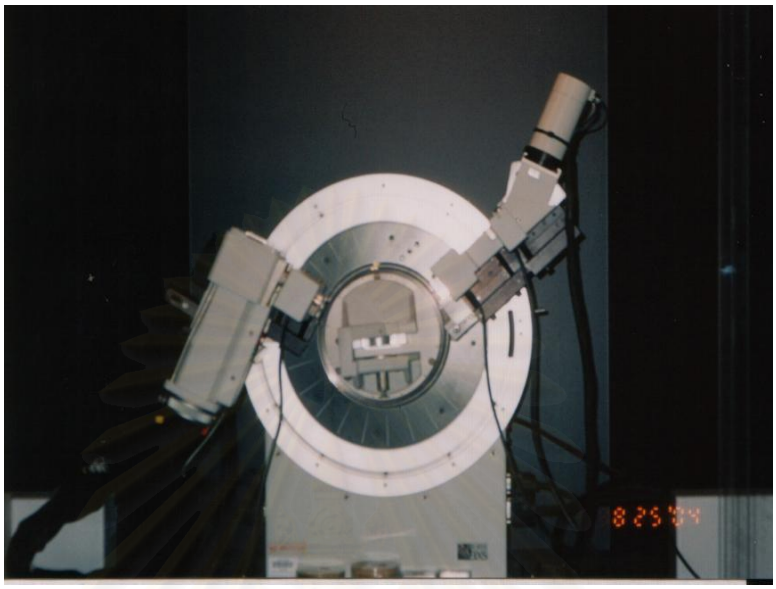

Figure A-3 Brunker Powder X-ray Diffraction Spectrometer Model D8 Advance

Figure A-4 Inductive Couple Plasma-Optical Emission Spectroscopy (ICP-OES)

Figure A-5 Rotating Agitator for Leaching Test

Figure A-6 Microwave Assisted Acid Digestion

BIOGRAPHY

Miss. Onchuda Dumsri was born on February 5, 1981 in Nakhonsrithammarat Province, Thailand. She attended Yothinburana School in Bangkok and graduated in 1999. She received her Bachelor's Degree in General Science from Faculty of Science, Chulalongkorn University, Bangkok, Thailand in 2003. She pursued her Master Degree studies in International Postgraduate Programs in Environmental Management, Inter-Department of Environmental Management, Chulalongkorn University, Bangkok, Thailand in May 2003. She finished her Master Degree of Science in Environmental Management in May 2005.